

1300 1-1000 1-1000

21 JUNE 1961

RADC TRINIDAD TEST SITE

FINAL REPORT

VOLUME II

A STUDY OF THE LONG-TERM UTILIZATION
OF THE INCIDENT SCATTER TECHNIQUE

SYSTEMS OPERATION

HEADQUARTERS ELECTRONICS DEPARTMENT • SYRACUSE, N. Y.

GENERAL  ELECTRIC

CONTRACT AF 30(602) 2244

PREPARED FOR

ROME AIR DEVELOPMENT CENTER
AIR FORCE SYSTEMS COMMAND
UNITED STATES AIR FORCE
GRIFFISS AIR FORCE BASE - NEW YORK

401 912

1

•

1

•

•

1

1

7

TABLE OF CONTENTS

<u>Section</u>	<u>Title</u>	<u>Page</u>
I	INTRODUCTION -----	1
II	THEORY OF IONOSPHERIC INCOHERENT SCATTER -----	3
	A. Introduction -----	3
	B. Backscattered Power -----	3
	C. Scattering Cross Section -----	5
	D. Frequency Spectrum of Incoherent Backscatter -----	10
III	APPLICATION OF THE INCOHERENT SCATTER TECHNIQUE FOR PROBING THE EARTH'S ATMOSPHERE -----	26
	A. Introduction -----	26
	B. Incoherent Scatter Power Measurements -----	27
	C. Incoherent Scatter Spectral Measurements -----	30
IV	IONOSPHERIC FARADAY EFFECT -----	32
	A. Introduction -----	32
	B. Angular Polarization Rotation -----	32
	C. Magnetic Field Measurements by Incoherent Scatter-Faraday Rotation Phenomenon -----	34
	D. Calibration of the Relative Electron Density Profile -----	37
V	EXPERIMENTAL CONSIDERATIONS -----	39
	A. Data Collection and Processing -----	39
	B. Characteristics of Incoherent Backscatter Echoes -----	41
VI	DATA ANALYSIS -----	46
	A. Backscatter Measurements in the Direction of Bogota, Colombia -	46
	B. Backscatter Measurements in the Direction of Puerto Rico -----	51
	C. Backscatter Measurements Near Vertical Incident at Trinidad ---	58
	D. Electron Density Profiles -----	65
	E. Ionospheric Movements -----	69
	F. Data Correlation -----	74
VII	SUMMARY AND CONCLUSIONS -----	75
VIII	REFERENCES -----	77
APPENDIX	System Requirements for the Detection of Ionospheric Incoherent Backscatter -----	81

TABLE OF CONTENTS

<u>Section</u>	<u>Title</u>	<u>Page</u>
I	INTRODUCTION -----	1
II	THEORY OF IONOSPHERIC INCOHERENT SCATTER -----	3
	A. Introduction -----	3
	B. Backscattered Power -----	3
	C. Scattering Cross Section -----	5
	D. Frequency Spectrum of Incoherent Backscatter -----	10
III	APPLICATION OF THE INCOHERENT SCATTER TECHNIQUE FOR PROBING THE EARTH'S ATMOSPHERE -----	26
	A. Introduction -----	26
	B. Incoherent Scatter Power Measurements -----	27
	C. Incoherent Scatter Spectral Measurements -----	30
IV	IONOSPHERIC FARADAY EFFECT -----	32
	A. Introduction -----	32
	B. Angular Polarization Rotation -----	32
	C. Magnetic Field Measurements by Incoherent Scatter-Faraday Rotation Phenomenon -----	34
	D. Calibration of the Relative Electron Density Profile -----	37
V	EXPERIMENTAL CONSIDERATIONS -----	39
	A. Data Collection and Processing -----	39
	B. Characteristics of Incoherent Backscatter Echoes -----	41
VI	DATA ANALYSIS -----	46
	A. Backscatter Measurements in the Direction of Bogota, Colombia -	46
	B. Backscatter Measurements in the Direction of Puerto Rico -----	51
	C. Backscatter Measurements Near Vertical Incident at Trinidad ---	58
	D. Electron Density Profiles -----	65
	E. Ionospheric Movements -----	69
	F. Data Correlation -----	74
VII	SUMMARY AND CONCLUSIONS -----	75
VIII	REFERENCES -----	77
APPENDIX	System Requirements for the Detection of Ionospheric Incoherent Backscatter -----	81

LIST OF ILLUSTRATIONS

<u>Figure</u>	<u>Title</u>	<u>Page</u>
1	Total Scattered Power as a Function of Inverse Wavelength for Various Electron-to-Ion Temperature Ratios (after Buneman) ----	9
2	Frequency Spectrum as a Function of Different Electron-to-Ion Temperature Ratios for Wavelengths much Larger than the Debye Length (after Fejer) -----	14
3	Frequency Spectrum as a Function of the Ratio of Hydrogen Ion-to-Oxygen Ion Density for Wavelengths much Larger than the Debye Length (after Fejer) -----	15
4	Frequency Spectrum as a Function of the Propagation Angle Near Perpendicularity for Wavelengths much Larger than the Debye Length (after Farley, Dougherty and Barron) -----	20
5	Relative Power as a Function of Off-Perpendicular Angle for Wavelengths much Larger than the Debye Length (after Renau, Camnitz and Flood) -----	22
6	Effect of the Earth's Magnetic Field on the Spectrum of Incoherent Backscatter Observed at 425 Megacycles at Trinidad, 26 January 1961 (after Pineo, Kraft, Briscoe and Hynek) -----	24
7	Spectral Bandwidth of Incoherent Backscatter as a Function of Off-Perpendicular Angle for Observations Taken at 425 Megacycles at Trinidad (after Pineo and Hynek) -----	25
8	The Function, $f(h) H \cos \theta$, as Viewed from Trinidad -----	35
9	Vertical Incidence Incoherent Backscatter Observed at Millstone Hill at 440 Megacycles on the Afternoon of 8 February 1960 (after Pineo, Kraft and Briscoe) -----	42
10	Range vs. Time Photographs of Incoherent Backscatter Echoes Showing Faraday Rotation. Observations Taken at Trinidad at 10° Elevation Angle in the Direction of Bogota, Colombia, on 2 February 1961 -----	43
11	A-Scope Photographs of Integrated Incoherent Backscatter Observed at Trinidad at 10° Elevation Angle in the Direction of Bogota, Colombia on 2 February 1961, 1318 through 1326 AST. Data Processed by Computer at the MIT Lincoln Laboratory, Millstone Hill Radar Station -----	45
12	Distribution of Electron Density Observed by Incoherent Backscatter at 10° Elevation Angle in the Direction of Bogota, Colombia, on 2 February 1961 -----	47
13	Incoherent Backscatter Electron Density Profile Compared with Profile Deduced from Ionospheric Soundings Taken at Bogota, Colombia on 2 February 1961, 1330 AST -----	48

LIST OF ILLUSTRATIONS (Continued)

<u>Figure</u>	<u>Title</u>	<u>Page</u>
14	Comparison of Theoretical Estimate of Faraday Rotation with Incoherent Backscatter Observations Taken at Trinidad at 10° Elevation Angle in the Direction of Bogota, Colombia, on 2 February 1961 -----	50
15	Distribution of Electron Density Observed by Incoherent Backscatter at Trinidad at 13° Elevation Angle in the Direction of Puerto Rico on 27 January 1961 -----	52
16	Incoherent Backscatter Electron Density Profile Compared with Profile Deduced from Ionospheric Soundings Taken at Puerto Rico on 27 January 1961, 1445 AST -----	53
17	Comparison of Theoretical Estimate of Faraday Rotation with Incoherent Backscatter Observations Taken at Trinidad at 13° Elevation Angle in the Direction of Puerto Rico on 27 January 1961 -----	55
18	Distribution of Electron Density Observed by Incoherent Backscatter at Trinidad at 13° Elevation Angle in the Direction of Puerto Rico on 1 February 1961 -----	56
19	Incoherent Backscatter Electron Density Profile Compared with Profile Deduced from Ionospheric Soundings Taken at Puerto Rico on 1 February 1961, 1615 AST -----	57
20	Comparison of Theoretical Estimate of Faraday Rotation with Incoherent Backscatter Observations Taken at Trinidad at 13° Elevation Angle in the Direction of Puerto Rico on 1 February 1961 -----	59
21	Distribution of Electron Density Observed by Incoherent Backscatter at Trinidad at 45° Elevation Angle in the Direction of Puerto Rico on 27 January 1961 -----	60
22	Incoherent Backscatter Electron Density Profile Compared with Profile Deduced from Ionospheric Soundings Taken at Trinidad on 27 January 1961 -----	61
23	Comparison of Theoretical Estimate of Faraday Rotation with Incoherent Backscatter Observations Taken at Trinidad at 45° Elevation Angle in the Direction of Puerto Rico on 27 January 1961 -----	62
24	Distribution of Electron Density Observed by Incoherent Backscatter at Trinidad at Vertical Incidence on 2 February 1961 --	63
25	Incoherent Backscatter Electron Density Profile Compared with Profile Deduced from Ionospheric Soundings Taken at Trinidad on 2 February 1961 -----	64
26	Comparison of Theoretical Estimate of Faraday Rotation with Incoherent Backscatter Observations Taken at Trinidad at Vertical Incidence on 2 February 1961 -----	66

LIST OF ILLUSTRATIONS (Concluded)

<u>Figure</u>	<u>Title</u>	<u>Page</u>
27	Electron Density Profiles Deduced from Incoherent Backscatter at Trinidad in the Direction of Bogota, Colombia, and Puerto Rico -----	67
28	Electron Density Profiles Deduced from Incoherent Backscatter at Trinidad at Near Vertical Incidence -----	68
29	Range vs. Time Photograph Showing Range Movement of Incoherent Backscatter Echoes Observed at Trinidad at 5° Elevation Angle and 180° Azimuth Angle on 25 January 1961, 2233 AST -----	70
30	Range vs. Time Photograph Showing Range Movement of Incoherent Backscatter Echoes Observed at Trinidad at 10° Elevation Angle in the Direction of Bogota, Colombia, on 27 January 1961, 1815 AST -----	70
31	Range vs. Time Photograph Showing Range Movement of Incoherent Backscatter Echoes Observed at Trinidad at 10° Elevation Angle in the Direction of Bogota, Colombia, on 2 February 1961, 1342 through 1345 AST -----	70
32	Electron Density Profiles Deduced from Ionospheric Soundings Taken at Bogota, Colombia, on 2 February 1961 -----	72
33	Contours of Constant Plasma Frequency at Bogota, Colombia, on 23 January 1961 -----	73
A-1	Incoherent Backscatter Signal-to-Receiver Noise Ratio as a Function of System Parameters -----	83
A-2	Estimate of the Bandwidth of Incoherent Signals Backscattered from a Normal Ionosphere at 425 and 1300 Megacycles -----	84
A-3	Estimate of Incoherent Signal-to-Receiver Noise Ratio from a Normal Ionosphere at 425 Megacycles -----	86

ACKNOWLEDGEMENTS

The magnetic recording of the incoherent backscatter experimental data and the data reduction reported in this work would not have been possible without the assistance of the Lincoln Laboratory's personnel, equipment and facilities. The author wishes especially to thank V.C. Pineo of the Lincoln Laboratory for his cooperation in making this experiment a success. The assistance of D.P. Hynek, W. Smith, and R. Silva, all of the Lincoln Laboratory, in the experimental measurements is also greatly appreciated.

The participation in this program of J.W. Wright and G.H. Stonehocker of the National Bureau of Standards in maintaining the operation of the ionosonde equipment and in furnishing the ionosonde data is also gratefully acknowledged.

RADC TRINIDAD TEST SITE
FINAL REPORT
VOLUME V

A STUDY OF THE IONOSPHERE UTILIZING
THE INCOHERENT SCATTER TECHNIQUE

I. INTRODUCTION

In January and February 1961, incoherent backscatter measurements were performed at a frequency of 425 megacycles at the U.S. Air Force Trinidad Test Site (10.7° N, 61.6° W), the experimental program being the joint effort of the Rome Air Development Center, the General Electric Company, the Lincoln Laboratory, and the National Bureau of Standards.

The main objectives of the program were as follows:

1. To obtain, from vertical incidence incoherent scattering, the electron density distribution as a function of height at a low latitude; to determine the diurnal characteristics of the profile in the region above the peak of the F-layer; to determine the effects of magnetic disturbances on the distribution; and to obtain electron density profiles measured at various elevation angles along the geographic meridian for studying the characteristics of the equatorial ionosphere,
2. To determine the characteristics of the frequency spectra of ionospheric incoherent backscattered radiation as a function of altitude and the angle between the direction of propagation and the lines of force of the earth's magnetic field; and to determine the effect of the orientation of the magnetic field on the total incoherent backscattered power, and
3. To study the effect of the polarization rotation induced by the ionospheric Faraday phenomenon on the incoherent backscatter echoes.

The Trinidad Test Site was well suited for this investigation because, at this location, the orientation of the magnetic field was such that it was possible to transmit radio waves in directions which would intersect the field lines at F-layer heights at various aspect angles. This requirement was necessary in the investigation of the effect of the magnetic field on the spectral characteristics of incoherent backscatter. An additional factor which favored the Trinidad Test Site was that this was the only radar installation in the low latitudes, available at the time, which had sufficient sensitivity to detect the radiation scattered incoherently from the ionosphere and which was capable of satisfying the condition of perpendicularity.

This report is mainly concerned with the investigation of the incoherent scatter-Faraday rotation phase of the experiment. A discussion is given on the theoretical concepts of incoherent scattering. The application of this technique for probing the earth's atmosphere is also considered.

It is anticipated that, in the near future, a report will be published jointly by the Lincoln Laboratory and the General Electric Company which will incorporate an analysis of all the experimental data obtained under the three categories described above.

II. THEORY OF IONOSPHERIC INCOHERENT SCATTER

A. INTRODUCTION

A random distribution of free electrons in an ionized medium such as exists in the ionosphere is capable of scattering electromagnetic waves incoherently. Although the energy scattered by this mechanism is very weak, Gordon¹ postulated in 1958 that it would be possible to detect the radiation backscattered from the ionosphere when a high powered radar system was employed.

Experimental verification of the existence of this phenomenon was first demonstrated at the National Bureau of Standards' facility in Illinois, as reported by Bowles.^{2,3} The NBS equipment, employed in this investigation, consisted of a conventional high-powered pulsed radar operating at a frequency of 40.9 megacycles. Transmissions were directed vertically utilizing, as the antenna, a simple broad-side array measuring 116 meters by 140 meters.

Additional evidence of the existence of incoherent backscatter radiation has been confirmed by Pineo, Kraft and Briscoe^{4,5} of the Lincoln Laboratory, and also by Millman, Moceyunas, Sanders, and Wyrick⁶ of the General Electric Company. The observations of the Lincoln Laboratory group were conducted with the Millstone Hill radar which operated at 440 megacycles with an 84-foot diameter parabolic antenna. The General Electric experimental work was performed at the U.S. Air Force Trinidad Test Site under the cognizance of the Rome Air Development Center.

Since Gordon's original hypothesis,¹ various facets of the theory of ionospheric incoherent scatter have been investigated by Salpeter,⁷ Dougherty and Farley,⁸ Fejer,^{9,10} Renau,^{11,12} Laaspere,¹³ Hagfors,¹⁴ and Buneman.¹⁵

The electron scattering cross section, which influences the magnitude of the backscattered radiation, is considered in this section. The effect of the earth's magnetic field on the spectral distribution of the incoherent radiation is also discussed.

B. BACKSCATTERED POWER

The radiation backscattered by the free electrons in the ionosphere and incident at a radar antenna can be written as

$$P_r = \left[\frac{P_t G}{4\pi R^2} \right] \left[\frac{\pi \lambda^2 R^2 h}{4 A_e} \right] \left[\frac{A_e}{R^2} \right] \sigma \quad (1)$$

where the first parenthesized term is the power density of the incident wave at the scatterers, the second term is the volume of the medium filled with scatterers and observed at an instant of time, the third term is the solid angle subtended by an antenna with an effective area, A_e , at a radar range, R , from the scatterers, and σ is the scattering coefficient defined as the power scattered per unit solid angle per unit incident power density per unit scattering volume. The parameter, P_t , is the transmitted peak power, G is the gain of the antenna relative to an isotropic antenna, λ is the transmitted wavelength, and h is one-half the pulse length in space.

The gain of an antenna is defined in terms of the effective antenna area by

$$G = \frac{4\pi A_e}{\lambda^2} \quad (2)$$

while

$$h = \frac{c \tau}{2} \quad (3)$$

where c is the free space velocity and τ is the pulse length.

According to Nyquist's formulation of the thermal noise concept,¹⁶ the total internal receiver noise power, N , is given by

$$N = K T B F \quad (4)$$

where K is Boltzmann's constant (1.38×10^{-23} watt-second per degree Kelvin), T is the ambient temperature, B is the receiver bandwidth (cps), and F is the receiver noise figure.

Utilizing the above relationships, it follows that the incoherent back-scattered signal-to-receiver noise ratio becomes, for a monostatic radar system,

$$\frac{P_r}{N} = \frac{\pi P_t c \tau A_e \sigma}{8 R^2 K T B F} \quad (5)$$

It is evident from this relationship that, for the condition in which the antenna beam is completely filled with scatterers, the power received by the incoherent scattering mechanism is independent of the transmission frequency and

inversely proportional to the square of the radar range. For a radar target which is smaller than the antenna beamwidth, the echo intensity varies inversely as the fourth power of the range.

It should be mentioned that it is necessary to consider the doppler spread imposed by the scattering medium in the evaluation of the incoherent signal-to-receiver noise ratio. If the receiver bandwidth is greater than the scattering bandwidth, then the former must be inserted in Equation (5). If, on the other hand, the receiver bandwidth is narrower than the width of the scatter spectrum, then the latter is used in defining the internal receiver noise power.

Since the doppler spread is a function of the transmission frequency impinging on the medium (as discussed in the following sections), the signal-to-noise ratio therefore decreases with increasing frequency. This applies only to the condition when the bandwidth of the receiver is equal to or less than the spectral width of the backscattered radiation.

Estimates of the radar system configurations necessary for detecting ionospheric incoherent backscatter are discussed in the appendix.

C. SCATTERING CROSS SECTION

According to Fejer's analysis⁹ of the scattering of radio waves by electron density fluctuations which exist in an ionized gas in thermal equilibrium, in the absence of an external magnetic field, the scattering coefficient, σ , can be described by the function

$$\sigma = \sigma_e N_e \frac{\left[4\pi \ell_D \sin\left(\frac{\epsilon}{2}\right)\right]^2 + \lambda^2}{\left[4\pi \ell_D \sin\left(\frac{\epsilon}{2}\right)\right]^2 + 2\lambda^2} \quad (6)$$

where ϵ is the angle between the direction of propagation of the incident wave and that of the scattered wave, N_e is the electron density, σ_e is the scattering cross section of a single free electron, and ℓ_D is the Debye length.

The derivation of this expression was based on the assumption that only one type of singly charged positive ions was present in the gas, and that the electron and ion temperatures were equal.

The Debye length, or shielding distance, is a measure of the distance over which the electron density in a plasma can deviate from the ion density. It is related to the electron density and the temperature of the plasma, T , by¹⁷

$$\ell_D = \left[\frac{KT}{4\pi e^2 N_e} \right]^{1/2} \quad (7)$$

where e is the electron charge (4.8×10^{-10} e.s.u.).

When N_e is in units of electrons per cubic centimeter, T in degrees Kelvin, and K equal to 1.38×10^{-16} erg per degree Kelvin, this expression simplifies to

$$\ell_D = 6.9 \left[\frac{T}{N_e} \right]^{1/2} \quad (8)$$

where ℓ_D is in centimeters.

The scattering coefficient of a single free electron is given, in gaussian units, by

$$\sigma_e = \left[\frac{e^2}{m_e c^2} \right]^2 \sin^2 \chi \quad (9)$$

$$\sigma_e = 7.94 \times 10^{-26} \sin^2 \chi \text{ (cm}^2\text{)} \quad (10)$$

where m_e is the electron mass (9.1×10^{-28} gram), and χ is the angle between the direction of polarization of the incident electric field and the direction of scattering. The term, $(e^2/m_e c^2)$, is the classical electron radius having the dimensions of 2.818×10^{-13} centimeter.

It should be noted that the radar cross section of an electron is merely the cross section, defined by Equation (9), integrated over 4π solid angle, and is approximately equal to $(4\pi)(e^2/m_e c^2)^2$ or 10^{-24} square centimeter.

The Thomson scattering cross section of an electron is the cross section also integrated over 4π solid angle, the electrons, in this case however, being illuminated by unpolarized radiation. It can be shown¹⁸ that this parameter is equal to $(8\pi/3)(e^2/m_e c^2)^2$ or 6.65×10^{-25} square centimeter.

It is evident that, when $\lambda \ll 4\pi \ell_D \sin(\epsilon/2)$, the scattering coefficient reduces to

$$\sigma = \sigma_e N_e \quad (11)$$

It should be noted that this value of σ applies to the condition in which the electrons are randomly distributed in space and are radiating energy incoherently. The total energy backscattered is merely the sum of the power scattered by each individual electron.

When $\lambda \gg 4\pi l_D \sin(\epsilon/2)$

$$\sigma = (1/2) \sigma_e N_e \quad (12)$$

In other words, this implies that, for wavelengths greater than 4π times the Debye length, the total power backscattered would be one-half of what it would be if the electrons were randomly distributed.

Gordon¹ originally assumed that the scattering coefficient defined by Equation (11) was applicable to all wavelengths. In essence, it is only valid for frequencies greater than about 9200 megacycles. This can be readily seen from Equation (8), since the Debye length in the F-layer (300 kilometers) is estimated to be on the order of 0.26 centimeter, the calculations being based on the assumption that $T = 1400^\circ \text{K}$ and $N_e = 10^6$ electrons per cubic centimeter.

The experimental results of Bowles³ have indicated that the intensity of the incoherent backscattered signal from the ionosphere is in approximate agreement to within ± 3 db with Gordon's predictions, as given by Equations (5) and (11).

Pineo,¹⁹ on the other hand, has reported that the backscatter power measurements at 440 megacycles were approximately 7 db less than that predicted on the basis of Gordon's hypothesis¹ or about 4 db less than that predicted by the revised theories on ionospheric incoherent scatter, i.e., Equations (5) and (12).

It should be mentioned that, in the limit of short wavelengths, the scattering coefficients obtained by Kahn,²⁰ Pines and Bohm,²¹ and Fejer,⁹ are the same. Kahn derived expressions for the charge and electron density fluctuations in an ionized gas containing electrons and discrete positive ions. When the positive ions are singly charged, Kahn's result, for the long wavelength case, is also in agreement with Fejer's.

Pines and Bohm were concerned with the density fluctuations in an electron gas in the presence of a uniform positive charge density. Fejer's analysis is a modified version of their paper without the restrictive assumption of a uniform

positive charge density. For long wavelengths, Pines' and Bohm's scattering coefficient is reduced by a factor of $(4\pi \ell_D \sin(\epsilon/2)/\lambda)^2$ to that given by Equation (11).

Dougherty and Farley⁸ independently derived the relationship for the scattering cross section given by Equation (6). Their analysis of the scattering of radio waves by the random thermal fluctuations of electron density was based on a generalized version of Nyquist's noise theorem.

For positive ions having an arbitrary net charge, Z , Salpeter⁷ and Renau¹¹ have shown that the total scattering cross section is modified to

$$\sigma = \sigma_e N_e \frac{[4\pi \ell_D \sin(\frac{\epsilon}{2})]^2 + Z\lambda^2}{[4\pi \ell_D \sin(\frac{\epsilon}{2})]^2 + (1+Z)\lambda^2} \quad (13)$$

It is noted that, when $Z = 1$, which corresponds to Fejer's assumption⁹, this expression reduces to Equation (6).

Buneman²² has investigated the scattering of radiation by the fluctuations in a non-equilibrium plasma and arrived at an expression for the cross section as a function of the temperature of the electrons and the ions. In terms of the nomenclature used in this paper, his results for the backscatter case can be written in the form

$$\sigma = \sigma_e N_e \left[1 - \frac{1}{1 + (\frac{4\pi}{\lambda} \ell_D)^2} + \frac{1}{\left[1 + (\frac{4\pi}{\lambda} \ell_D)^2 \right] \left[1 + (\frac{4\pi}{\lambda} \ell_D)^2 + \frac{T_e}{T_i} \right]} \right] \quad (14)$$

where ℓ_D is the electron Debye length defined by Equation (7), and T_e and T_i are the electron and ion temperature, respectively.

It is evident from Figure 1, which is a plot of Equation (14), that, at wavelengths much smaller than the Debye length, the scattering cross section is independent of the electron-ion temperature ratio. When the wavelength is large compared to the Debye length, the amount of scattered power is solely dependent upon the temperature of the electron and ion in the plasma. The scattered power decreases with increasing T_e/T_i ratio. This has also been confirmed by Fejer.¹⁰

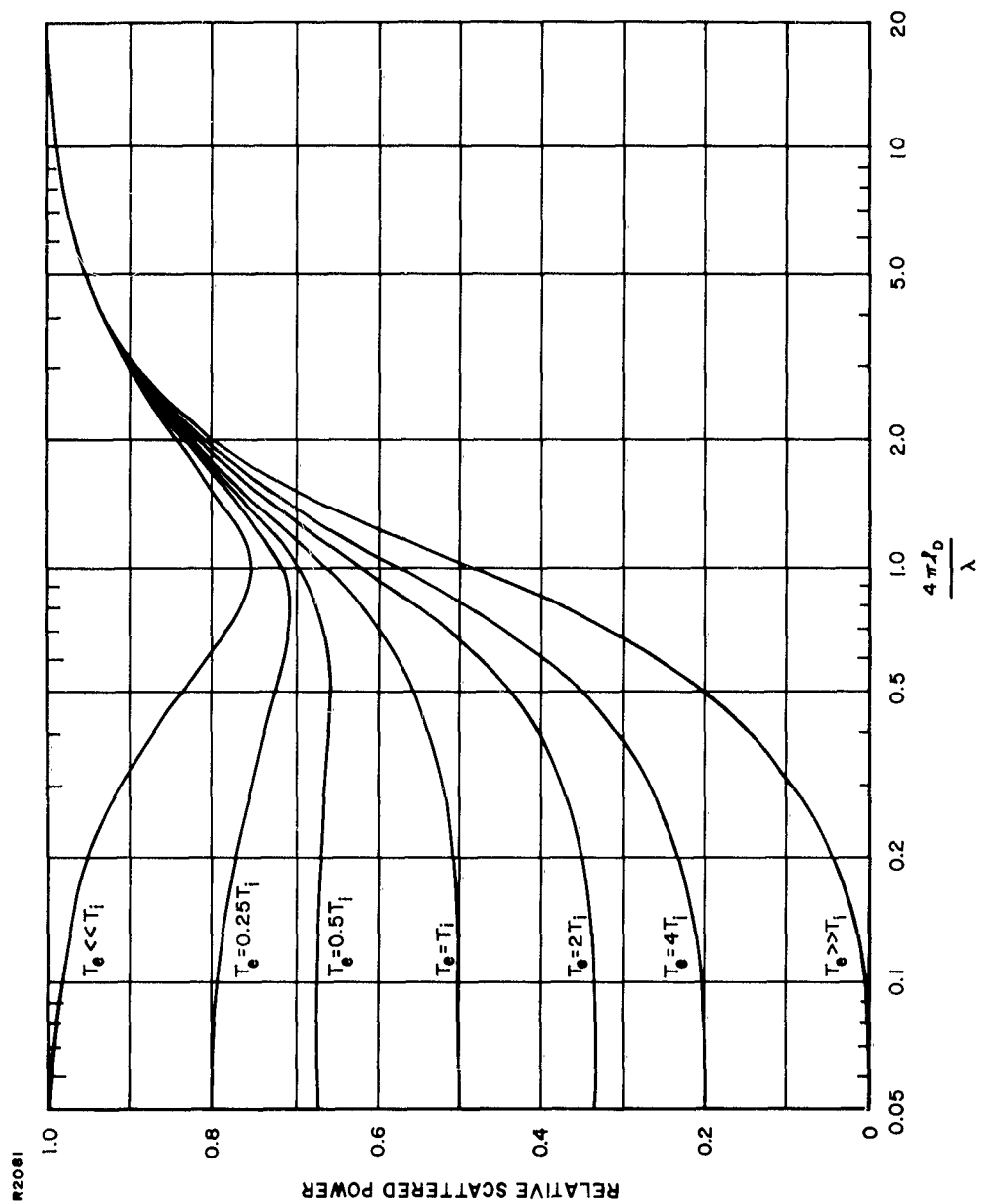


Figure 1. Total Scattered Power as a Function of Inverse Wavelength for Various Electron-to-Ion Temperature Ratios (after Buneman)

When $T_e = T_i$, Buneman's²² results agree with those derived by Fejer,⁹ Salpeter,⁷ Renau,¹¹ and Dougherty and Farley.⁸

With regard to the effect of a uniform external magnetic field, Fejer,¹⁰ Hagfors,¹⁴ and Farley, Dougherty and Barron²³ have all theoretically shown that the presence of a magnetic field can never alter the total backscattered signal power.

Experimental confirmation of the validity of this prediction has been reported by Pineo.²⁴ From the ionospheric incoherent backscatter measurements performed at a frequency of 425 megacycles at the U.S. Air Force Trinidad Test Site in January and February 1961, Pineo²⁴ has found that the total backscattered power does not appear to be a function of the orientation of the earth's magnetic field.

D. FREQUENCY SPECTRUM OF INCOHERENT BACKSCATTER

1. General

In Gordon's original paper on incoherent backscatter,¹ it was assumed that the signal scattered from the ionosphere would be doppler shifted from that of the incident wave, the width of its spectrum being determined by the random thermal velocity of each individual electron. He estimated that the spectral width of energy scattered from free electrons at F-region heights would be about 100 kilocycles at an operating frequency of 200 megacycles.

Bowles' observations³ have revealed that the doppler broadening is spread over a much narrower frequency range than that predicted by Gordon. At a frequency of 41 megacycles he was able to determine that the spectrum was considerably less than nine kilocycles.

Backscatter measurements at 440 megacycles by Pineo, Kraft and Briscoe⁵ indicate a half-power spectral width of approximately five kilocycles and 11 kilocycles at a height of about 120 kilometers in the E-region and 330 kilometers in the F-region, respectively. The increase in the frequency spread with height results from the fact that the doppler broadening is proportional to the square root of the kinetic temperature and that the temperature in the ionosphere increases with height.

In attempting to explain the discrepancy in the spectral width as postulated by Gordon and experimentally measured, Bowles³ predicted that the Coulomb forces between the electrons and ions in the plasma played an important part in the scattering process. He hypothesized that the scattering was brought about by fictitious particles which had a thermal velocity comparable to that of the ions and a cross section equal to that of the electrons.

More refined theoretical expositions on the incoherent scattering phenomenon have recently appeared in the literature.^{7-15,22,23}

2. In the Absence of an External Magnetic Field

a. Neglecting the Effects of Particle Collisions

Fejer⁹ has determined that, when neglecting the effect of collisions and the presence of an external magnetic field and assuming $\lambda \ll 4\pi \ell_D \sin(\epsilon/2)$, i.e., incoherent scattering from individual electrons, the frequency spectrum has a gaussian shape. This gaussian form is characteristic of the doppler broadening resulting from the random thermal motions of the electrons and is described by the function

$$S_1(\omega) = e^{-\left[(\omega - \omega_0)/\Omega_1\right]^2} \quad (15)$$

where

$$\Omega_1 = \left[\frac{8 KT}{m_e} \right]^{1/2} \frac{\omega_0}{c} \sin\left(\frac{\epsilon}{2}\right) \quad (16)$$

and where ω_0 and ω are the angular frequencies of the incident and scattered wave, respectively.

It can be readily shown that, for the backscatter case ($\epsilon = 180^\circ$), the spectral bandwidth, Δf , i.e., the limits of the power density spectrum at one-half its maximum value, is given by

$$\Delta f = \frac{3.32}{\lambda_0} \left[\frac{2 KT}{m_e} \right]^{1/2} \quad (17)$$

$$\Delta f = \frac{18.3}{\lambda_0} \sqrt{T} \quad (18)$$

where Δf is in kilocycles, λ_0 is in meters, and T is in degrees Kelvin.

For the case where the wavelength of the radio wave is greater than the Debye length, $\lambda \gg 4\pi \ell_D \sin(\epsilon/2)$, the spectrum is greatly narrowed mainly because its width is, to a large extent, determined by the thermal motion of the ions rather than that of the electrons. According to Fejer⁹, the function describing the spectrum has the form

$$S_{cl}(\omega) = \frac{e^{-x^2}}{4 \left[1 - x e^{-x^2} \int_0^x e^{u^2} du \right]^2 + \pi \left[x e^{-x^2} \right]^2} \quad (19)$$

where

$$x = \frac{\omega - \omega_0}{\Omega_1} \quad (20)$$

The parameter, Ω_1 , is defined by Equation (16) with the exception that the electron mass, m_e , is replaced by m_i , the mass of the positive ion.

The spectral distributions defined by Equations (15) and (19) were derived on the assumption that the plasma consisted of one type of charged positive ions whose temperature was the same as that of the electrons.

An evaluation of Equation (19) reveals that the spectrum is somewhat flat in the region near the transmitted frequency and that it contains two raised shoulders symmetrically located about the center frequency.⁹

It is of interest to note that the "saddle" type spectrum was also theoretically postulated independently by Salpeter⁷ and Dougherty and Farley.⁸

Experimental evidence of a flat-topped shape or a slight dip at the center frequency of incoherent backscatter spectral measurements has been reported by Pineo.²⁵

Laaspere²⁶ has indicated that, for an incident wavelength greater than the Debye length and for a region containing oxygen ions which are at the same temperature as the electrons, the spectral width at the half-power points can be represented, to a first approximation, by the function

$$\Delta f = \frac{0.204}{\lambda_0} \sqrt{T} \quad (21)$$

where λ_0 is the wavelength of the incident wave in meters, f is the bandwidth in kilocycles, and T is the temperature in degrees Kelvin.

Salpeter⁷ has considered the intermediate case where $\lambda = 4\pi l_D \sin(\epsilon/2)$, a condition which could exist at altitudes on the order of 1000 kilometers or higher and at frequencies less than about 500 megacycles. His results for the extreme conditions in which the wavelength is much greater or less than the Debye length compare favorably with those obtained by Fejer,⁹ and Dougherty and Farley.⁸

Fejer⁹ has modified his original theory by removing the restriction of the relationship of the wavelength of the radio wave with the Debye length and also by considering that the ions and electrons in the plasma were at different temperatures.

The backscattered power spectra deduced by Fejer¹⁰ in his revised paper are plotted in Figure 2 as a function of different ratios of electron-to-ion temperature. These curves are applicable to wavelengths which are greater than the Debye length. It is evident that the total integrated scattered power decreases as the ratio of the electron temperature to the ion temperature increases. This effect has also been predicted by Buneman²² as depicted in Figure 1.

The abscissa or relative frequency scale of Figure 2 actually represents the parameters ω_d/Ω_1 , where ω_d is the angular frequency difference between the incident wave and the scattered wave, i.e., the angular doppler frequency shift. The term, Ω_1 , is identical to the expression defined by Equation (16), with the exception that m_e is replaced by the ionic mass m_i , and T is replaced by the ionic temperature, T_i . It should be evident, therefore, that a measure of the spectral bandwidth would be indicative of the temperature of the ions.

For a plasma consisting of oxygen ions, hydrogen ions, and electrons, the spectral shape could vary considerably depending upon the concentration of the ions. According to Fejer,¹⁰ the width of the frequency spectrum decreases quite noticeably as the ratio of the density of the hydrogen ions to the oxygen ions is reduced. This is illustrated in Figure 3, the computations being based on the assumption that the temperature of all the constituents are the same and that the radio wavelength is much greater than the Debye length.

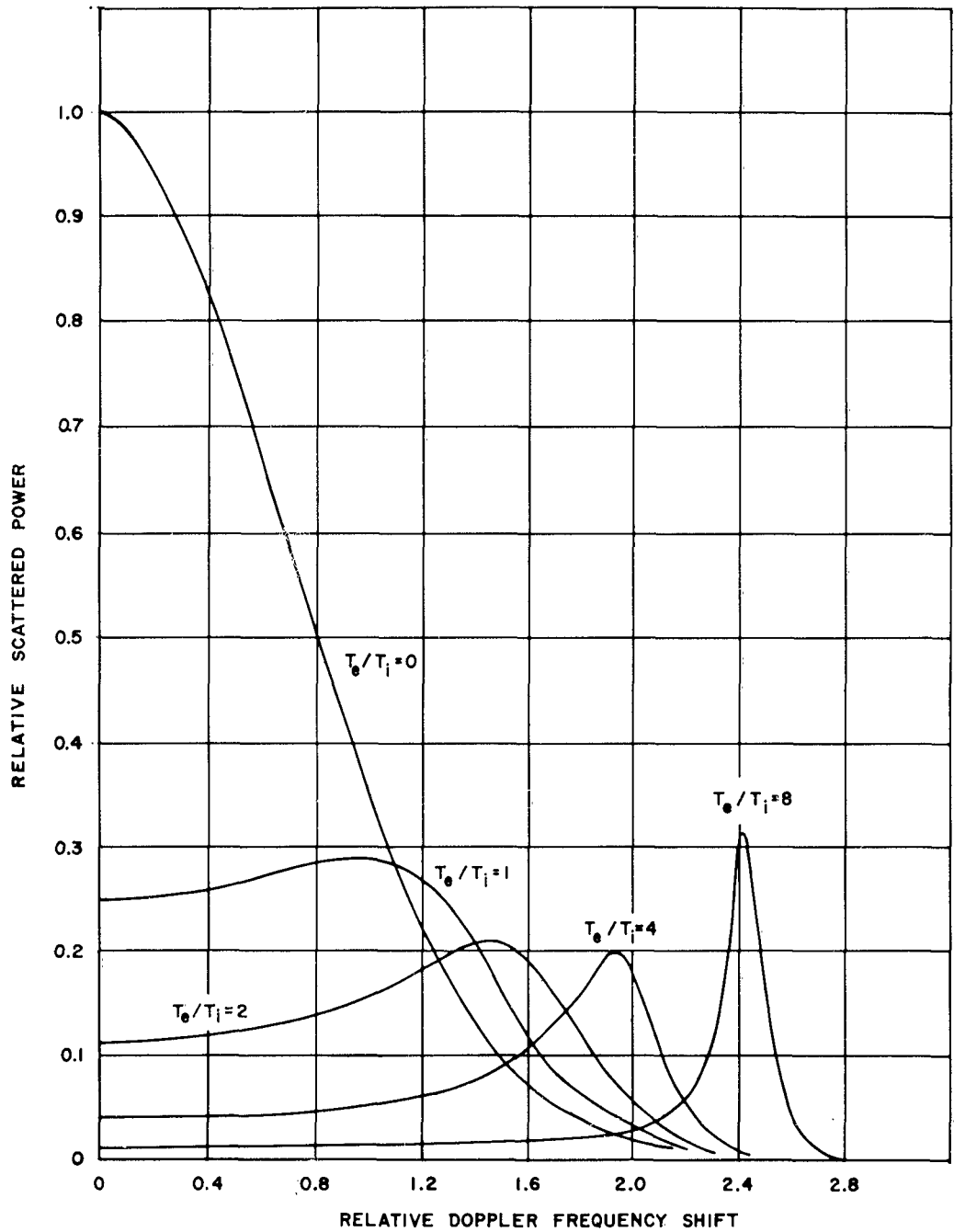


Figure 2. Frequency Spectrum as a Function of Different Electron-to-Ion Temperature Ratios for Wavelengths much Larger than the Debye Length (after Fejer)

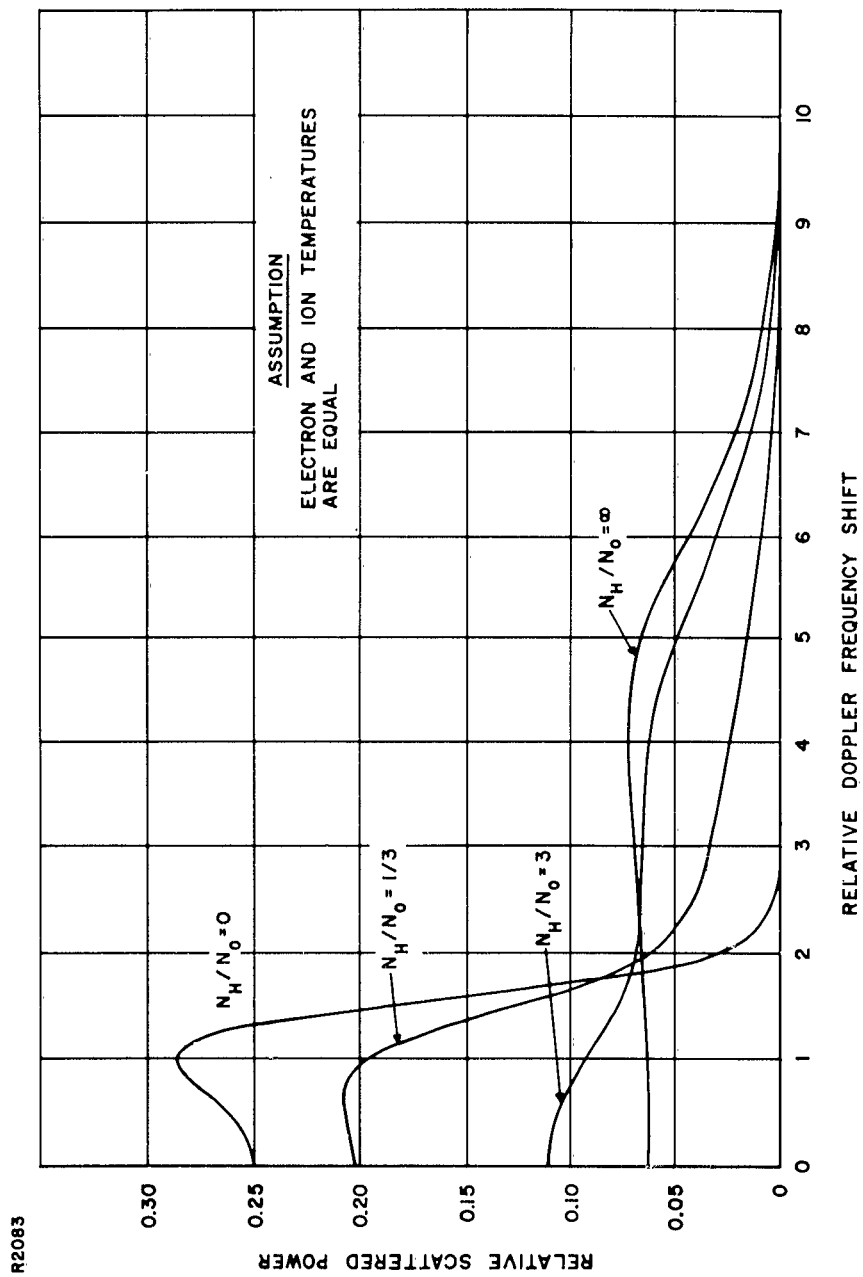


Figure 3. Frequency Spectrum as a Function of the Ratio of Hydrogen Ion-to-Oxygen Ion Density for Wavelengths much Larger than the Debye Length (after Fejer)

Changes in both the spectral width and shape from daytime to nighttime which seemed to correlate with changes in the scale height above the F-layer maximum have been observed by Pineo.²⁷ The nighttime spectral widths and topside scale heights were both less than those measured during the midday hours. In addition, he noted that the values of the scattering cross section were smallest near sunrise and greatest near midnight.

Based on Fejer's¹⁰ and Buneman's²² theories, the difference in the scattering cross section implies that the nighttime ratio of electron-to-ion temperature is less than the presunrise value. Pineo's²⁷ spectral data also indicate that the temperature ratio was smallest during the nighttime. A cursory examination of both the spectral and cross section measurements reveals the existence of a diurnal variation in the ratio of the temperature of the electrons to that of the ions.

b. Particle Collisions Present

The effect of particle collisions on the frequency spectrum of scattered radiation has been theoretically investigated by Fejer.⁹ He showed that for equal electron and ion temperatures and $\lambda \ll 4\pi \ell_D \sin(\epsilon/2)$, i.e., the incoherent scattering results from the random thermal motion of the electrons, the spectral distribution can be described by the function

$$S_2(\omega) = \frac{1}{\left[1 - \left[\frac{\omega - \omega_0}{\Omega_2} \right]^2 \right]} \quad (22)$$

where

$$\Omega_2 = \frac{4 D_e \omega_0^2}{c^2} \sin^2 \left[\frac{\epsilon}{2} \right] \quad (23)$$

The coefficient of diffusion of the electrons, D_e , is expressed by

$$D_e = \frac{KT}{m_e \nu_e} \quad (24)$$

where ν_e is the collision frequency of the electrons with neutral and other particles.

The electron collisions are effective and should be taken into account in determining the scattered spectrum⁹ when $\lambda \gg \pi^2 \ell_{me} \sin(\epsilon/2)$, where ℓ_{me} , the mean free path of the electrons, is given by

$$\ell_{me} = \frac{1}{\nu_e} \left[\frac{8 KT}{\pi m_e} \right]^{1/2} \quad (25)$$

A comparison of the frequency spectrums defined by Equation (15), which is valid for $\lambda \ll \pi^2 \ell_{me} \sin(\epsilon/2)$, and Equation (22) reveals that, for wavelengths much less than the Debye length, the presence of electron collisions, in effect, decreases the spectral width of the scattered radiation.

When $\lambda \gg 4\pi \ell_D \sin(\epsilon/2)$, i.e., the random thermal motion of the ions is the influencing factor which determines the characteristics of the scattered spectrum, the relationship describing the spectral distribution for the collision case is written in the form

$$S_{c2}(\omega) = \frac{1}{\left[4 + \left[\frac{\omega - \omega_0}{\Omega_2} \right]^2 \right]} \quad (26)$$

This expression, as derived by Fejer,⁹ is applicable to high frequency collisions which satisfy the condition, $\lambda \gg \pi^2 \ell_{mi} \sin(\epsilon/2)$, where ℓ_{mi} is the mean free path of the ions.

The parameter, Ω_2 , defined by Equation (23), must be modified to include the coefficient of diffusion of the ions, D_i , instead of the electron diffusion coefficient, D_e . In addition, for both Equations (24) and (25), the electron collision frequency and mass are replaced by the collision frequency of the ions, ν_i , and the ion mass, m_i , respectively.

It is noted that, for wavelengths greater than the Debye length and $\lambda \ll \pi^2 \ell_{mi} \sin(\epsilon/2)$, the frequency spectrum is given by the function, $S_{cl}(\omega)$, defined by Equation (19).

3. In the Presence of an External Magnetic Field

The effects of an external magnetic field on the characteristics of the frequency spectrum of incoherent scatter were qualitatively considered by Bowles.³ He predicted that, for ionospheric incoherent scattering, the earth's magnetic field

would have little influence on spectral distribution for ordinary radar transmission frequencies, except when the direction of propagation is approximately perpendicular to the lines of force of the field. Bowles³ postulated that, near perpendicularity, and at wavelengths greater than the Debye length, the spectrum should develop toward a line spectrum with sharp resonance peaks at the gyrofrequencies of the ions and peaks at all the harmonics of this frequency.

More complete theoretical investigations of the effects of the earth's magnetic field on the scattered frequency spectrum have been performed by Fejer,¹⁰ Renau, Camnitz and Flood,¹² Laaspere,¹³ Hagfors,¹⁴ and Farley, Dougherty and Barron.²³

Laaspere¹³ has analyzed the case in which the electrostatic interactions between the charged particles are negligible or, in other words, the influence of the ions is insignificant. This condition would apply for incoherent scatter at wavelengths which are much smaller than the Debye length, i.e., $\lambda \ll 4\pi \ell_D \sin(\epsilon/2)$. His results disclose that, when the propagation direction is perpendicular to the magnetic field lines, the frequency spectrum is composed of lines which are symmetrically located about the transmitted frequency at multiples of the gyromagnetic frequency of the electrons. In other words, the spectrum can be described by the relationship

$$f = f_o \pm n f_H \quad (27)$$

where f_o is the transmitted frequency, n is an integer, and f_H is the electron gyromagnetic frequency which is given in gaussian units by

$$f_H = \frac{H e}{2\pi m_e c} \quad (28)$$

where H is the intensity of the earth's magnetic field. The other parameters, e , m_e and c , have been previously defined.

It should be mentioned that the presence of a line spectrum would be applicable to backscatter occurring at great altitudes, i.e., 1000 to 3000 kilometers above the earth's surface, and for frequencies in the microwave region.

The envelope of the line spectrum, according to Laaspere,¹³ is found to approximate the gaussian doppler shift spectrum which would normally exist in the absence of a magnetic field. This characteristic is evident for wavelengths that are small compared to the radius of gyration of the electrons, R_e , defined by

$$R_e = \left[\frac{2 KT}{m_e} \right]^{1/2} \left[\frac{m_e c}{H e} \right] \quad (29)$$

The first term in this expression is the most probable velocity which the electrons could attain based on the assumption that their velocities are Maxwellian distributed. The second term is the inverse of the angular gyromagnetic frequency of the electrons.

Laaspere¹³ showed that, as the angle between the wave vector and the magnetic lines of force is decreased, the line spectrum becomes somewhat smeared and tends to approach the gaussian shaped curve obtained for the nonmagnetic field case.

The magnetic field effects for wavelengths larger than the Debye length, i.e., $\lambda \gg 4\pi l_D \sin(\epsilon/2)$, have been analyzed by Hagfors¹⁴ and Farley, Dougherty and Barron.²³ While the two approaches to the solution of the problem are decidedly different, their final results are compatible.

Hagfors's¹⁴ work is concerned with the fluctuation in the density of electrons in a plasma containing an arbitrary number of one type of ions and takes into account the effect of two-body collisions. In the case of the ionosphere and neglecting the collisions of the constituents, the frequency spectra are not influenced by the magnetic field except for density fluctuations which are approximately perpendicular to the magnetic field lines.

Buneman¹⁵ has extended Hagfors's¹⁴ theory by introducing the assumption that the plasma is comprised of several species of ions. For a plasma containing an equal mixture of singly charged oxygen and hydrogen ions, the computed spectrum revealed the presence of the oxygen and hydrogen gyrofrequency resonances, the latter being the more predominant.

A typical example illustrating the effect of the orientation of the magnetic field on the spectral density function is shown in Figure 4. These data, which are a composite of the theoretical calculations by Farley, Dougherty and Barron,²³ apply to a transmission frequency of 40 megacycles incident on a plasma whose kinetic temperature is 1500°K, plasma frequency is one megacycle, and ionic constituents are oxygen ions.

It is seen that when the propagation angle, θ (the angle between the directions of propagation and the lines of force of the magnetic field), is 87°, the

R2084

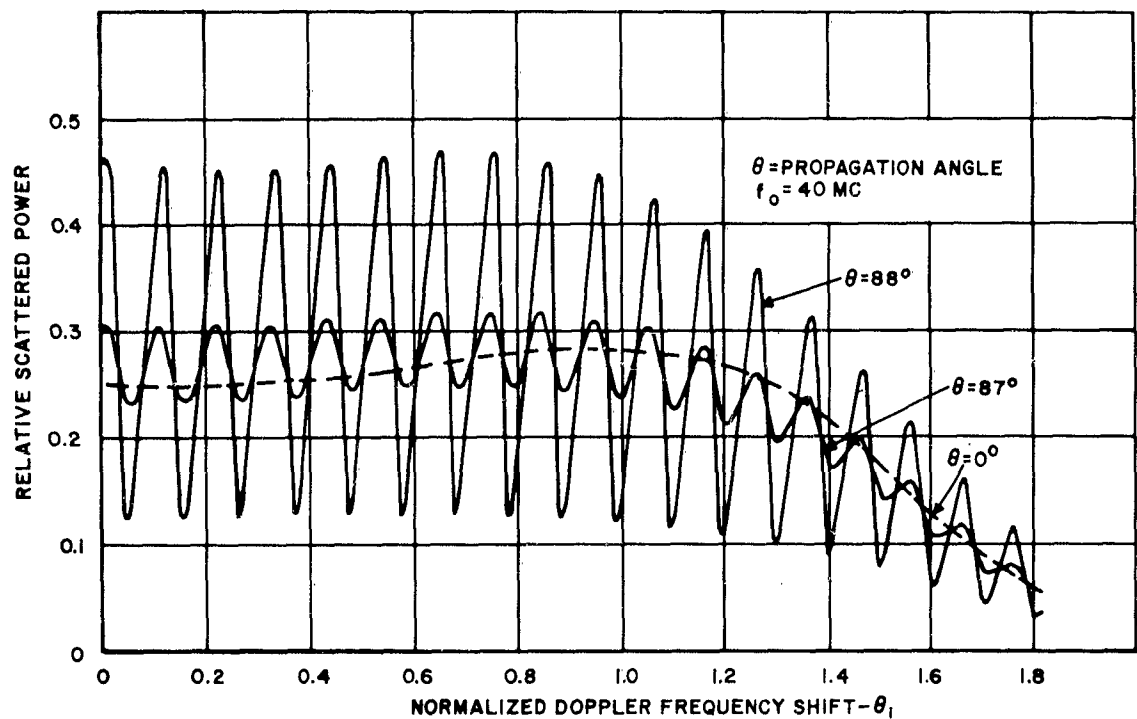


Figure 4. Frequency Spectrum as a Function of the Propagation Angle Near Perpendicularity for Wavelengths much Larger than the Debye Length (after Farley, Dougherty and Barron)

scattered spectrum consists of an oscillatory function which closely approximates the spectral curve for the nonmagnetic field case shown by the dashed curve. When θ is increased slightly, the amplitude of oscillation becomes greatly enhanced.

According to Farley, Dougherty and Barron,²³ whose scattering theory is derived utilizing a generalized version of Nyquist's noise theorem, near perpendicularity the resonance peaks should occur at approximately

$$\theta_{i,n} = n \Phi_i \left[1 + \frac{\Phi_i}{\sqrt{\pi}} \right] \quad (30)$$

where θ_i is the normalized doppler frequency shift given by

$$\theta_i = \frac{\omega_d \lambda_o}{4\pi} \left[\frac{m_i}{2 KT} \right]^{1/2} \quad (31)$$

and Φ_i is the normalized angular gyromagnetic frequency of the ions defined by

$$\Phi_i = \frac{\lambda_o H e}{4\pi m_i c} \left[\frac{m_i}{2 KT} \right]^{1/2} \quad (32)$$

The term, λ_o , is the wavelength of the transmitted radiation while ω_d is the angular doppler shifted frequency. Since the mass of the oxygen ion, m_i , is about 2.66×10^{-23} gram, and assuming the values of the parameters on which Figure 4 is based, it follows that for this particular example, the resonance peaks are at a frequency

$$\theta_{i,n} = 0.108 n \quad (33)$$

where n is an integer.

In general, for small Debye lengths, the frequency spectrum of the scattered radiation is influenced by the magnetic field only if the angle between the propagation direction and the perpendicular to the magnetic field is within about $\Phi_i/2$ radian.²³ At 425 megacycles and normal ionospheric conditions, the off-perpendicular angle would have to be less than approximately 0.3° .

When the direction of propagation deviates from orthogonality with the magnetic field, the power per unit bandwidth of the spectrum decreases. This is evident from Figure 5, which is derived by Renau, Camnitz and Flood¹² on the assumption that the doppler frequency shift of the backscattered radiation is zero and the incident wavelength is much larger than both the Debye length and the ion gyroradius.

R2085

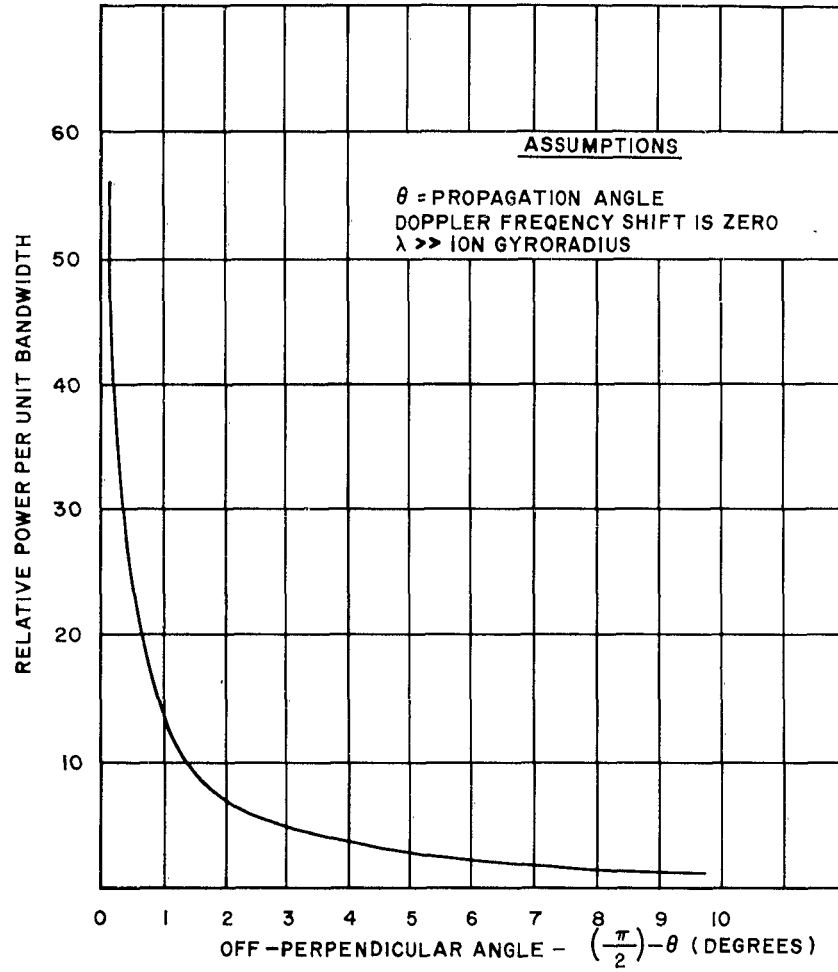


Figure 5. Relative Power as a Function of Off-Perpendicular Angle for Wavelengths much Larger than the Debye Length (after Renau, Camnitz and Flood)

Renau, Camnitz and Flood's¹² analytical treatment is based also on the generalized Nyquist theorem similar to that employed by Farley, Dougherty and Barron.²³

With regard to experimental verification of the affect of the earth's magnetic field on the spectral characteristics of incoherent scatter, Pineo's²⁵ analysis of the doppler frequency measurements conducted at 425 megacycles at the United States Air Force Trinidad Test Site early in the winter of 1961 indicates that the spectral width decreases quite noticeably when the direction of propagation is perpendicular to the magnetic field line. As depicted in Figure 6, the half-power width observed from scattering taking place at F-layer heights is on the order of 12 kilocycles.²⁵ When the angle between the antenna beam axis and the magnetic field lines approaches 90°, there is a marked decrease in the spectral width to about six kilocycles.

According to Pineo,^{24,28} the greatest variation in the spectral spread appears to take place in the region where the angle of incidence changes from perpendicular to $\pm 2^\circ$ off perpendicular. This is evident in Figure 7, which is a plot of the doppler bandwidth as a function of the angle off-perpendicularity.²⁸ These measurements were also made at 425 megacycles at the United States Air Force Trinidad Test Site with the antenna beam axis oriented at an elevation angle of 41° and at 0° azimuth angle. The determination of the aspect angle of the magnetic field was accomplished by the method discussed in Section IV.

It is noted that the spectrum attains a minimum half-power width of approximately six kilocycles within $\pm 0.25^\circ$ from orthogonality and that there is a marked transition of spectral widths through the height of normal incidence which occurs at about 330 kilometers. It would appear that any changes in the orientation of the magnetic field, possibly brought about by a severe magnetic disturbance, could perhaps be detected from such spectral observations.

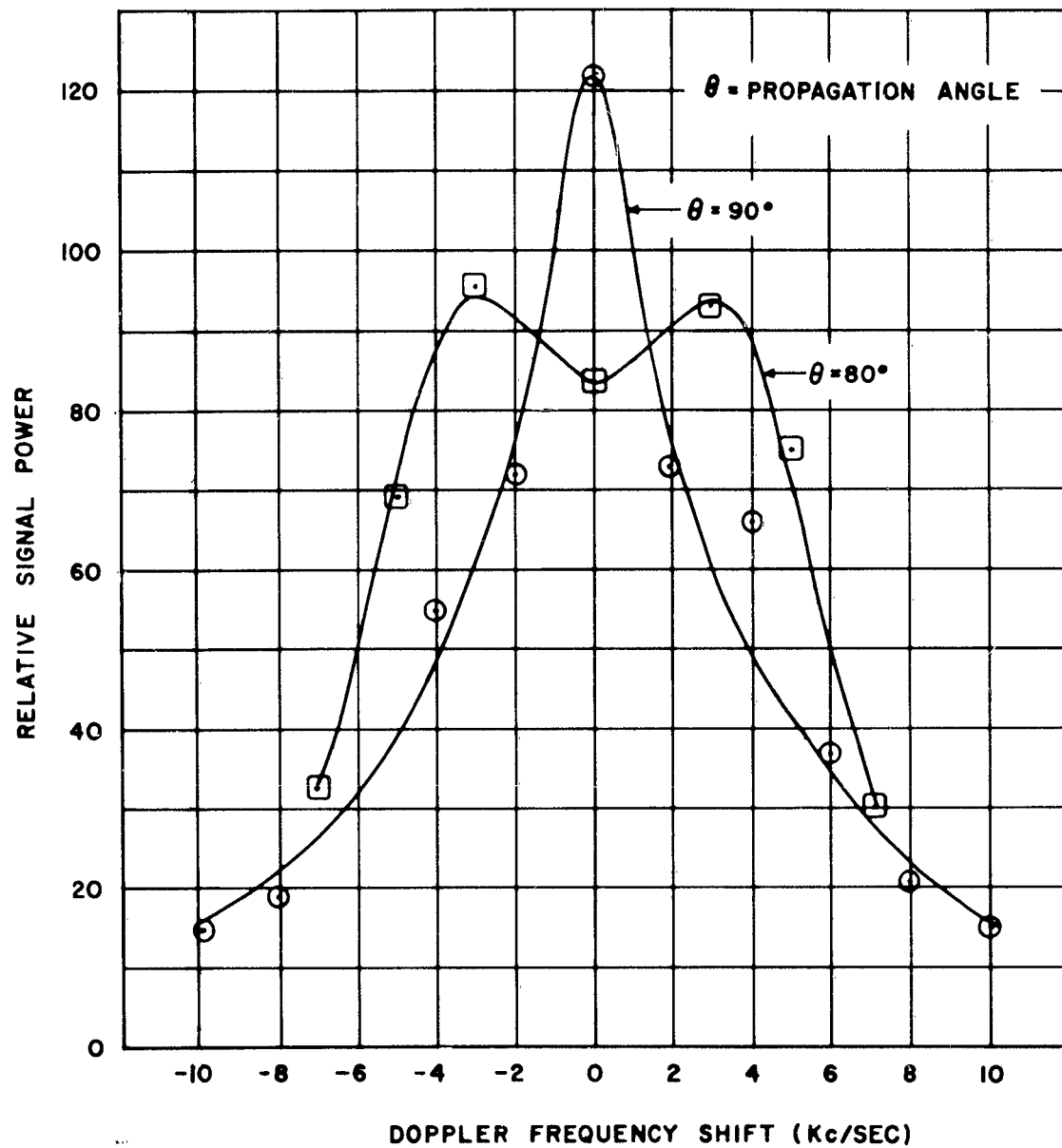


Figure 6. Effect of the Earth's Magnetic Field on the Spectrum of Incoherent Backscatter Observed at 425 Megacycles at Trinidad, 26 January 1961 (after Pineo, Kraft, Briscoe and Hynek)

R2087

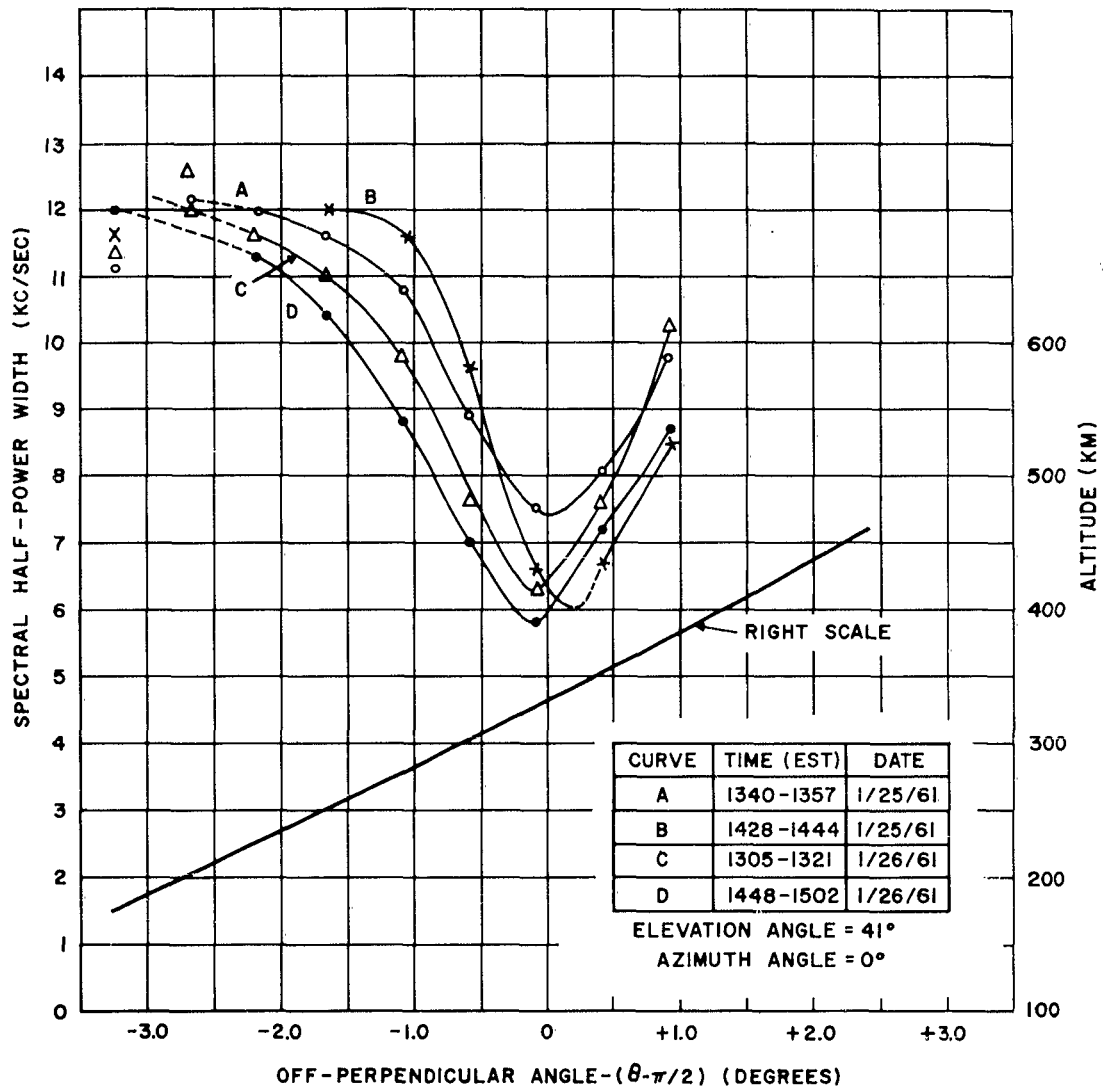


Figure 7. Spectral Bandwidth of Incoherent Backscatter as a Function of Off-Perpendicular Angle for Observations Taken at 425 Megacycles at Trinidad (after Pineo and Hynek)

III. APPLICATION OF THE INCOHERENT SCATTER TECHNIQUE FOR PROBING THE EARTH'S ATMOSPHERE

A. INTRODUCTION

Experimental investigations of the characteristics of the ionosphere have to a great extent been accomplished, prior to the development of space vehicles, by ground-based active and passive radio systems.

Vertical incidence sweep frequency pulsed sounders have been employed to render electron density profiles up to the maximum ionization level of the F-layer. Fixed frequency sounders, on the other hand, have generally been used in the study of such phenomena as ionospheric absorption, and also ionospheric turbulence and wind movements, the latter being performed by the three-spaced receiver technique.²⁹ The data deduced from the fixed frequency sounder measurements reveals only the physical status of the ionosphere in the region below the peak of the F-layer.

The passive monitoring of the radiation emitted from radio stars has been a useful technique for investigating the irregularities of electron density in the ionosphere. However, the level of the irregularities which cause the comparatively constant extraterrestrial signals impinging on the earth's surface to fluctuate in a random manner has still not been definitely established.

With the availability of rockets and satellites, the state of knowledge of the structure and composition of the ionosphere has been greatly enhanced.

Radio wave transmissions originating from these vehicles and recorded at the ground have yielded such data as the electron density distribution above the F-layer maximum,³⁰⁻³⁴ the integrated electron density along the transmission path,³³⁻³⁷ the dynamics,³⁸ and temperature³⁹ of the ionosphere, and the intensity of the earth's magnetic field.⁴⁰

From radar signals reflected off the surface of the moon⁴¹ and spherical satellites,⁴² and undergoing Faraday rotation fades, the electron content in the ionosphere has been readily inferred.

The development of high powered sensitive radar systems has opened a new technological approach for studying the properties of the ionosphere, since it has made possible the detection of the electromagnetic waves incoherently scattered by the free electrons in the ionosphere.

The scientific data that can be deduced from incoherent scatter measurements are discussed in this section.

B. INCOHERENT SCATTER POWER MEASUREMENTS

1. Electron Density Distribution

A unique method for determining the electron density distribution in the atmosphere is the incoherent backscatter technique. Since the radiation scattered by the free electrons in the ionosphere and received at a radar antenna is directly proportional to the number of electrons in a unit volume at the particular point in space (see Equations (5) and (12)), the intensity of the incoherent signal as a function of radar range is therefore representative of the distribution of electron density along the propagation path. The conversion into a relative electron density profile is accomplished by multiplying the signal intensity by the square of the radar range to the scattering volume.

The relative electron density scale can be readily calibrated into an absolute measurement by adjusting its maximum value to the maximum ionization density deduced from vertical incidence ionospheric sweep frequency soundings which should be recorded at approximately the same time and in the near vicinity of the incoherent scatter measurements.

It should be noted that the calibration adjustment is required when the incoherent backscatter observations are made with circular polarization both on transmission and reception. When linear polarization is employed on transmission and the backscattered signal is received simultaneously on the transmitted and the orthogonal polarization, the ionosonde data adjustment is not necessary. The Faraday rotation phenomenon which the scattered linear wave encounters in its passage through the ionosphere should provide the calibration scale factor for converting the relative electron density distribution into an absolute measurement. The application of the Faraday effect to the incoherent scattering problem is more fully discussed in the next section.

2. Ionospheric Movements

For radar observations conducted with the antenna beam axis oriented in a fixed azimuth-elevation position, it is possible to detect movements and turbulence in the ionization if the intensity of the incoherent backscatter return is somewhat intense to warrant little signal integration. The desired information can

be acquired from the electron density-versus-time plots at fixed radar range increments and also from range-versus-time film recordings of incoherent echoes. The latter method has been used at the United States Air Force Trinidad Test Site in the detection of radial motions of ionization ranging as high as one to six kilometers per second.

An examination of Trinidad range-versus-time film records, samples of which are presented in Section V, definitely confirm that the resolution of the regions in space in which ionospheric movements are taking place can be attained by employing linear polarization in conjunction with the Faraday phenomenon.

It should be mentioned that spatial resolution can also be achieved, in the case of the electron density-versus-time plots, by the use of short pulse lengths. This is applicable when the incoherent scatter signal requires a minimum of integration.

3. Electron-to-Ion Temperature Ratio

It may be possible to determine the variation of the ratio of the electron temperature to the ion temperature from the backscattered signal intensity. This necessitates that the radar system be calibrated with great accuracy at periodic intervals of time throughout an experimental measurement program. It is believed that a system calibration accuracy of ± 2 db is feasible within the present state of the art.

Since the total scattering cross section of a plasma, as determined by Buneman,²² is directly proportional to the scattering coefficient of a single free electron, the electron density, and the temperature-ratio function (see Equation (14)), an absolute measurement of the received incoherent scattered power and the true height distribution of electron density adjusted from ionospheric soundings should enable the ratio of the electron-to-ion temperature to be computed.

4. The Earth's Magnetic Field

The phenomenon of Faraday rotation can be applied to the study of the earth's magnetic field. In order to perform this measurement, the transmitted signal must be linearly polarized while the scattered signal must be received simultaneously on two linear orthogonal polarization channels. The relative signal amplitudes in the two channels are a measure of the rotation of the plane of polarization that the wave encounters in the ionosphere.

Since the amount of Faraday rotation is a function of the integrated product of the electron density and the intensity and orientation of the magnetic field, it is possible to relate the polarization angle to the elements of the magnetic field for a given distribution of electron density. It should be noted that the electron density distribution is determined independently from the total power measurement, i.e., the summation of the signal strengths in the two receiver channels.

It is possible that the existence of any major variations in the earth's magnetic field accompanying severe magnetic disturbances could perhaps be detectable by means of the incoherent backscatter Faraday rotation technique.

Inasmuch as the parameters of the magnetic field, such as the intensity and the inclination and declination angles, vary slightly with height above a given location on the earth's surface, the experimental observations should be performed for propagation directed near the zenith.

A complete mathematical formulation of this subject is contained in Section IV.

5. Exploration of Ionization in Space and Planetary Atmospheres

In experimental studies of the ionosphere by the radar-lunar technique,^{41,43} the radar data may be difficult to analyze because of the ambiguity in the number of angular rotations of the wave encountered when only one frequency is used on transmission. The incoherent backscatter displaying the Faraday effect is one scheme which may be employed for resolving the polarization ambiguity problem since the contribution of the discernible ionosphere to the polarization rotation can be made known.

The difference in the rotation angle observed with lunar reflections and incoherent scattering could then be attributed to the polarization rotation taking place in the region bounded by the maximum scattering height and the lunar surface. This would infer the presence of ionization in outer space.

Similarly, this same process can be applied to the investigation of the existence of an ionized atmosphere and also a magnetic field surrounding the neighboring planets, Venus and Mars.

C. INCOHERENT SCATTER SPECTRAL MEASUREMENTS

1. Electron and Ion Temperature

The doppler frequency shift of ionospheric incoherent scattered radiation is caused by the thermal velocity of the particles present in the medium, the particle velocity being determined by its kinetic temperature and its mass (see Equation (29)).

For incoherent scattering conducted in a direction which is not normal to the earth's magnetic field and at frequencies in the VHF and UHF band, the spectral bandwidth is a measure of the temperature of the ions while at microwave frequencies and for the normal ionosphere, it is directly related to the temperature of the electrons.

Since the spectral shape at centimeter wavelength and above is a function of the ratio of the electron-to-ion temperature, it should, therefore, be possible to determine from the frequency spectrum, when the ionic species, mass and height distribution are known, the temperature of both the electrons and ions as a function of height. It should be recalled that the electron-ion temperature ratio can also be deduced independently from the signal power measurement.²²

2. Ionic Constituents

From the spectral distribution obtained at the long wavelengths when the direction of propagation is approximately perpendicular to the direction of the earth's magnetic field, information on the ionic constituents present in the ionosphere can be evaluated. For example, since the frequencies of the resonant peaks appearing in the line spectra are approximately equal to the gyromagnetic frequency of the ions and its harmonics, the ionic mass can be readily derived. For a medium containing several ionic components, periodic lines would appear in the spectrum which would correspond to the gyromagnetic frequency of the individual type of ion.

When the propagation direction is not perpendicular to the magnetic field, supplementary data concerning the ionic constituents can be obtained. The ratio of the densities of the various ionic particles existing in the plasma can be estimated from the spectral shape.¹⁰ Inasmuch as the spectral shape is also controlled by the temperature of the electrons and ions,¹⁰ these parameters must be known before the ionic density ratio can be specified.

3. Earth's Magnetic Field

The characteristics of the earth's magnetic field can be studied from the frequency spectrum associated with the incoherent scattering of electromagnetic waves occurring at normal incidence to the field.

At millimeter wavelengths, the spectrum is composed of lines which are at multiples of the gyromagnetic frequency of the electron. Thus, it follows that, for each spectrum corresponding to a given height increment, the magnetic field intensity can be calculated from any frequency line. In practice, however, this measurement does not appear feasible in this frequency range because of the unavailability of extremely sensitive radar systems which are required for detecting the scattered radiation.

On the other hand, at the long wavelengths, the ion gyromagnetic frequency line spectrum can be processed to yield the magnetic field strength when the height distribution of the ionic components are known. It should, therefore, be readily possible to determine the effect of a magnetic storm on the earth's magnetic field intensity by comparing the frequencies of the line spectra prior to and during such a disturbance.

The spectrum, which does not show the individual gyrofrequency lines of the ions because of smearing resulting from insufficient frequency resolution, can still be used for magnetic field investigations. Since the half-power doppler bandwidth of such a spectrum is a minimum at perpendicularity,²⁸ variations in the orientation of the magnetic field accompanying a magnetic disturbance should be detectable from the spectral width-versus-off perpendicular angle function obtained under normal and perturbed conditions.

IV. IONOSPHERIC FARADAY EFFECT

A. INTRODUCTION

When a linearly polarized electromagnetic wave enters an ionized medium in the presence of an external magnetic field, such as encountered in the ionosphere, the wave separates into two independent components, both, in the general case, elliptically polarized with opposite senses of rotation. For frequencies in the UHF range, the two components are circularly polarized.

As the ionosphere is traversed, the two waves progress with different velocities of propagation which result in the phase relationship between them to be continuously changing. On leaving the ionosphere, the circularly polarized components recombine to form a linearly polarized wave which is rotated with respect to the original linear wave.

In this section, this phenomenon, which is commonly referred to as the Faraday effect, is discussed with application to the study of the earth's magnetic field by means of incoherent scattering and to the calibration of the relative electron density distribution available from the incoherent scatter power measurements.

B. ANGULAR POLARIZATION ROTATION

The amount of angular rotation experienced by a linearly polarized wave traversing a two-way path in the ionosphere can be represented by the relationship⁴⁴

$$\phi = \frac{4.7233 \times 10^4}{f_o^2} \int_0^h f(h) H \cos \theta N_e dh \quad (34)$$

where ϕ is the rotation in radians, f_o is the transmission frequency in cycles per second, H is the magnetic field intensity in gauss, N_e is the electron density in electrons per cubic centimeter, dh is the height differential in centimeters, and θ is the propagation angle, i.e., the angle between the direction of the earth's magnetic lines of force and the direction of electromagnetic propagation.

The function, $f(h)$, which is basically the secant of the angle between the ray path and the zenith, is given by

$$f(h) = \frac{r_o + h}{\left[(r_o + h)^2 - (r_o \cos E)^2 \right]^{1/2}} \quad (35)$$

where r_0 is the radius of the earth and E is the elevation angle of the antenna beam.

Equation (34) is representative of the quasi-longitudinal mode of propagation. For frequencies in the 425 megacycles range, this relationship is valid for $0^\circ \leq \theta \leq 89^\circ$.

It can be shown⁴⁵ that

$$\theta = \cos^{-1} \left[-\cos e \sin I - \sin e \cos I \cos (\gamma - D) \right] \quad (36)$$

where I and D are the magnetic inclination and declination angles, respectively. These parameters specify the direction of the total magnetic intensity vector in space.

The angle, γ , is the geographic azimuth bearing of the observer's location measured with respect to the subionospheric point, i.e., the location on the earth's surface directly underneath the particular point in space. The angle, e , is simply given by

$$e = \sin^{-1} \left[\frac{r_0}{r_0 + h} \cos E \right] \quad (37)$$

where h is the height of the point in space above the earth's surface.

The technique employed in evaluating H and θ in this report is as follows: the parameters, H , I and D , have been scaled in 2.5° and 5.0° latitude and longitude steps over the entire surface of the earth from isomagnetic maps issued by the U.S. Navy Hydrographic Office and the Canadian Department of Mines and Technical Surveys. The ground observed magnetic data, scaled from these maps, are stored in matrix form in an IBM-7090 digital computer. Linear interpolation is used for obtaining the values of the magnetic field elements at other geographic locations.

For propagation through the ionosphere, the angles I and D at the subionospheric point are assumed to be invariant at all heights. The magnetic field intensity at the point in space, on the other hand, is derived from the surface value which is assumed to decrease inversely as the cube of the distance from the earth's center.

It is believed that this method for determining H and θ is far more accurate than that obtained by assuming a dipole model for the earth's magnetic field. The evaluation of the magnetic field elements based on spherical harmonic expansion^{46,47} is another method which could be employed. However, utilization of such a sophisticated technique is believed not warranted in the Faraday rotation problem.

The value of the function, $f(h) H \cos \theta$, contained in Equation (34) is plotted in Figure 8, as a function of height for various azimuth-elevation directions as viewed from Trinidad. It is evident that, at low elevation angles oriented towards the south in the direction of Bogota, Colombia (240° azimuth), and towards the north in the direction of Puerto Rico (327° azimuth), the function varies over quite a wide range. As the elevation angle is increased, there is a noticeable reduction in the spread of its value with height.

In the theoretical computation of the magnitude of the Faraday rotation, the electron density distribution deduced from ionosonde data can be employed. Since vertical incidence sweep frequency sounders are capable of yielding only the characteristics of the ionosphere up to the height of maximum ionization of the F-layer, it is necessary to postulate a model above this region. As a first approximation, it can be assumed that, above the F-layer maximum, the distribution of electron density with height (under equilibrium conditions) follows a Chapman model of the form

$$N_e = N_m e^{1/2 \left[1 - (h-h_m)/H - e^{-(h-h_m)/H} \right]} \quad (38)$$

where N_m is the electron density at the level of maximum ionization, h_m , and H is the scale height of the neutral particles. In this study, a constant scale height of 80 kilometers is assumed for all the electron density distribution above the F region.

C. MAGNETIC FIELD MEASUREMENTS BY INCOHERENT SCATTER-FARADAY ROTATION PHENOMENON

The Faraday effect when employed in conjunction with ionospheric incoherent scattering can be applied to the study of the characteristics of the earth's magnetic field.

In order to simplify the analysis of the data resulting from this type of an investigation, the incoherent scatter observations should be performed at high elevation angles.

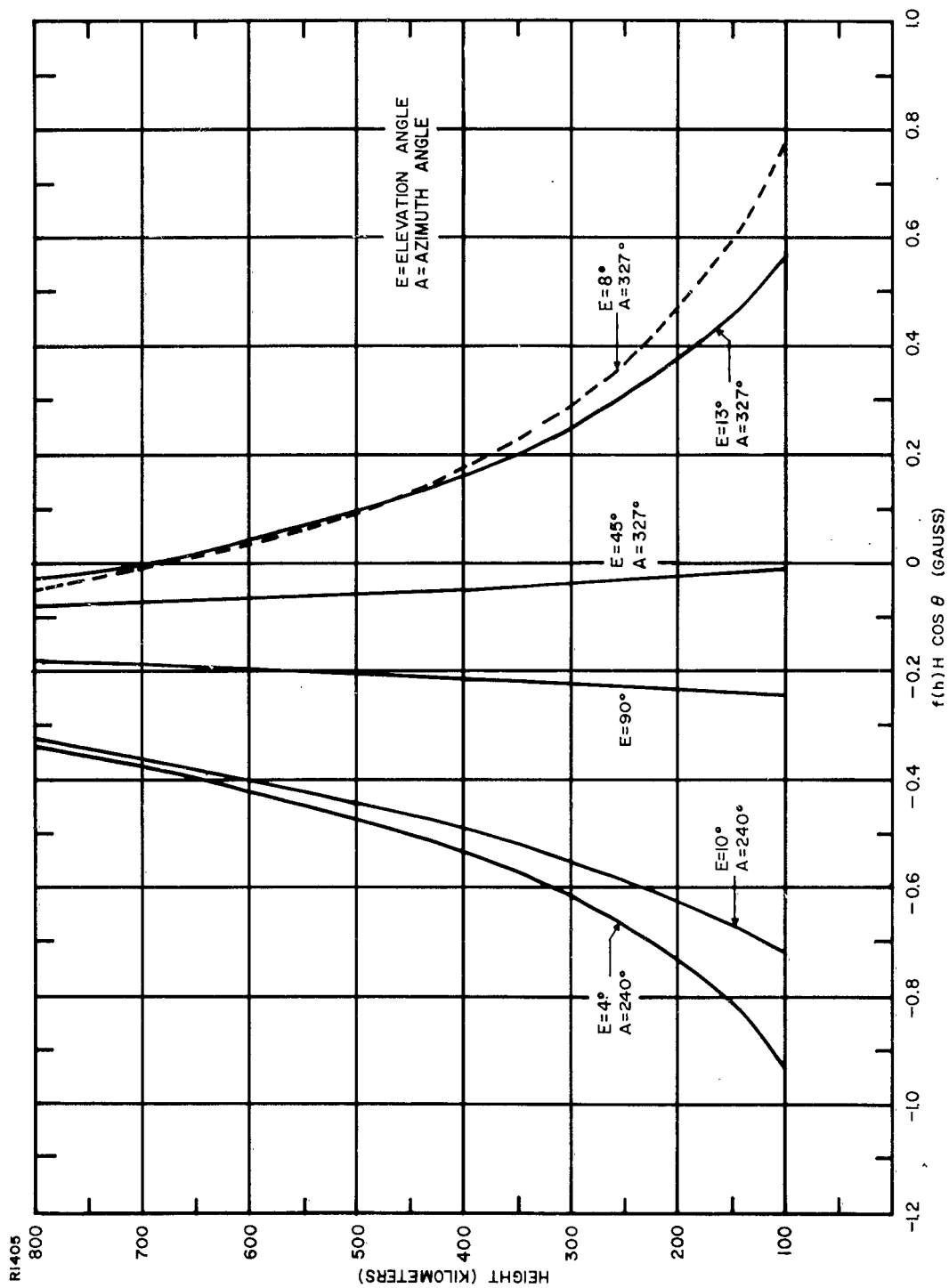


Figure 8. The Function, $f(h) H \cos \theta$, as Viewed from Trinidad

According to Equations (35), (36) and (37), it is seen that, at vertical incidence, the function, $f(h)$, reduces to unity and that

$$\cos \theta = - \sin I \quad (39)$$

It should be noted that the inclination or dip angle, I , is measured positive downward from the horizontal component of the magnetic field.

On substituting Equation (39) in Equation (34), it is found that the magnitude of the angular rotation reduces to

$$\phi = \frac{4.7233 \times 10^4}{f_o^2} \int_0^h H \sin I N_e dh \quad (40)$$

Since the inclination angle and the intensity of the earth's field vary slightly within small intervals of height,⁴⁸ it is valid to rewrite this relationship in terms of

$$\phi_{i,j} = \frac{4.7233 \times 10^4}{f_o^2} \overline{[H \sin I]_{h_i}^{h_j}} \int_{h_i}^{h_j} N_e dh \quad (41)$$

where $\overline{[H \sin I]_{h_i}^{h_j}}$ is the mean value of the function, $H \sin I$, between the height increment, h_i and h_j , while $\phi_{i,j}$ is the rotation occurring within that interval.

The integrated electron density, defined by the integral, can be obtained from the summation of the range-normalized signal intensities detected in the two orthogonal receiver channels. The calibration of these data can be achieved by adjusting the scale of the resultant electron density profile with the distribution deduced from vertical incidence ionospheric sounders recorded in the vicinity of the incoherent scatter measurements.

Inasmuch as the rotation between fixed height intervals is readily measurable from the signal amplitudes in each channel, it, therefore, follows that

$\overline{[H \sin I]_{h_i}^{h_j}}$ can be resolved as a function of height.

The effect of a magnetic disturbance on the field components can be estimated by taking into account the differential changes in the parameters contained in Equation (41).

It can be shown that the variations in the elements of the magnetic field can be described by the function

$$\delta \left[H \sin I \right]_{h_i}^{h_j} = \frac{f_o^2}{4.7233 \times 10^4} \delta \phi_{i,j} - \frac{\left[H \sin I \right]_{h_i}^{h_j} \delta \int_{h_i}^{h_j} N_e dh}{\int_{h_i}^{h_j} N_e dh} \quad (42)$$

The angular rotation and the electron content can both be experimentally measured by independent means and, hence, a significant change in the magnitude of these quantities which should be detectable implies an alteration in the mean value of $H \sin I$. It is of interest to note that this term is, in essence, the vertical component of the magnetic field. Correlation of the incoherent scatter Faraday rotation data with magnetometer recordings of the magnetic field made at the earth's surface should provide extremely valuable information on the characteristic of the geomagnetic field.

D. CALIBRATION OF THE RELATIVE ELECTRON DENSITY PROFILE

The signal intensity of ionospheric incoherent scattered radiation is proportional to the distribution of the electron density along the scatter path. The conversion into an absolute measurement of the electron density can be performed by utilizing linear polarization both on transmission and reception so that the angular rotation of the plane of polarization brought about by the Faraday effect can be resolvable.

According to Equation (41), it is seen that, for a given measured angular rotation, $\phi_{i,j}$, the electron content in a vertical height increment, h_i and h_j , is specifiable. This is contingent on the magnetic field intensity and inclination angle being known, to a first approximation, as a function of altitude.

Once the integral of Equation (41) is evaluated, the relative electron density distribution obtained from the power measurement, i.e., the sum of the

range-normalized signals received in the two orthogonal channels, can then be adjusted to a calibrated scale.

In other words, this simply means that

$$\int_{h_i}^{h_j} N_e \, dh = \alpha \int_{h_i}^{h_j} N'_e \, dh \quad (43)$$

where α is the calibration factor and N'_e is the relative electron density.

V. EXPERIMENTAL CONSIDERATIONS

A. DATA COLLECTION AND PROCESSING

The experimental observations discussed in this report were performed at the United States Air Force Trinidad Test Site located on the island of Trinidad, W.I. (10.7°N, 61.6°W).

The radar data were acquired in January and February 1961 under an experimental program jointly conducted by the Rome Air Development Center, the General Electric Company, the Lincoln Laboratory, and the National Bureau of Standards.

The objectives of the program were: (1) to obtain the electron density profiles in the ionosphere above the peak of the F-layer, (2) to determine the effect of the orientation of the magnetic field on the frequency spectrum of the scattered radiation and on the total backscattered power, and (3) to study the effect of Faraday rotation on incoherent backscattered echoes.

For items (1) and (2), transmissions were made utilizing right-hand circular polarization, while the returned signals were received on left-hand circular polarizations. Item (3), with which this study is concerned, and, at times, item (1), were carried out with linear polarization on transmission, and with the transmitted and the orthogonal polarization on reception.

A more complete description of the parameters of the radar system used in the experimental measurements is outlined in Table 1.

The IF receiver incoherent backscatter signals were recorded on an Ampex FR-100 multichannel magnetic tape recorder (Lincoln Laboratory equipment) together with timing and synchronizing signals. The magnetic tapes were then processed in the CG-24 digital computer at the Millstone Hill facility of the Lincoln Laboratory.

The processing of the IF data was accomplished by dividing the range sweep into intervals of 250 microseconds. The digital numbers associated with a fixed range increment were summed until sufficient enhancement of the incoherent signal-to-receiver noise ratio was attained. This same procedure was duplicated for the entire range sweep. It is estimated that approximately a 20-db signal-to-noise improvement was obtained by this integration technique.

Because only one IF magnetic tape recorder was available for this experiment, the backscattered radiation was received separately in the two linear receiver channels in consecutive intervals of time. The recording time in each channel varied

TABLE 1
RADAR SYSTEM PARAMETERS EMPLOYED IN THE
INCOHERENT SCATTER EXPERIMENT AT TRINIDAD

Radar Parameters	EXPERIMENTAL MEASUREMENT		
	Electron Density Profile (No. 1)	Scatter Spectrum (No. 2)	Faraday Effect (No. 3)
Transmission Frequency	425 megacycles	425 megacycles	425 megacycles
Transmitted Power (Peak)	2 megawatts	2 megawatts	2 megawatts
Antenna (Parabolic)	84-foot diameter	84-foot diameter	84-foot diameter
Pulse Duration	800 usec	800 usec	800 usec
Pulse Repetition Frequency	25 and 32 pps	25 and 32 pps	32 pps
Transmitted Polarization	a. Circular-right hand b. Linear-horizontal	Circular-right hand Circular-left hand	Linear-horizontal
Received Polarization	a. Circular-left hand b. Linear-horizontal and vertical	Circular-left hand	Linear-horizontal and vertical
Receiver Noise Figure	3.5 db	3.5 db	3.5 db

from approximately 8 to 15 minutes depending upon the conditions of the ionosphere, i.e., daytime or nighttime, and the azimuth-elevation orientation of the antenna beam.

In addition to the IF recordings, Polaroid photographs of radar range versus time coordinates were made for visual examination of the quality of the data.

The true height-electron density data deduced from the vertical incidence ionospheric sweep frequency soundings taken at the Ramey Air Force Base, Puerto Rico, and at Bogota, Colombia, were made available by the Central Radio Propagation Laboratory of the National Bureau of Standards for inclusion in the incoherent backscatter data analysis of the Faraday effect.

A Lincoln Laboratory C-4 ionospheric sounder was installed at Trinidad for the specific purpose of furnishing the calibration factors to convert the relative electron density profiles obtained by incoherent scattering into a true distribution. The Trinidad ionosonde data was also reduced by the National Bureau of Standards into true height profiles.

B. CHARACTERISTICS OF INCOHERENT BACKSCATTER ECHOES

The incoherent scattered signal from the ionosphere is noiselike in nature, as illustrated in Figure 9. The A-scope photograph shows vertical incidence backscatter recorded at Millstone Hill at a frequency of 440 megacycles, during an afternoon in February 1960.⁵ It is seen that the ground clutter is followed by a noise signal which is extended in range between 200 and 700 kilometers.

Since incoherent scattering would normally take place at an altitude of 100 kilometers and above, lowering the elevation angle of the antenna beam would result in both the signal intensity to decrease and the radar range to the backscatter return to increase.

A sample range versus time (Polaroid) photographic recording of incoherent backscatter echoes taken in the early afternoon of 2 February 1961 is presented in Figure 10. For these observations, the antenna beam was oriented in the direction of Bogota, Colombia, at an elevation angle of 10°.

In order to enhance the noise-type echoes with respect to the background noise, the vertical range sweep was slowly moved across the face of an intensity modulated oscilloscope. This permitted a form of integration, or averaging, of the signal by the overlapping of oscilloscope traces on the film.

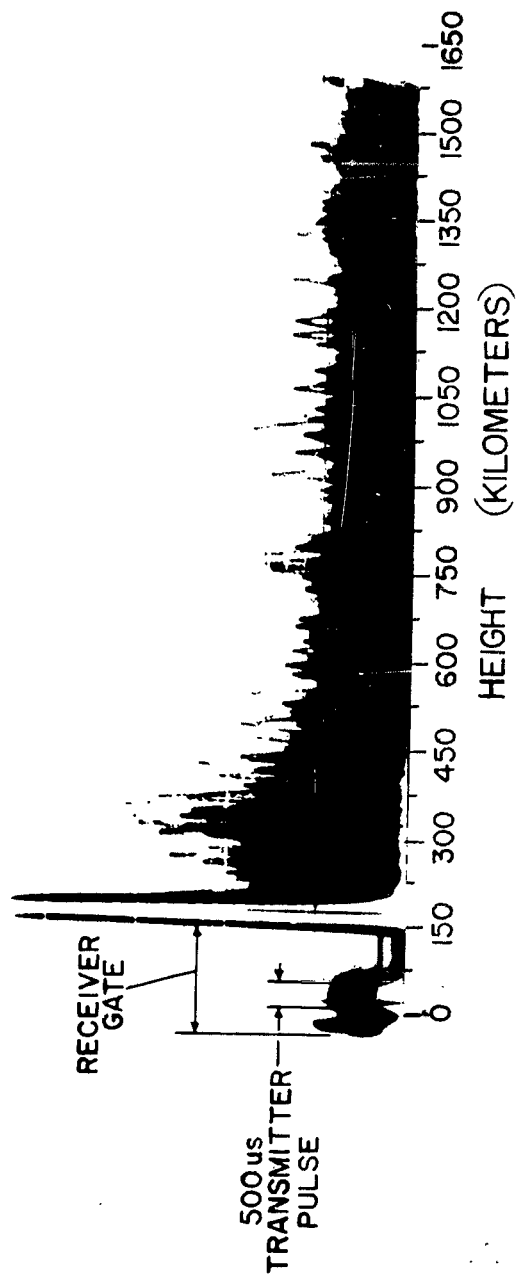


Figure 9. Vertical Incidence Incoherent Backscatter Observed at Millstone Hill at 440 Megacycles on the Afternoon of 8 February 1960 (after Pineo, Kraft and Briscoe)

RI426

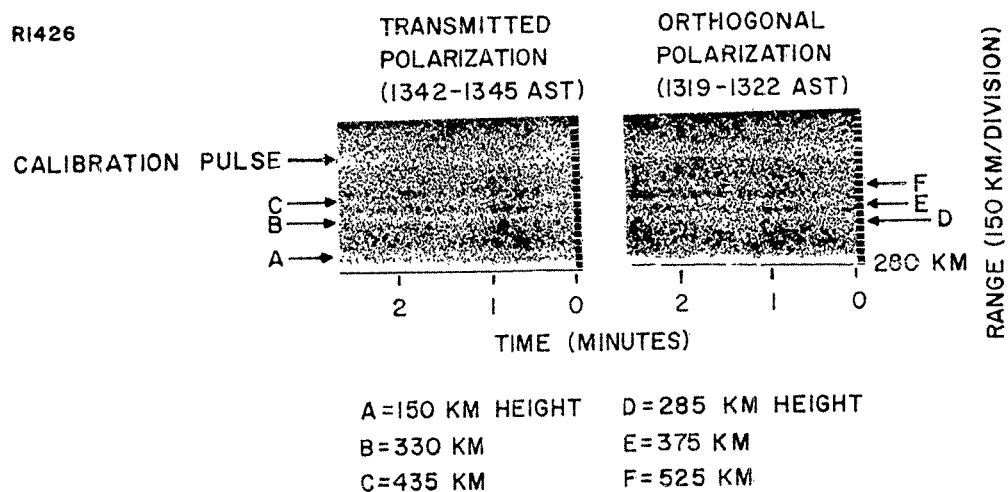


Figure 10. Range vs. Time Photographs of Incoherent Backscatter Echoes Showing Faraday Rotation. Observations Taken at Trinidad at 10° Elevation Angle in the Direction of Bogota, Colombia, on 2 February 1961

It is noted that the signals received on the two orthogonal polarization channels maximize at decidedly different radar ranges. This effect is conclusive evidence of the Faraday rotational properties of the ionosphere.

The IF signals, corresponding to the data depicted in Figure 10, were recorded on magnetic tape and then processed on the Millstone Hill CG-24 computer. An A-scope display of the integrated signal detected in the orthogonal channel is shown in the upper photograph of Figure 11. The lower picture is a processed version of the same data. The conversion into a relative electron density was accomplished by normalizing the relative signal intensity with respect to the square of the radar range.

The calibration pulse, also evident in Figure 11, was inserted at the receiver input continuously throughout the entire data recording of each radar measurement and was maintained at a temperature level of approximately 90°K.

RI429

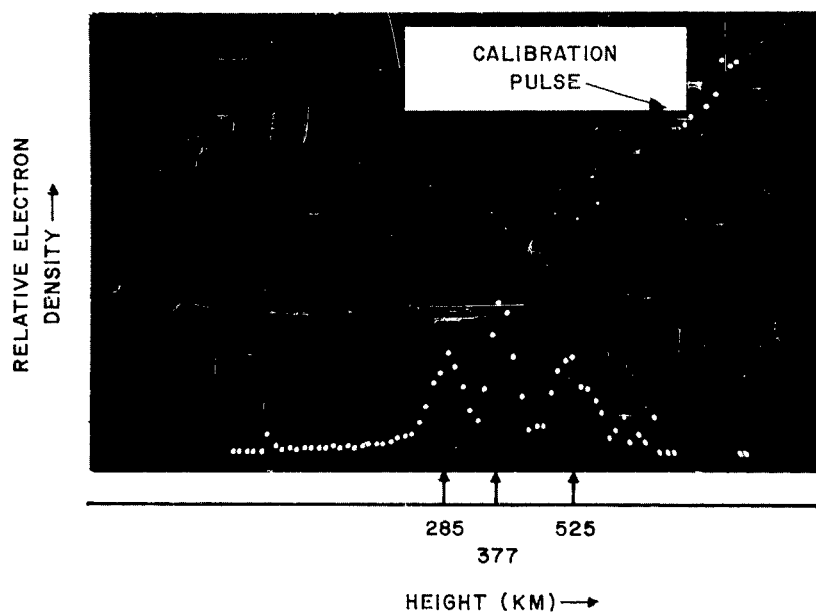
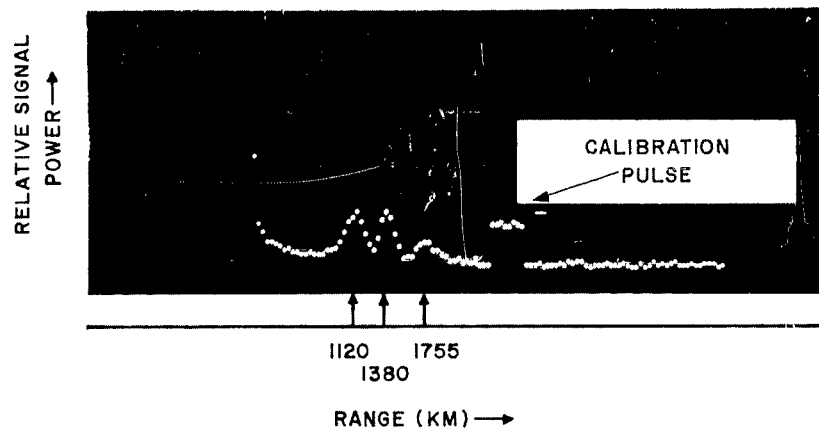


Figure 11. A-Scope Photographs of Integrated Incoherent Backscatter Observed at Trinidad at 10° Elevation Angle in the Direction of Bogota, Colombia on 2 February 1061, 1318 through 1326 AST. Data Processed by Computer at the MIT Lincoln Laboratory, Millstone Hill Radar Station

VI. DATA ANALYSIS

A. BACKSCATTER MEASUREMENTS IN THE DIRECTION OF BOGOTA, COLOMBIA

A representative sample of incoherent backscatter echoes, recorded at the Trinidad Radar Site in the afternoon of 2 February 1961, is shown in Figure 12. These data, which are the processed output of the Millstone Hill CG-24 digital computer, were acquired with the antenna beam oriented in the direction of Bogota, Colombia (azimuth-bearing of 240°), at an elevation angle of 10° . It should be mentioned that the orthogonal polarization curve is a replot of the A-scope display shown in the lower portion of Figure 11.

Transmissions were made utilizing horizontal polarization, while the scattered signals were received separately on the transmitted and orthogonal linear polarization receiver channels in successive intervals of about 15 minutes each.

It is seen that the relative electron density distributions received on the two orthogonal polarizations maximize at decidedly different heights. The intertwining of the two profiles is characteristic of incoherent scatter data obtained when linear polarization is employed on transmission and reception, the "scallop" effect being due to the Faraday rotational characteristics of the ionosphere.

It is of interest to note that, at the height of signal maximum on one polarization, the signal on the other channel does not reduce to zero. This implies that, most likely, the plane of polarization of the incoherent scattered signal is to some extent randomly polarized with perhaps maximum polarization oriented in the direction of the incident field.

The sum of the relative electron densities in the two channels results in the electron density distribution depicted in Figure 13. The data were normalized with respect to the maximum ionization deduced from vertical incidence sweep frequency soundings taken at approximately the same time at the Bogota station of the National Bureau of Standards. The ionogram virtual height data were converted by the National Bureau of Standards into a true height profile by means of the Budden matrix technique.⁴⁹

It is quite apparent that the incoherent scatter distribution compares reasonably well with the ionosonde true height data, the profile above the F-layer maximum being extrapolated by means of a Chapman model having a scale height of 80 kilometers for the neutral particles.

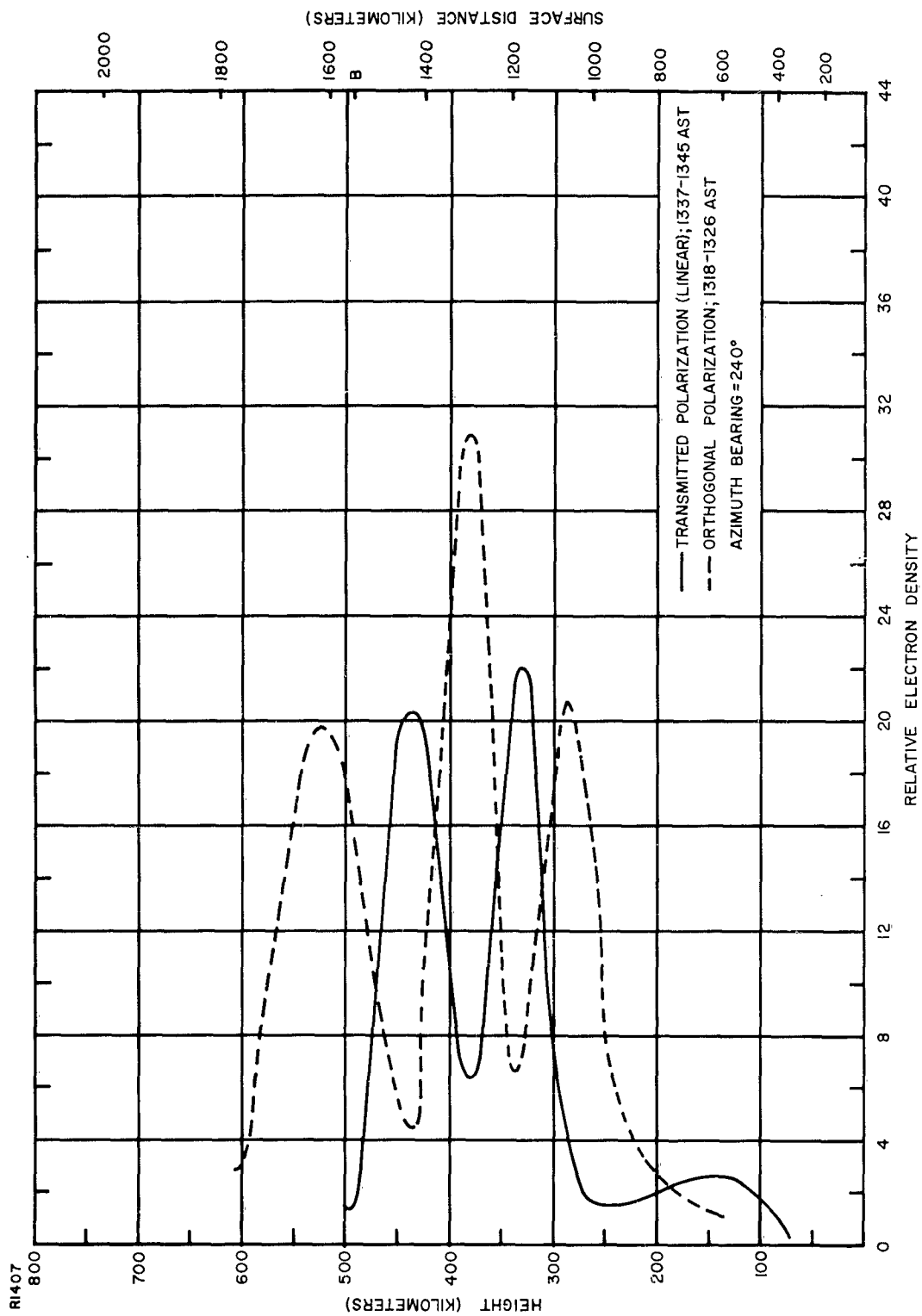


Figure 12. Distribution of Electron Density Observed by Incoherent Backscatter at 10° Elevation Angle in the Direction of Bogota, Colombia, on 2 February 1961

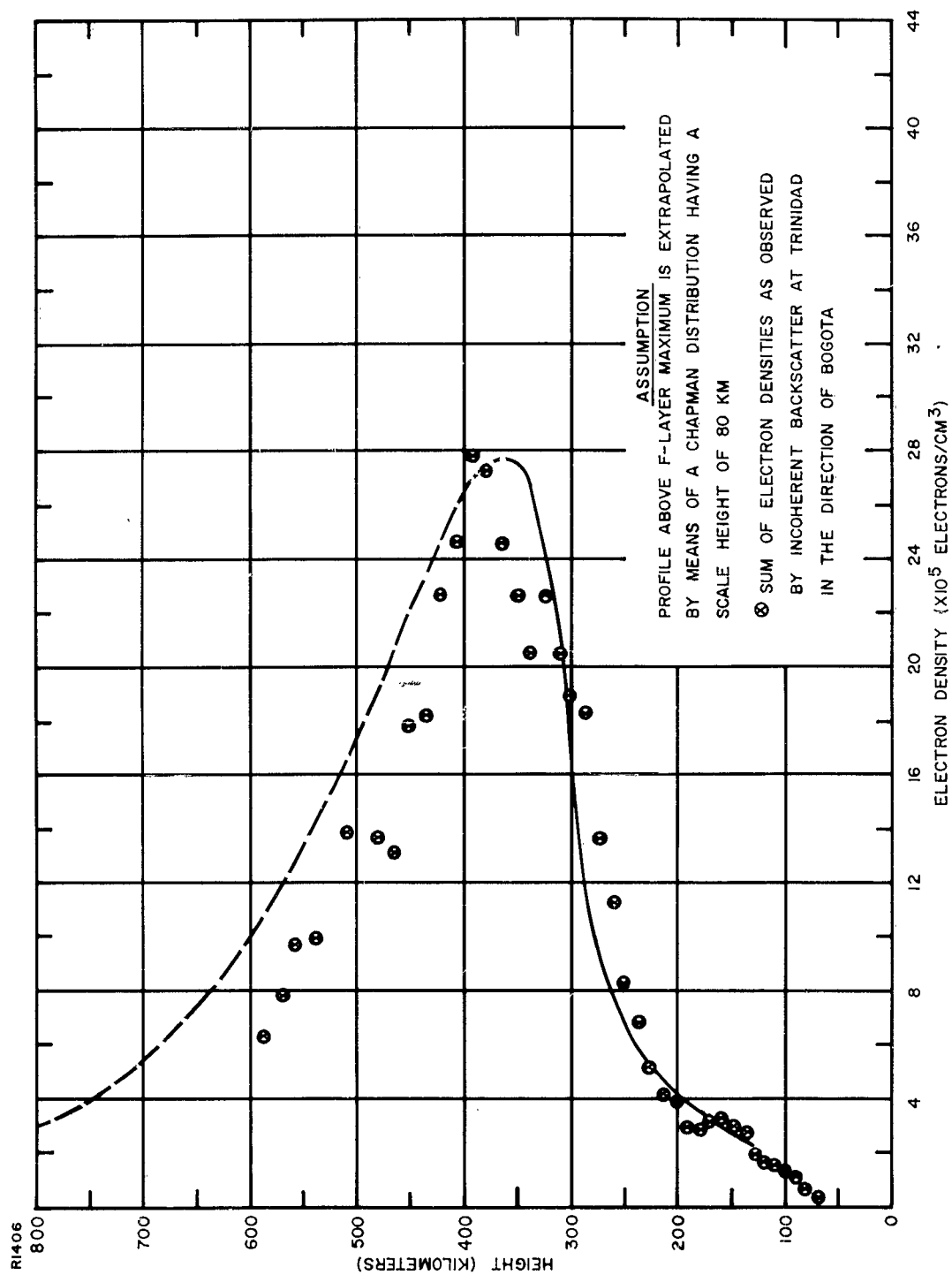


Figure 13. Incoherent Backscatter Electron Density Profile Compared with Profile Deduced from Ionospheric Soundings Taken at Bogota, Colombia on 2 February 1961, 1330 AST

It should be noted that the total electron density profile plotted in Figure 13 would be the same as that obtained when using circularly polarized radio waves in the experimental measurements.

With regard to the heights of the signal maxima shown in Figure 12, it is interesting to find that they correlate with those theoretically predicted from Faraday rotation computations, as illustrated in Figure 14. The theoretical estimate of the ionospheric contribution to the polarization rotation was determined by the method discussed in Section IV utilizing the electron density distribution recorded at Bogota.

These measurements indicate that, for these particular observations, which were made at a frequency of 425 megacycles, the total amount of angular rotation of the plane of polarization for a two-way propagation path through the ionosphere was on the order of 450° .

Since there is excellent correlation between the experimental results and the theoretical predictions of the Faraday effect, it appears that it may be feasible to study the variability of the elements of the earth's magnetic field by means of the incoherent scatter-Faraday rotation technique.

The Faraday effect can also be used to provide the calibration factor for converting the relative electron density profiles into an absolute measurement.

Rewriting Equation (34) in terms of the integrated electron density evaluated from Faraday measurements, it follows that, as a first approximation, at 425 megacycles

$$\int_{h_1}^{h_2} N_e \, dh = \frac{3.81 \times 10^{12} \phi}{\left[f(h) H \cos \theta \right]_{h_1}^{h_2}} \quad (44)$$

It is seen from Figure 8 that, at a 10° elevation angle and 240° azimuth angle, the average value of the function, $f(h) H \cos \theta$, between 100 and 525 kilometer altitude, is on the order of -0.605 gauss. Thus, for $\phi = 2.5\pi$ radians, which is the two-way angular rotation encountered up to an altitude of 525 kilometers, as shown in Figure 12,

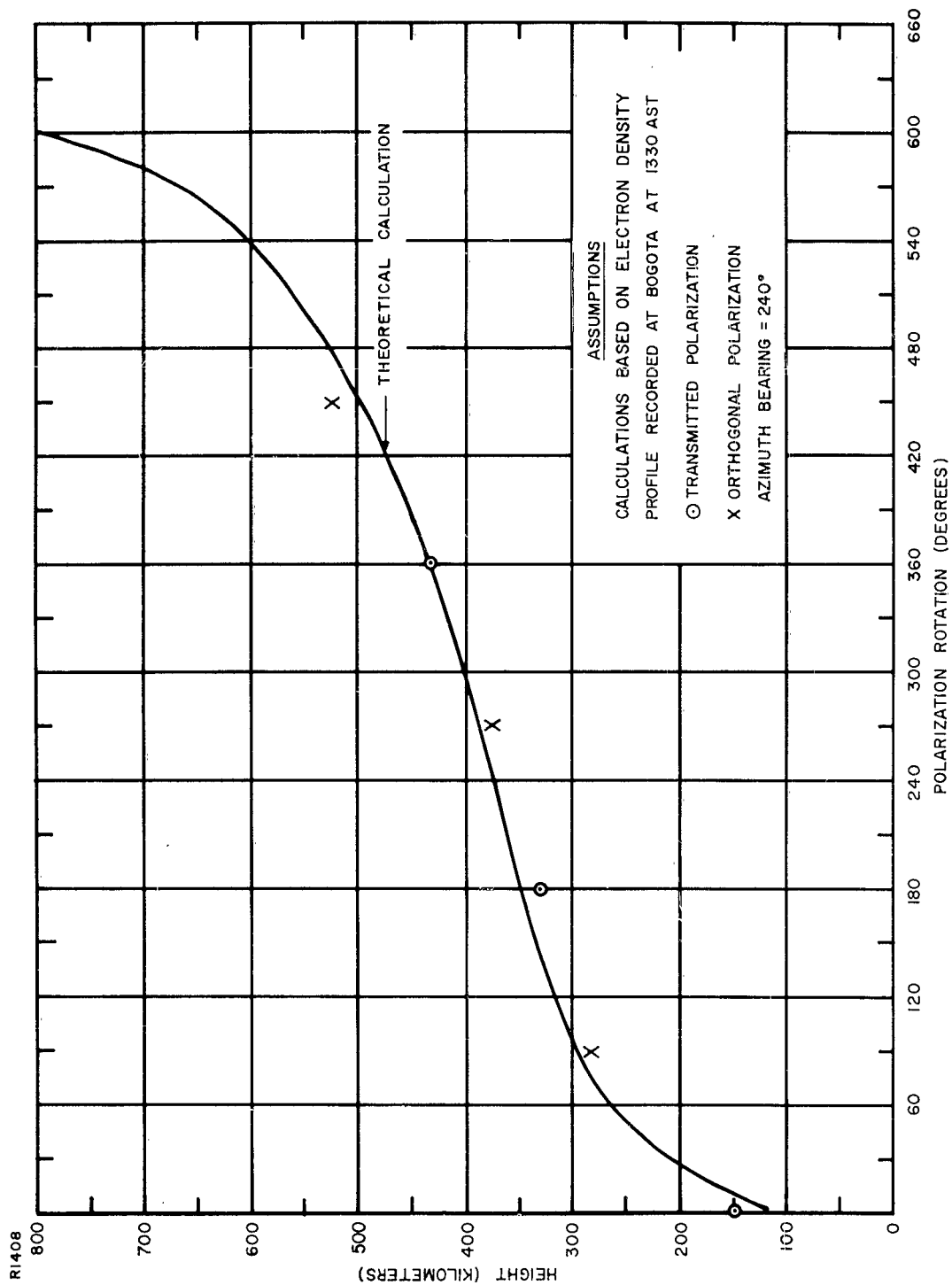


Figure 14. Comparison of Theoretical Estimate of Faraday Rotation with Incoherent Backscatter Observations Taken at Trinidad at 10° Elevation Angle in the Direction of Bogota, Colombia, on 2 February 1961

$$\int_{100 \text{ km}}^{525 \text{ km}} N_e dh = 49.3 \times 10^{12} \text{ electrons per square centimeter}$$

According to Figure 12, the total relative electron density distribution integrated up to an altitude of 525 kilometers yields a value of approximately 76×10^7 arbitrary units-centimeter.

From Equation (43), it follows that the calibration factor, $\alpha = 6.47 \times 10^4$ electrons per cubic centimeter. Utilizing this parameter, it can be readily shown that the maximum value of electron density, deduced from incoherent backscatter, becomes 24.4×10^5 electrons per cubic centimeter as compared to approximately 27.8×10^5 electrons per cubic centimeter obtained from ionospheric soundings taken at Bogota, the data being given in Figure 13. The slight discrepancy in the two values can be attributed to the assumption of removing the function, $f(h) H \cos \theta$, outside the integral of Equation (34).

B. BACKSCATTER MEASUREMENTS IN THE DIRECTION OF PUERTO RICO

The relative electron density profiles observed by incoherent backscatter at Trinidad at 13° elevation angle in the direction of Puerto Rico (azimuth angle of 327°) on 27 January 1961 is illustrated in Figure 15.

The conversion into the true distribution, shown in Figure 16, was performed using the Puerto Rico ionosonde data recorded at approximately the same time as the incoherent scatter observations.

It is seen that the theoretical profile above the F-layer maximum extrapolated by means of a Chapman model having a constant scale height of 80 kilometers is slightly higher than the experimental data. This would imply that, for this day, the scale height above the F-layer maximum during the daytime, in the vicinity of Puerto Rico, was most likely less than 80 kilometers.

With regard to calibrating the resultant relative electron density profile, given in Figure 15, by the Faraday method, it can be shown, utilizing Equations (43) and (44), that the calibration factor, α , equals 7.55×10^4 electrons per cubic centimeter. This computation is based on $\theta = \pi/2$ radians for propagation up to an altitude of 300 kilometers.

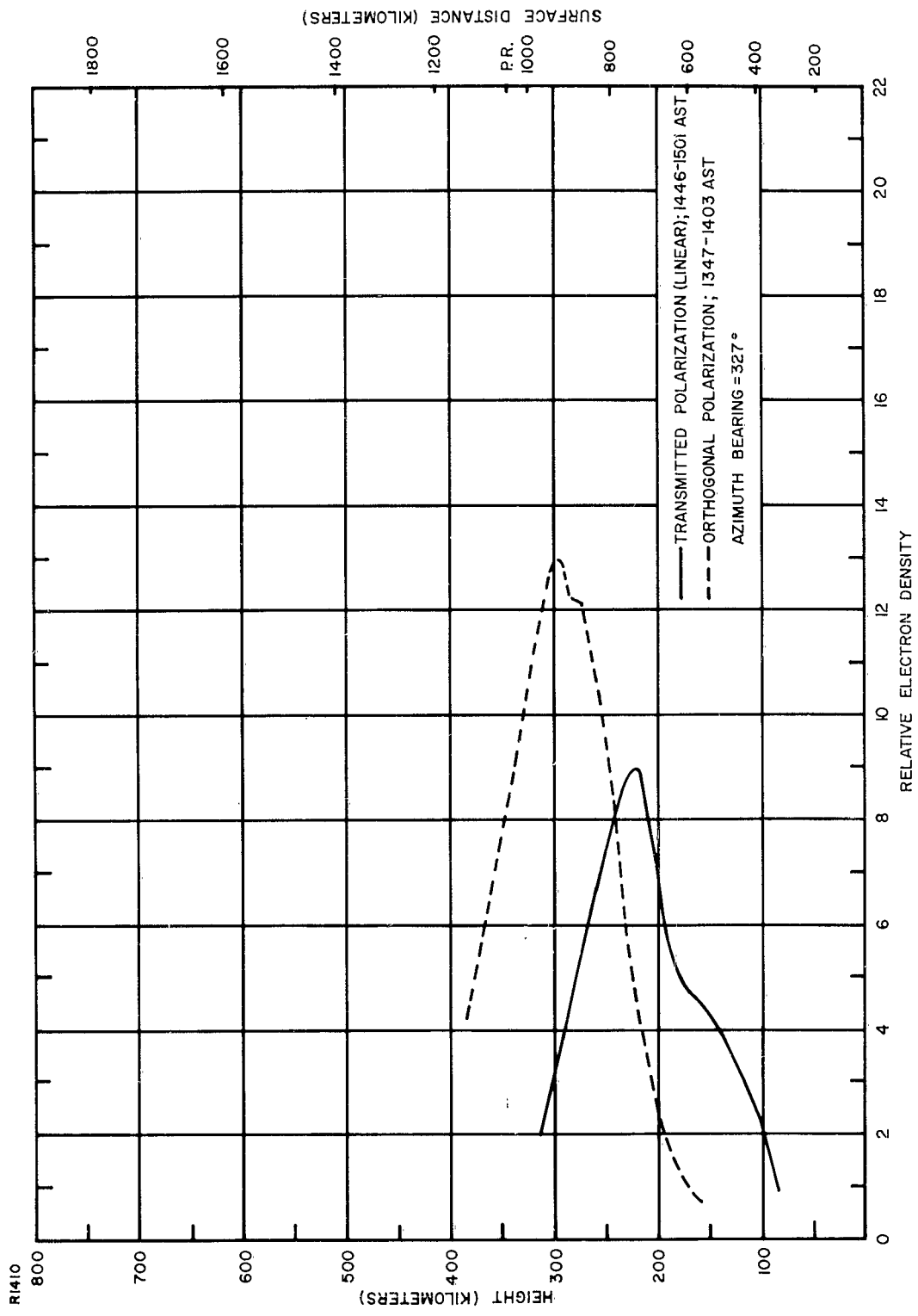


Figure 15. Distribution of Electron Density Observed by Incoherent Backscatter at Trinidad at 13° Elevation Angle in the Direction of Puerto Rico on 27 January 1961

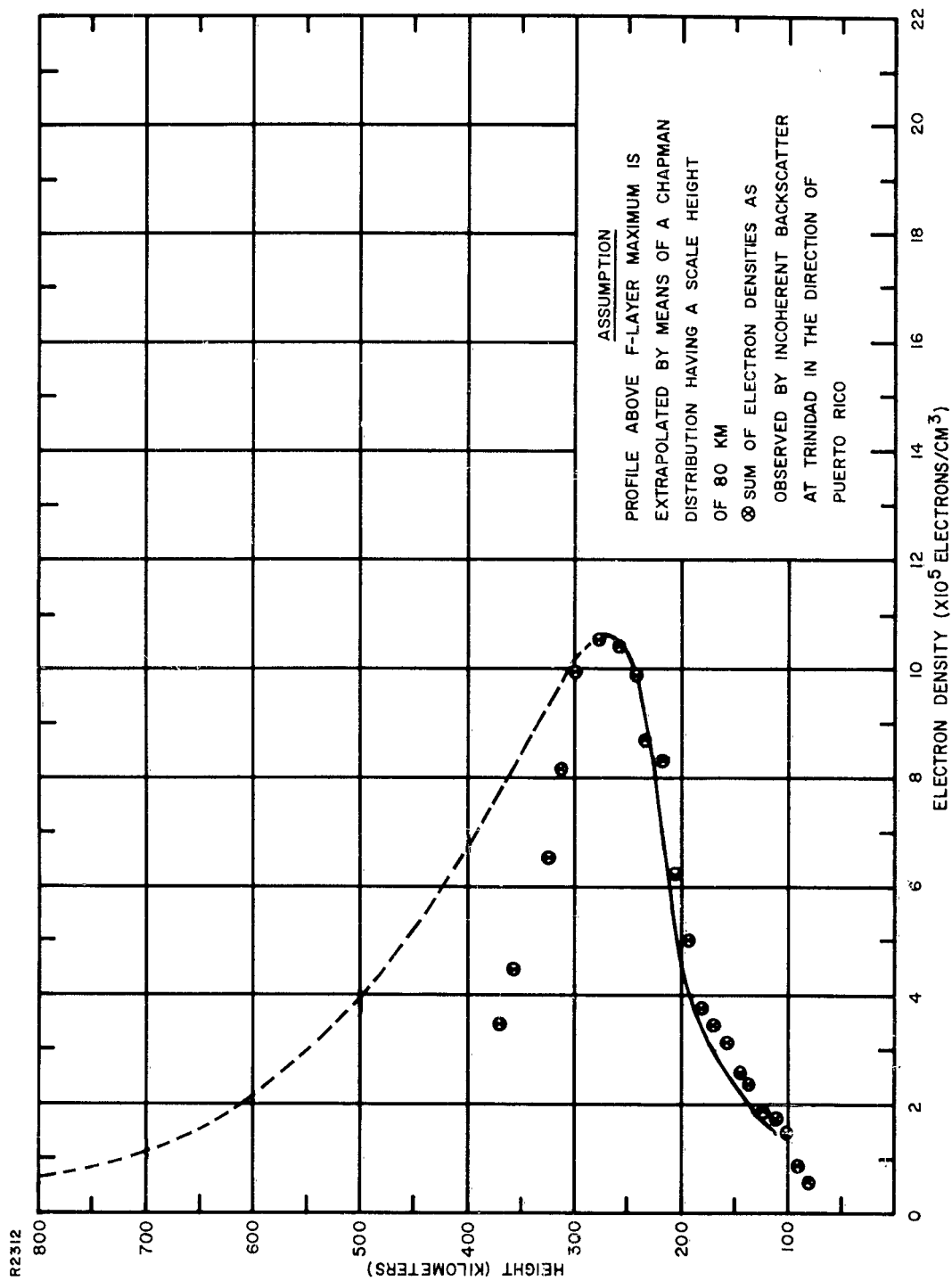


Figure 16. Incoherent Backscatter Electron Density Profile Compared with Profile Deduced from Ionospheric Soundings Taken at Puerto Rico on 27 January 1961, 1445 AST

$$\int_{100 \text{ km}}^{300 \text{ km}} N_e dh = 15.5 \times 10^{12} \text{ electrons per square centimeter}$$

$$\int_{100 \text{ km}}^{300 \text{ km}} N'_e dh = 20.5 \times 10^7 \text{ arbitrary units - centimeter,}$$

and the average value of $f(h) H \cos \theta$ between 100 and 300 kilometers, as determined from Figure 8, equal to 0.385 gauss. The maximum electron density, therefore, becomes 12.1×10^5 electrons per cubic centimeter which is comparable to the value of 12.6×10^5 per cubic centimeter deduced from the Puerto Rico ionogram depicted in Figure 16.

The comparison of the theoretical estimate of the angular rotation, induced by the ionosphere, with the incoherent backscatter observation, is shown in Figure 17. It is noted that the theoretical curve approximates, to some degree, the experimental measurements.

Incoherent backscatter-Faraday rotation measurements made on 1 February 1961, also in the direction of Puerto Rico, revealed the relative electron density distribution shown in Figure 18.

The conversion into an absolute profile from the Puerto Rico ionosonde data taken at the same time is given in Figure 19. It is quite evident that the incoherent experimental points agree with the distribution deduced from the ionospheric sweep frequency sounder, the ionosonde data being given by the solid curve below the maximum ionization level of 260 kilometers. The lack of agreement above the peak of the F-layer indicates that the scale height in this region must be less than 80 kilometers for the neutral particles. This conclusion is similar to the one arrived at from the measurements made on the afternoon of 27 January 1961, the results of the analysis being presented in Figure 16.

It is of interest to note that a study of the characteristics of the ionosphere by radar-lunar techniques, conducted at Trinidad between January and July 1960, also revealed similar daytime results.⁵⁰ It was found that the distribution of electron density above the peak of the F-layer can be represented, to a first approximation, by a Chapman model with a constant scale height of less than about 80 kilometers for the neutral particles during the daytime and more than about 80 kilometers during the nighttime.

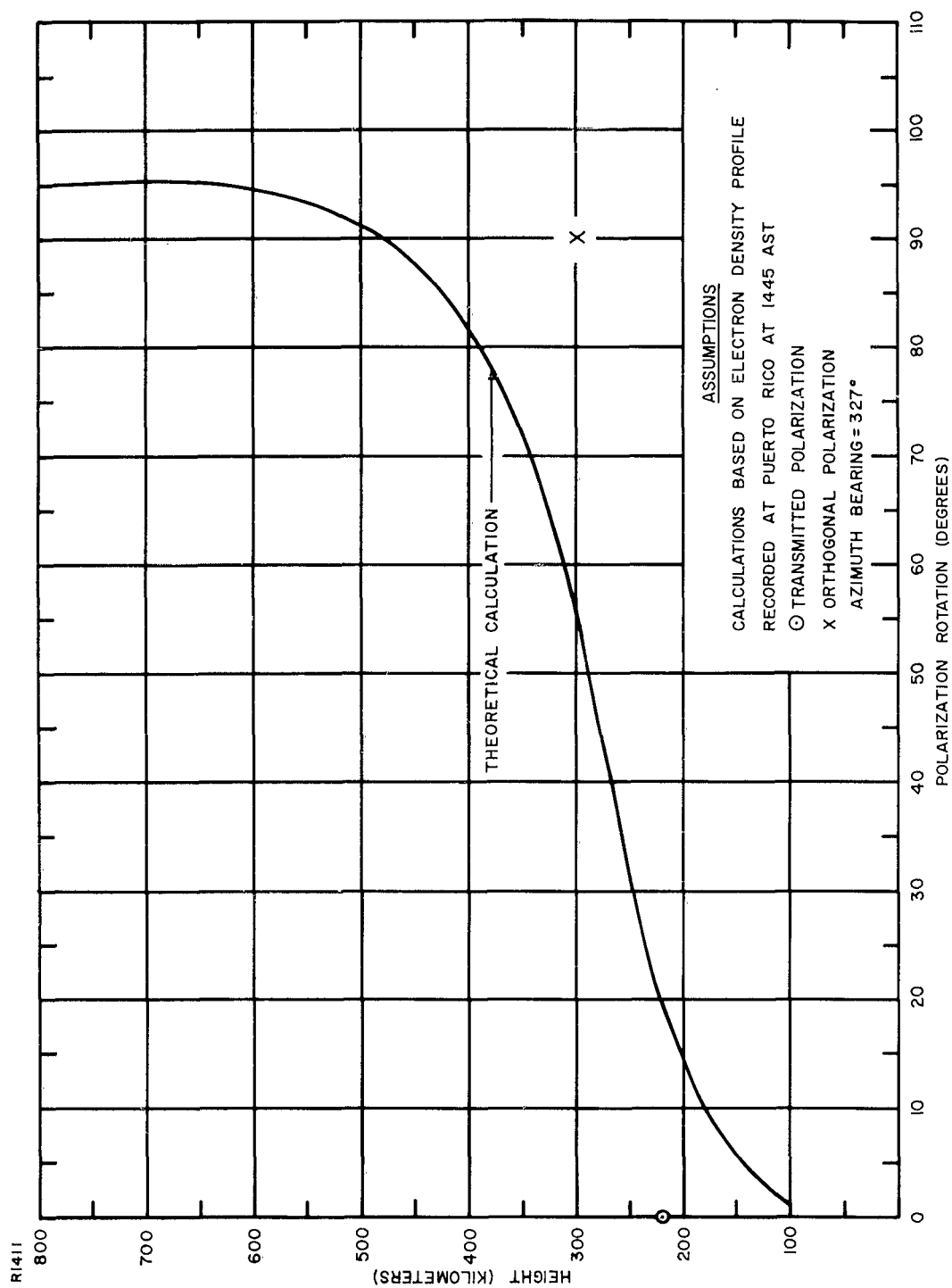


Figure 17. Comparison of Theoretical Estimate of Faraday Rotation with Incoherent Backscatter Observations Taken at Trinidad at 13° Elevation Angle in the Direction of Puerto Rico on 27 January 1961

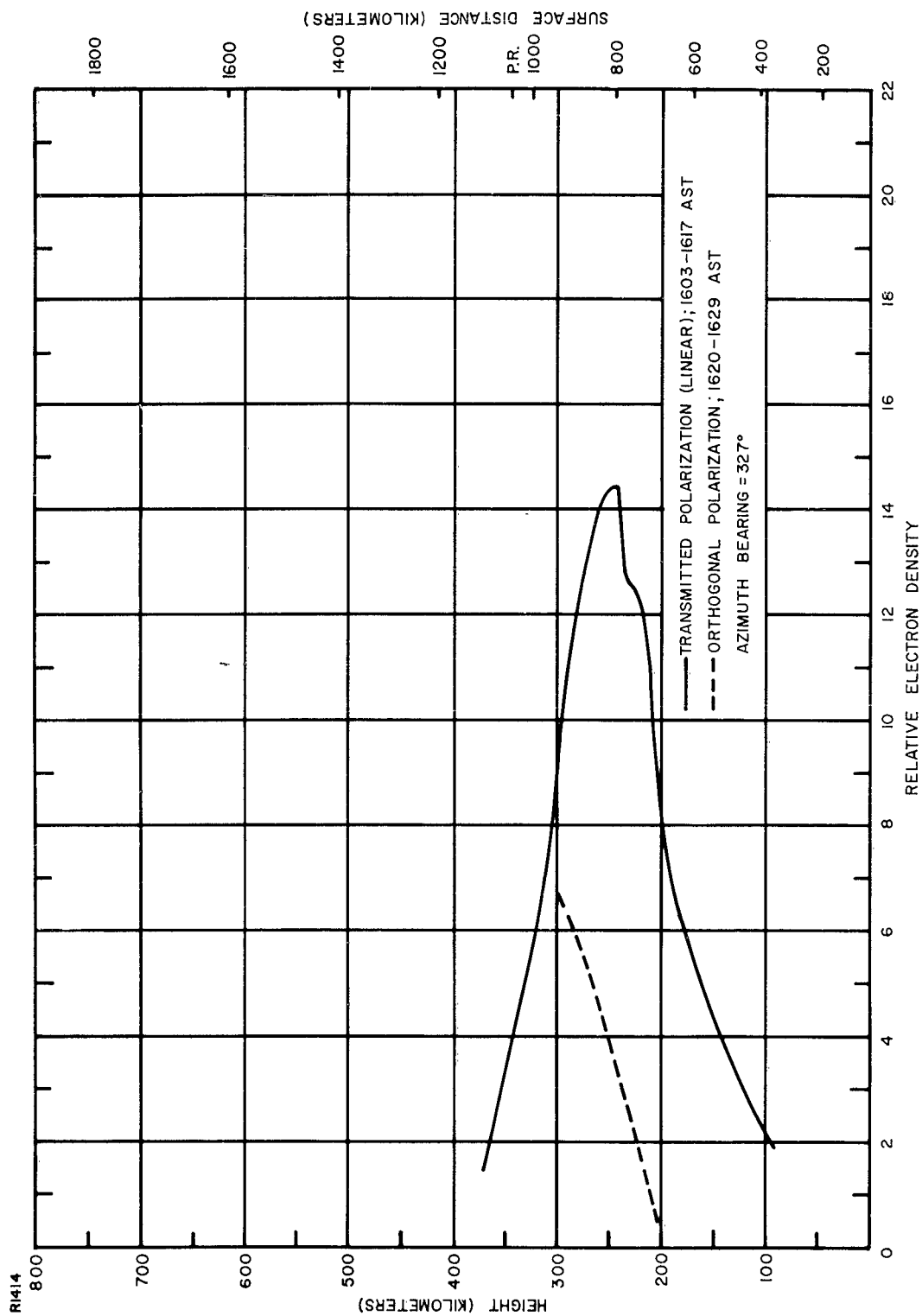


Figure 18. Distribution of Electron Density Observed by Incoherent Backscatter at Trinidad at 13° Elevation Angle in the Direction of Puerto Rico on 1 February 1961

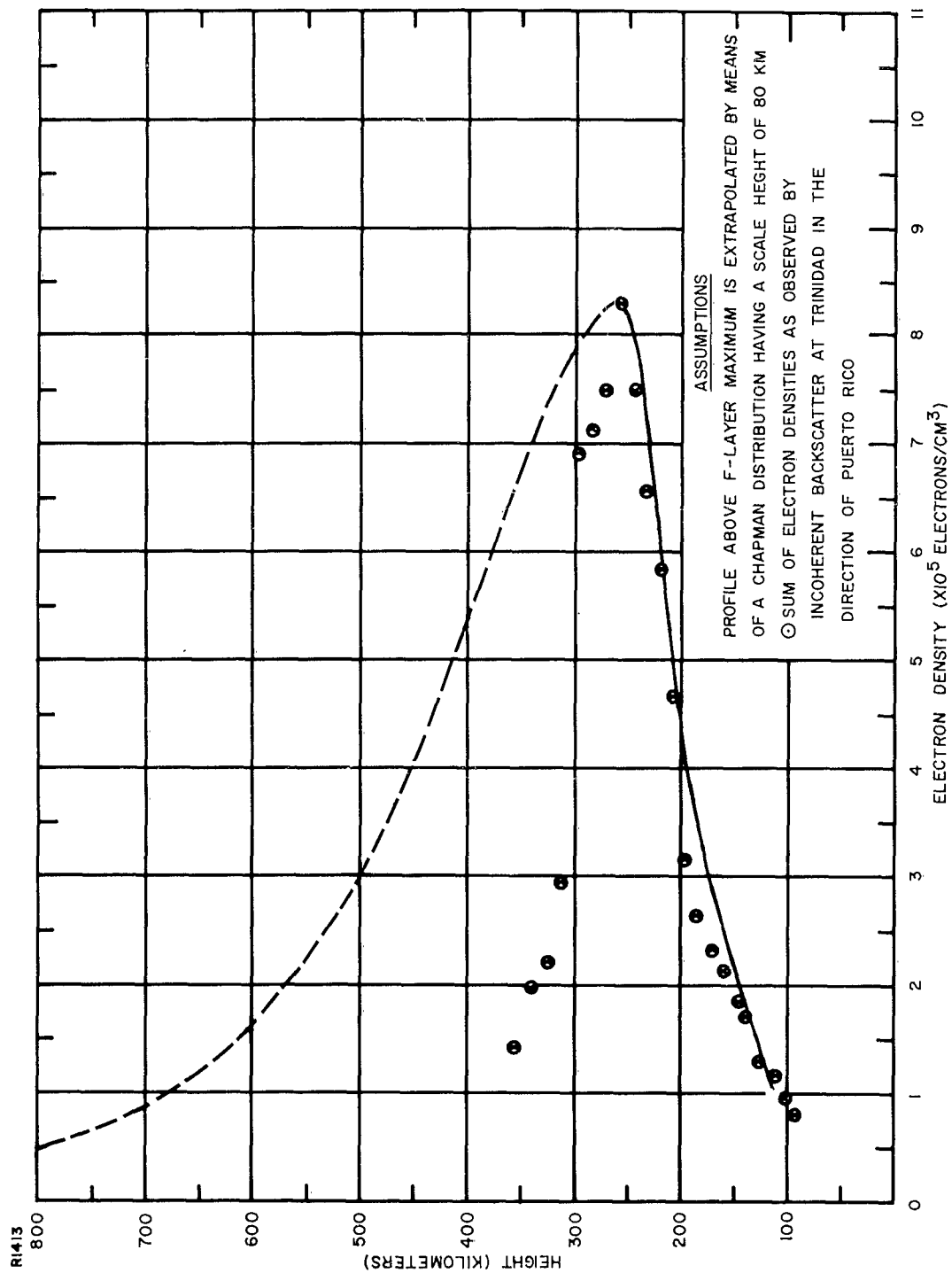


Figure 19. Incoherent Backscatter Electron Density Profile Compared with Profile Deduced from Ionospheric Soundings Taken at Puerto Rico on 1 February 1961, 1615 AST

According to Figure 20, the theoretical estimate of the Faraday rotation that could have taken place during the incoherent scatter recording period was less than 90° . This is partially confirmed by the experimental measurements.

It is of interest to note that the theoretical curve tends to reach a maximum at an altitude of about 700 kilometers. An examination of Figures 8 and 20 reveals that the height of maximum rotation corresponds to the height at which the propagation angle attains a value of 90° . It follows, therefore, that, when radio wave propagation occurs along a path in which the angle between the ray direction and the magnetic field vector changes quadrants, the sense of rotation of linearly polarized transmissions is reversed.

C. BACKSCATTER MEASUREMENTS NEAR VERTICAL INCIDENCE AT TRINIDAD

Incoherent scatter soundings conducted with the antenna beam directed at high elevation angles or vertically upwards are best utilized to obtain height profiles of electron density above the F-layer at a fixed location on the earth's surface.

The processed data from the measurements made on 27 January 1961 with the antenna beam axis elevated to an angle of 45° in the direction of Puerto Rico are plotted in Figures 21 and 22.

The measured true height profile of Figure 22 indicates that the scale height in the region immediately above the peak of the F-layer is less than 80 kilometers. The abrupt change in the slope of the curve at a height of 400 kilometers, on the other hand, signifies that the scale height is increasing.

The two data points at altitudes of 545 and 575 kilometers are believed to be in error, since the signal intensity at these heights was extremely weak.

The Faraday calculations, depicted in Figure 23, show that the total angular rotation is only on the order of 20° . The lack of signal power in the orthogonal receiver polarization channel, evident in Figure 21, necessarily confirms the theoretical predictions.

It should be mentioned that the calibration of the electron density curves of Figure 21 cannot be accomplished from the Faraday data because of insufficient angular rotation of the transmitted plane of polarization.

The vertical incidence incoherent scatter data, taken on 2 February 1961, are illustrated in Figures 24 and 25.

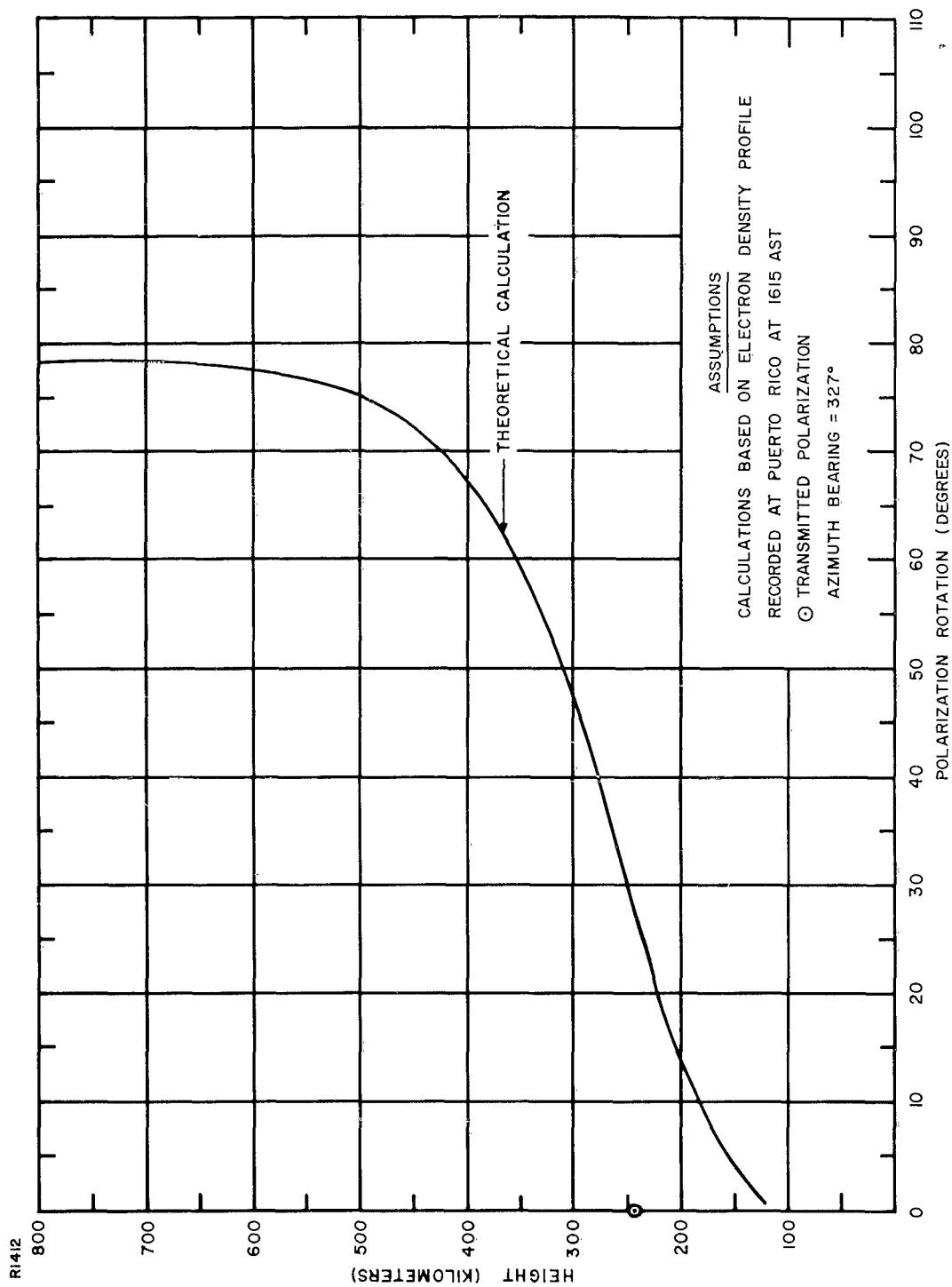


Figure 20. Comparison of Theoretical Estimate of Faraday Rotation with Incoherent Backscatter Observations Taken at Trinidad at 13° Elevation Angle in the Direction of Puerto Rico on 1 February 1961

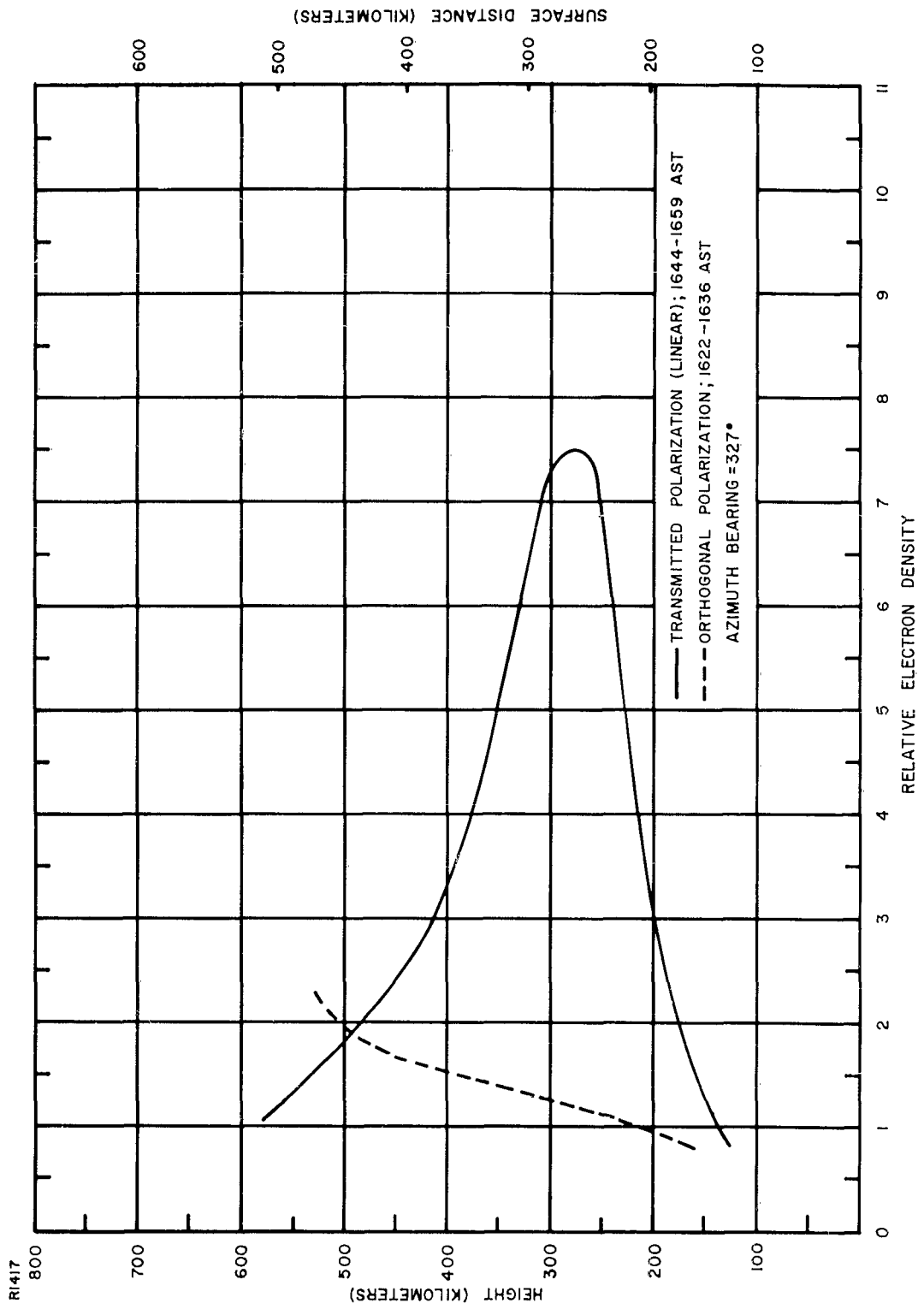


Figure 21. Distribution of Electron Density Observed by Incoherent Backscatter at Trinidad at 45° Elevation Angle in the Direction of Puerto Rico on 27 January 1961

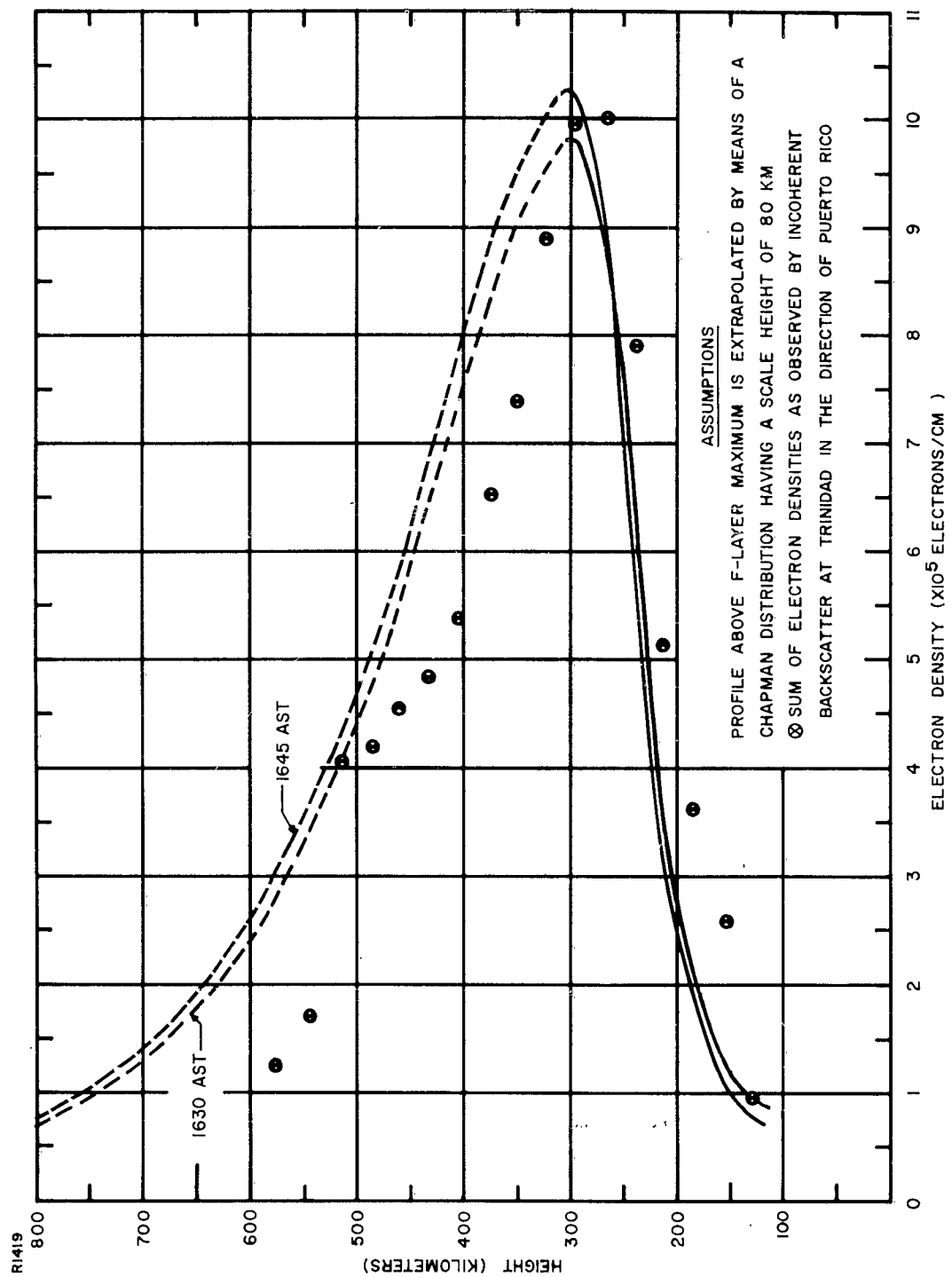


Figure 22. Incoherent Backscatter Electron Density Profile Compared with Profile Deduced from Ionospheric Soundings Taken at Trinidad on 27 January 1961

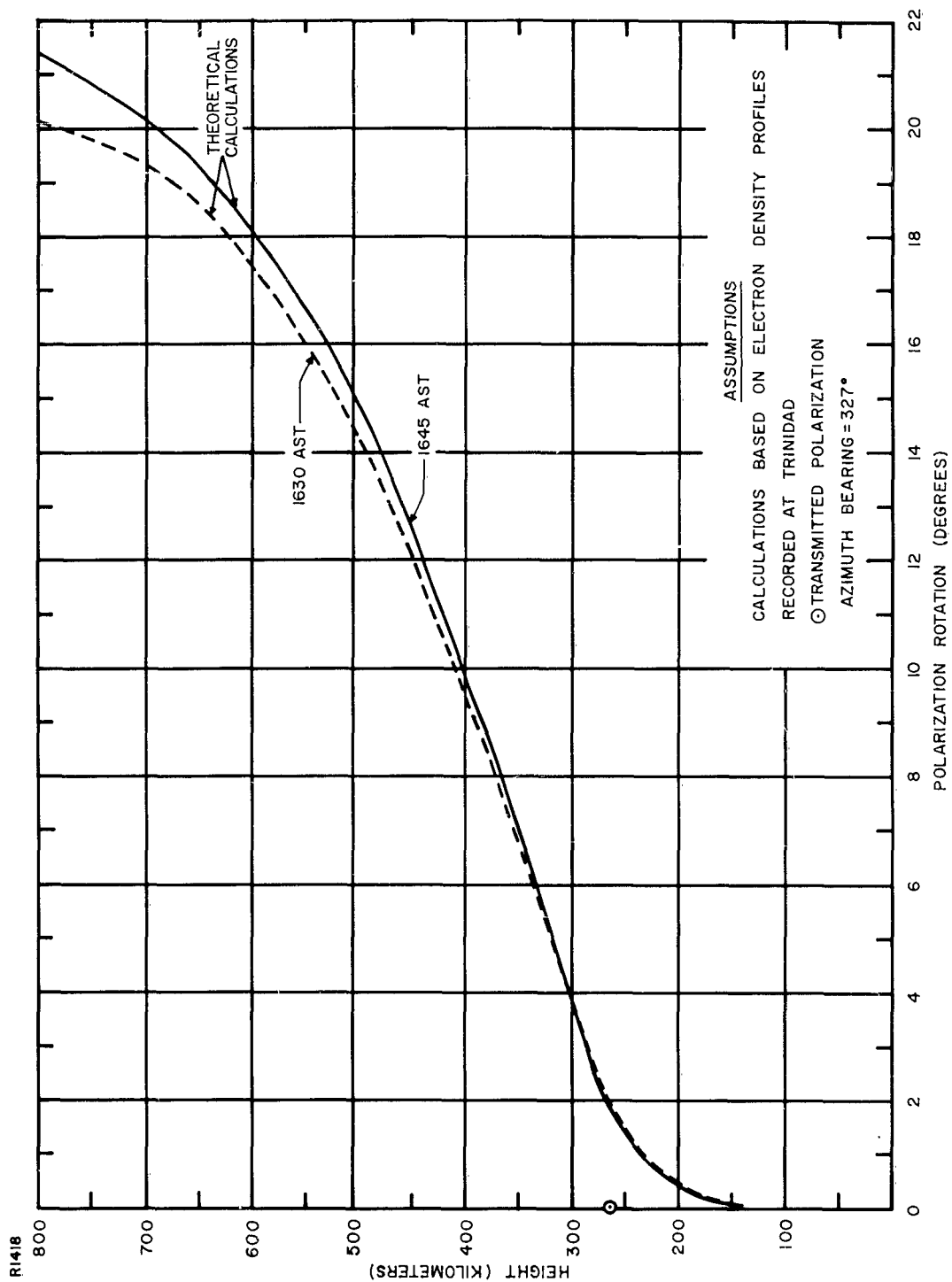


Figure 23. Comparison of Theoretical Estimate of Faraday Rotation with Incoherent Backscatter Observations Taken at Trinidad at 45° Elevation Angle in the Direction of Puerto Rico on 27 January 1961

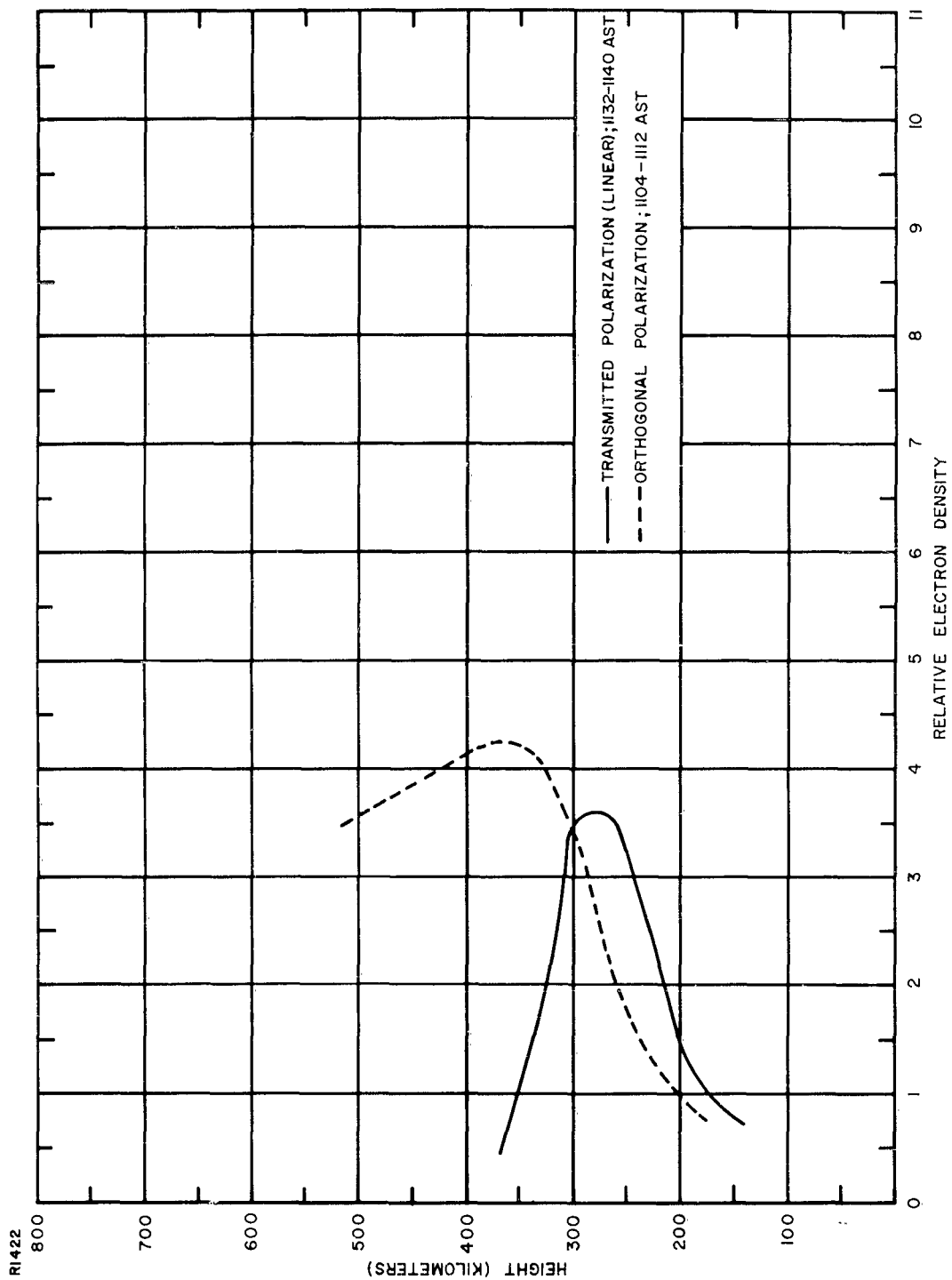


Figure 24. Distribution of Electron Density Observed by Incoherent Backscatter at Trinidad at Vertical Incidence on 2 February 1961

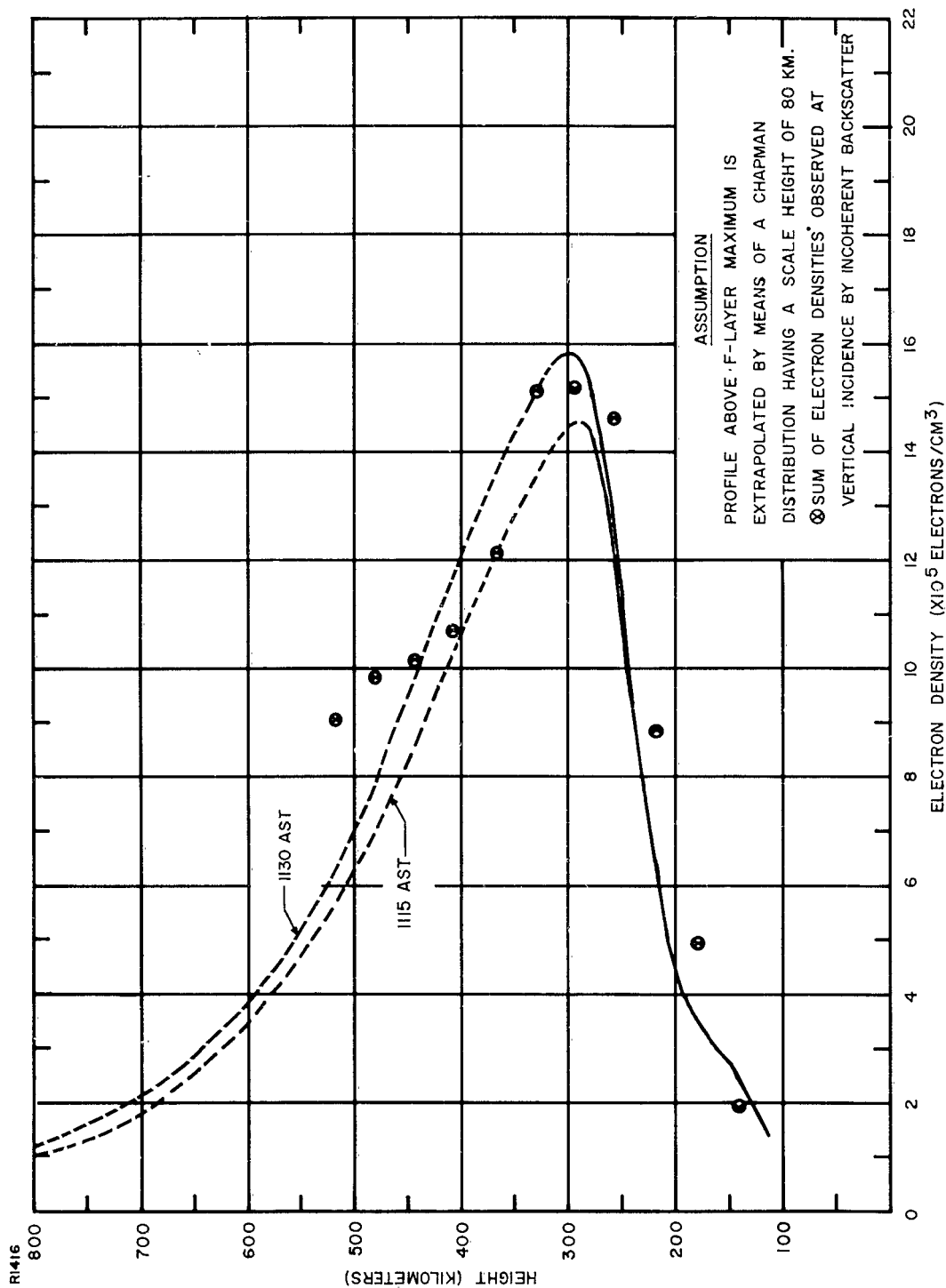


Figure 25. Incoherent Backscatter Electron Density Profile Compared with Profiles Deduced from Ionospheric Soundings Taken at Trinidad on 2 February 1961

According to Figure 25, the electron density profile discloses a marked slope change beginning in the region of about 368 kilometers. The effect is similar to the one presented in Figure 22.

The agreement between the experimental measurement and the theoretical estimate of angular rotation, shown in Figure 26, also validates the concept of the Faraday effect.

With regard to converting the relative experimental data, plotted in Figure 24, into an absolute measurement without the use of ionosonde data, it can be shown, utilizing the procedure previously described, that the calibration factor, α , evaluates to 2.44×10^5 electrons per cubic centimeter. The calculation of this parameter was determined on the basis of a total angular rotation of $\pi/2$ radians up to a height of 368 kilometers,

$$\left[f(h) H \cos \theta \right]_{100 \text{ km}}^{368 \text{ km}} = -0.23 \text{ gauss}$$

$$\int_{100 \text{ km}}^{368 \text{ km}} N_e dh = 26 \times 10^{12} \text{ electrons per square centimeter}$$

and

$$\int_{100 \text{ km}}^{368 \text{ km}} N'_e dh = 10.62 \times 10^7 \text{ arbitrary units - centimeter}$$

The solution of the elements of the magnetic field by means of the Faraday effect, as defined by Equation (41), can be readily obtained when the propagation direction is at vertical incidence. For this particular observation, it is found that the mean value of the vertical component of the magnetic field, $H \sin I$, between 100 and 368 kilometers, is on the order of 0.242 gauss, as compared to 0.230 gauss determined from Figure 8. The former computation is based on an integrated electron density of 24.7×10^{12} electrons per square centimeter up to an altitude of 368 kilometers, this value being deduced from Figure 25.

D. ELECTRON DENSITY PROFILES

A composite of the electron density profiles inferred from the incoherent scatter observations is depicted in Figures 27 and 28.

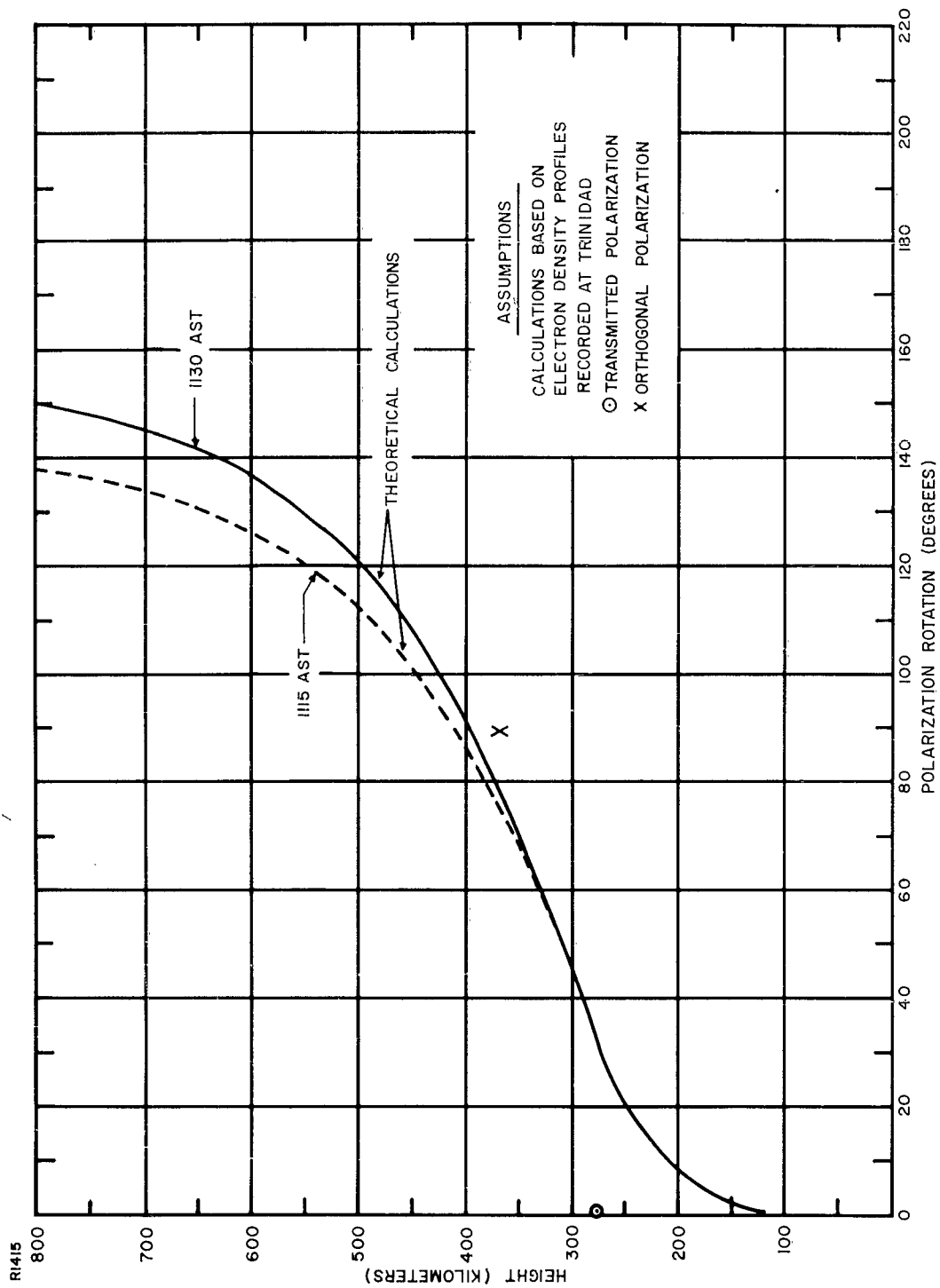


Figure 26. Comparison of Theoretical Estimate of Faraday Rotation with Incoherent Backscatter Observations Taken at Trinidad at Vertical Incidence on 2 February 1961

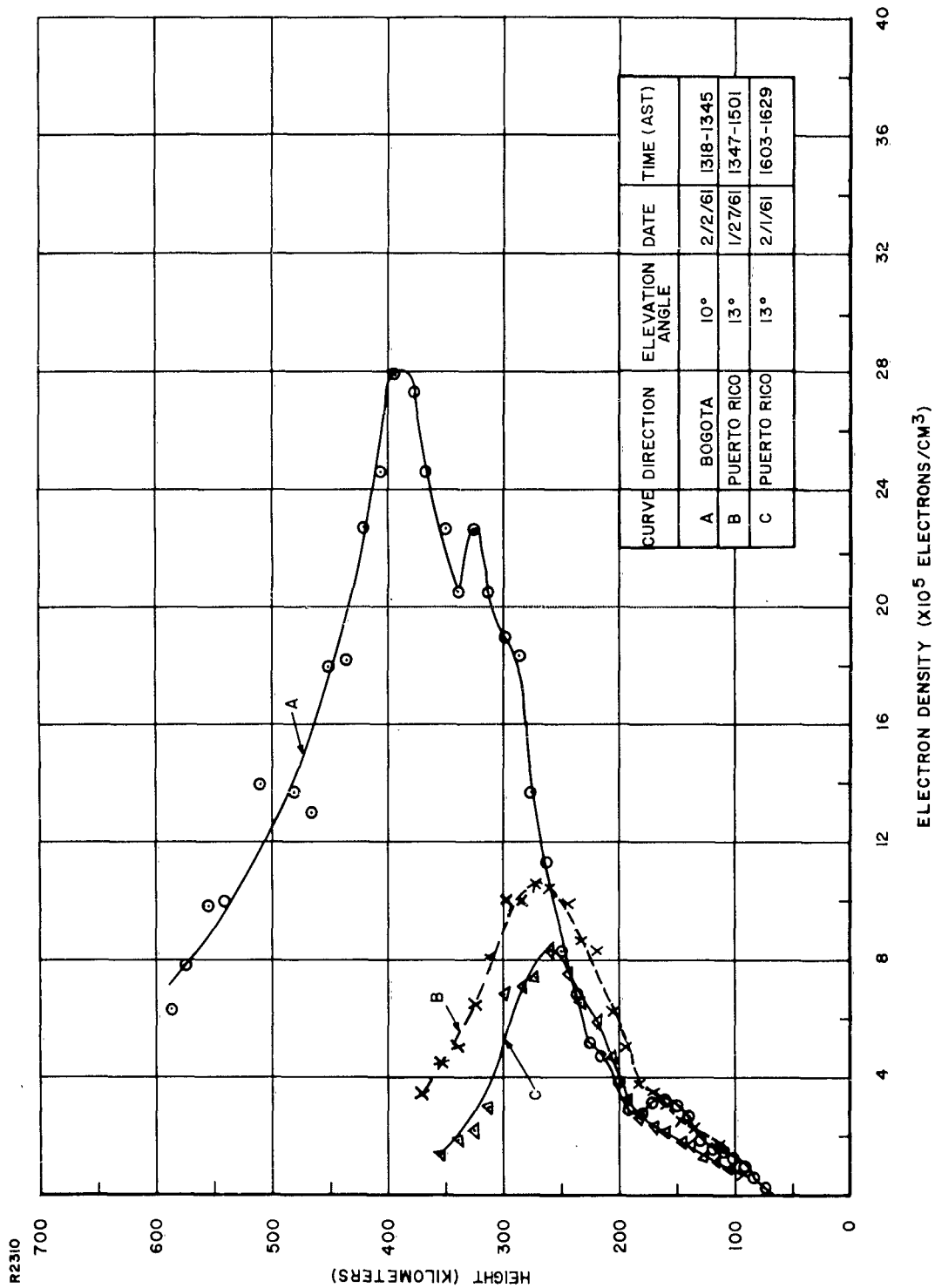


Figure 27. Electron Density Profiles Deduced from Incoherent Backscatter at Trinidad in the Direction of Bogota, Colombia, and Puerto Rico

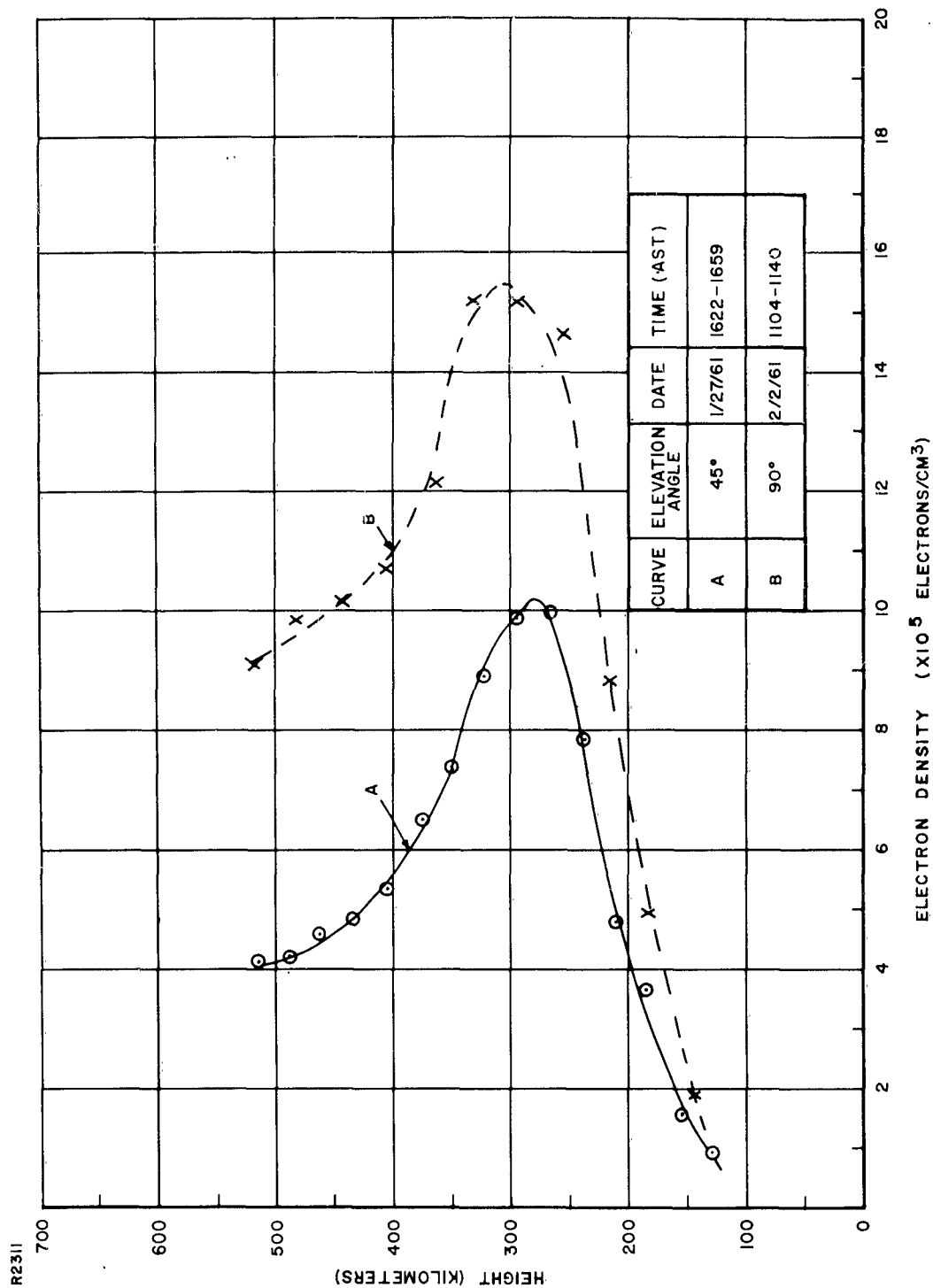


Figure 28. Electron Density Profiles Deduced from Incoherent Backscatter at Trinidad at Near Vertical Incidence

It is evident that the height and ionization density of the peak of the F-layer measured in the direction of Bogotá, as shown in Figure 27, are larger than those measured in the direction of Puerto Rico.

According to Wright,^{51,52} the electron density should maximize at about 5°N geographic latitude, which is in the region south of Trinidad. This inference is based on his study of electron density distributions along the 75°W geographic meridian.

The indentation in the Bogota curve at an altitude of 340 kilometers perhaps can be attributed to the presence of "blobs" or patches of intense ionization along the ray path. The observations directed towards the north, i.e., Puerto Rico, do not disclose any such reversal in the electron density profile.

It is seen that the two distributions obtained at near vertical incidence, shown in Figure 28, although displaced from one another, are somewhat identical in shape. The change in the slope, evident in both curves in the region between 368 and 400 kilometers, is indicative of an increasing scale height.

Wright⁵³ has suggested that a scale height gradient of approximately 0.2 kilometer per kilometer for the region above the maximum ionization of the F-layer may be more representative of an ionospheric model than one with a constant scale height.

Rocket sounding measurements of electron densities, as reported by Berning,³⁰ have disclosed a linear scale height gradient of 0.22 kilometer per kilometer for the neutral gas.

E. IONOSPHERIC MOVEMENTS

A range versus time photograph of incoherent backscatter echoes displaying radial movements of ionization is illustrated in Figure 29. The observations were made with circular polarization and with the antenna beam oriented at 5° elevation angle and 180° azimuth angle. A decreasing rate of range change on the order of six kilometers per second is found at a height of 312 kilometers. This extremely high range velocity corresponds to a height change of approximately two kilometers per second.

Ionospheric movements observed with linear polarization are shown in Figures 30 and 31.

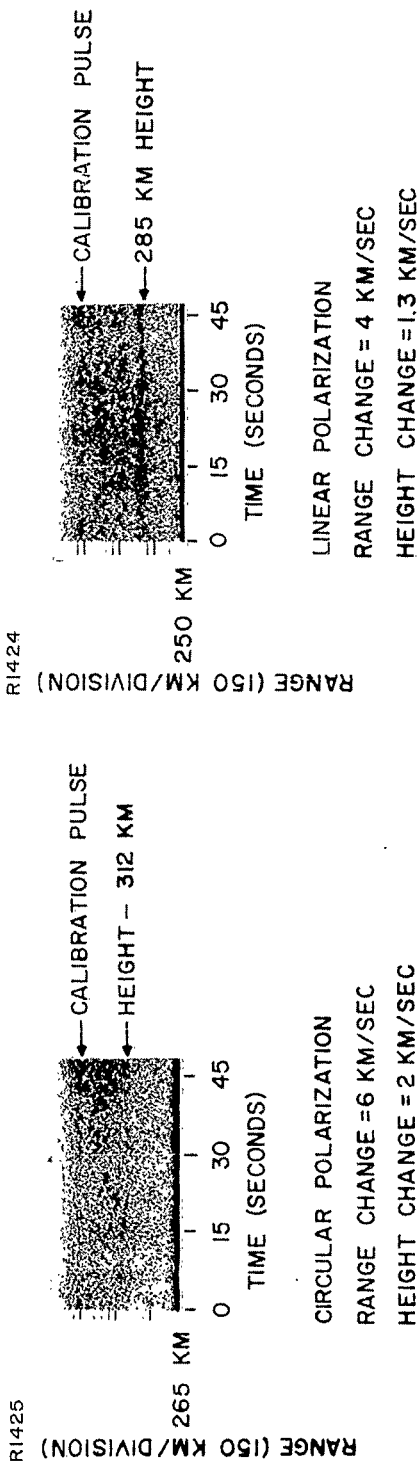


Figure 29. Range vs. Time Photograph Showing Range Movement of Incoherent Backscatter Echoes Observed at Trinidad at 5° Elevation Angle and 180° Azimuth Angle on 25 January 1961, 2233 AST

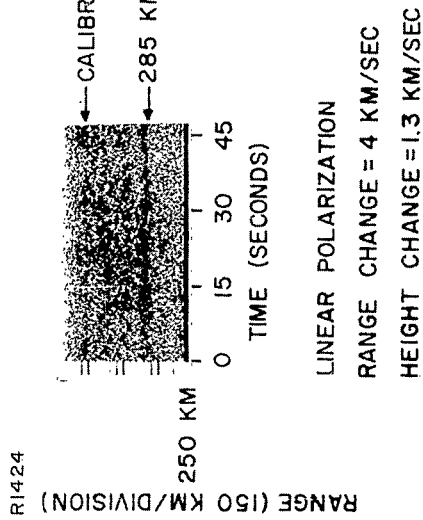


Figure 30. Range vs. Time Photograph Showing Range Movement of Incoherent Backscatter Echoes Observed at Trinidad at 10° Elevation Angle in the Direction of Bogota, Colombia, on 27 January 1961, 1815 AST

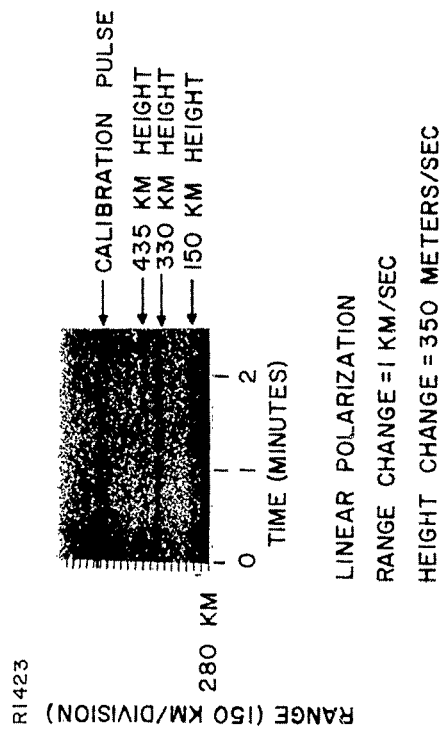


Figure 31. Range vs. Time Photograph Showing Range Movement of Incoherent Backscatter Echoes Observed at Trinidad at 10° Elevation Angle in the Direction of Bogota, Colombia, on 2 February 1961, 1342 through 1345 AST

The increasing range rate of Figure 30, which is approximately four kilometers per second, implies an upward height movement about 1.3 kilometers per second.

The interesting feature of Figure 31, which displays a range change of one kilometer per second, is that the ionization motion occurs only at a height of 330 kilometers in the F-region. The 150-km E-region echoes do not reveal any evidence of a radial disturbance.

It is important to realize that a decrease in radar range to the incoherent backscatter echoes may be produced by both a descent in the layer height and an increase in the ionization density. In the case of linear polarization, which shows the effect of Faraday rotation, both the layer motion and the change in the integrated electron density can be responsible for a variation in range.

For the observations made on 2 February 1961, between 1342 and 1345 AST, as given in Figure 31, the height of the F-layer at Bogota, according to Figure 32, appears to decrease at approximately eight meters per second. This average value, which is determined from vertical incidence sweep frequency sounders, is much lower than the 350 meters per second detected by incoherent backscatter. It is of interest to note that the virtual height data, on the other hand, showed a layer descent of 20 meters per second.

According to Wright,⁵⁴ there is often, in the early hours of the evening, a sudden rise in the F-layer beginning at the top of the layer and then later occurring at the bottom of the layer. As shown in Figure 33, which is a representative plot of the contours of constant plasma frequency deduced from Bogota ionosonde data, the height of the F-layer maximum rose at the rate of about 60 meters per second in the first 15 minutes, while the bottom of the F-layer ascended at about one-third this value. Calculations by Wright⁵⁴ indicate that the total electron content through the ionosphere decreased about 12.3 percent during this period.

It should be evident that, when circular polarization is employed on transmission and reception, the "scallop" effect of the signal intensity in range would not be present. Instead, the scattered return, as shown in Figure 29, appears to originate over a single band, its depth in range being dependent upon the elevation angle of the antenna beam and upon the height distribution of electron density in the ionosphere.

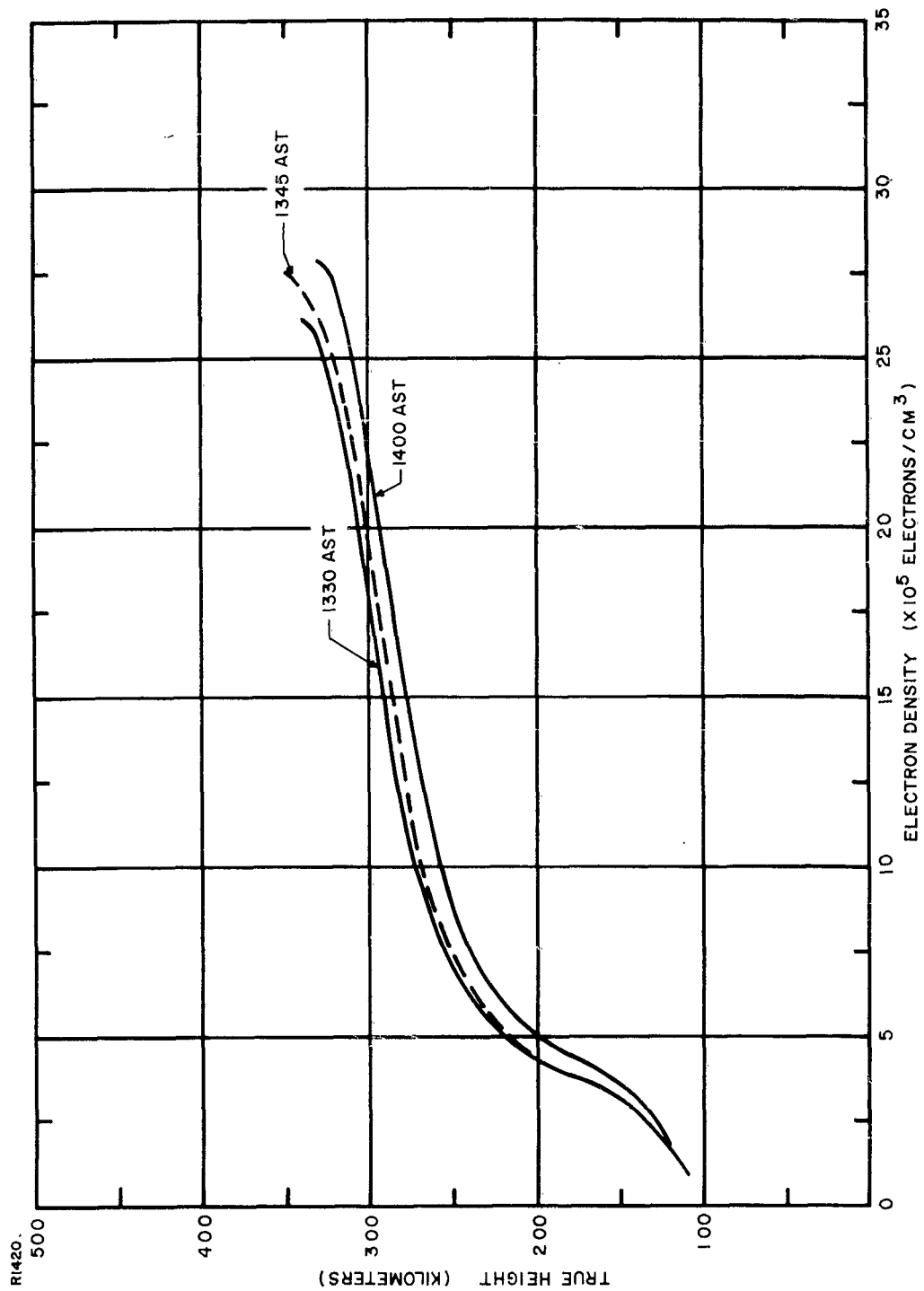


Figure 32. Electron Density Profiles Deduced from Ionospheric Soundings Taken at Bogota, Colombia, on 2 February 1961

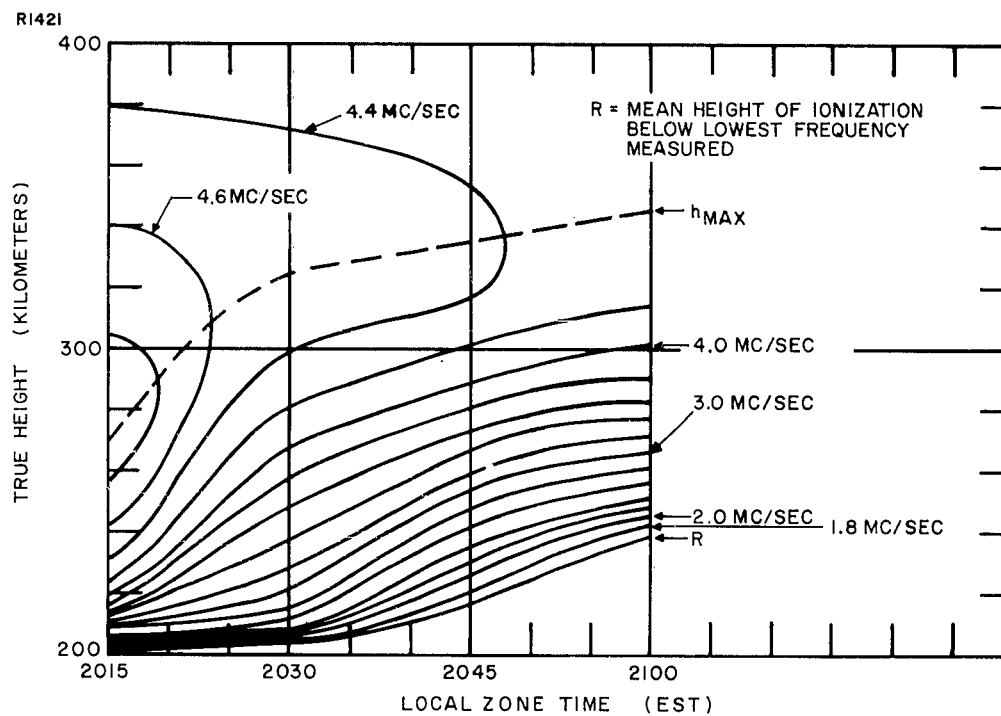


Figure 33. Contours of Constant Plasma Frequency at Bogota, Colombia, on 23 January 1961

Comparing Figure 29 with Figures 30 and 31, it is quite apparent that linear polarization is capable of resolving the regions in space at which ionospheric movements occur.

It should be mentioned that, of the hundreds of Polaroid photographs taken during the incoherent backscatter experiment at Trinidad, only three gave an indication of the presence of ionospheric motions. Moreover, the similarity in the three records was basically that the radial movement appeared only in the F-layer and in a southerly direction towards the equatorial ionosphere. The magnitudes of the radial and height rate changes are higher than previously reported by conventional ionospheric probing devices in the southern hemisphere.

Measurements of the motion of clouds of abnormal ionization in the auroral and polar regions which are comparable to the velocities detected at Trinidad, have been reported by Hagg and Hanson.⁵⁵

F. DATA CORRELATION

An attempt was made to determine whether there was any correlation between the incoherent backscatter measurements of the ionosphere, i.e., the electron density profile and the ionospheric movements, and the geophysical conditions existing during the time of the experiment.

According to the bulletins published by the National Bureau of Standards,⁵⁶ the magnetic conditions were quite normal during the observational period discussed in this paper, the geomagnetic planetary index, K_p , being 2-, 2-, 1-, 2- and 0° at the designated hours on 25 January 1961 (2235 AST), 27 January 1961 (1347 to 1501 AST and 1622 to 1649 AST), 27 January 1961 (1815 AST), 1 February 1961 (1603 to 1629 AST), and 2 February 1961 (1104 to 1140 AST and 1215 to 1345 AST), respectively.

The geomagnetic planetary index is a mean three-hour magnetic reading derived from observations located between 47° and 64° geomagnetic latitude. The scale of 0 to 9 is an arbitrary one, where 0 refers to a very quiet magnetic state and 9 to an extremely disturbed magnetic state. The symbols, + and - following the integer imply that the mean value of K_p is one-third of a unit more or one-third of a unit less, respectively, than the given integer, while ° signifies that K_p is a whole number, for example, 2+ = $2-1/3$, 2- = $1-2/3$, and 2° = 2.

Because of the lack of sufficient experimental incoherent backscatter data, it is not possible to arrive at a conclusion regarding the influence of a magnetic disturbance on the electron density profiles. However, it is definitely seen that the high radial velocities are detectable even on a magnetically quiet day, for example, 2 February 1961.

VII. SUMMARY AND CONCLUSIONS

The analysis of ionospheric incoherent backscattered echoes displaying Faraday rotational effects are treated in this report. The radar data were acquired in January and February 1961 at the United States Air Force Trinidad Test Site under an experimental program conducted jointly by the Rome Air Development Center, the General Electric Company, the Lincoln Laboratory, and the National Bureau of Standards.

The theoretical concepts of incoherent scattering are briefly reviewed and compared with existing experimental data.

The application of incoherent scattering as a technique for investigating the characteristics of the earth's atmosphere is considered.

A discussion is given on the theory of the Faraday effect. The possible utilization of this phenomenon in conjunction with ionospheric incoherent scatter for the study of the earth's magnetic field is also mentioned.

The radar, recording, and processing equipment used in the experimental work are briefly described. In addition, a description is given on the characteristics of incoherent backscatter echoes.

Experimental measurements show that, for linear polarized transmissions, the incoherent backscattered signals received on two linear orthogonal channels maximize at different radar ranges. It is found that the positions of the signal maxima correlate with those theoretically predicted based on the ionospheric Faraday effect.

Evidence is presented which indicates the feasibility of utilizing the Faraday effect to provide the calibration factor for converting the relative electron density profiles deduced from incoherent backscatter into an absolute measurement.

The average magnitude of the vertical component of the earth's magnetic field between altitudes of 100 and 360 kilometers at Trinidad, determined by means of incoherent scattering displaying Faraday rotation, is on the order of 0.242 gauss as compared to the value of 0.230 gauss extrapolated from isomagnetic maps.

During the daytime, the scale height of the neutral particles above the F-layer maximum appears to be less than 80 kilometers in the vicinity of Puerto Rico, and equal to approximately 80 kilometers in the vicinity of Bogota, Colombia.

Incoherent backscatter electron density profiles obtained at near vertical incidence at Trinidad indicate an increasing scale height gradient above the peak of the F-layer in the region between 368 and 400 kilometers.

It is shown that the incoherent scatter technique can be applied to the study of the movements of ionization in the ionosphere. Radial motions between one and six kilometers per second, which correspond to height changes of 0.35 to two kilometers per second, have been observed, the apparent motion occurring only in the F-layer and in a southerly direction towards the equatorial ionosphere.

VIII. REFERENCES

1. Gordon, W.E., "Incoherent Scattering of Radio Waves by Free Electrons with Applications to Space Exploration by Radar", Proceedings of I.R.E., Vol. 46, pp. 1824-1829, November 1958.
2. Bowles, K.L., "Observation of Vertical Incidence Scatter from the Ionosphere at 41 Mc/sec.", Physical Review Letters, Vol. 1, pp. 454-455, December 15, 1958.
3. Bowles, K.L., "Incoherent Scattering by Free Electrons as a Technique for Studying the Ionosphere and Exosphere: Some Observations and Theoretical Considerations", Journal of Research, National Bureau of Standards, Vol. 65D, pp. 1-14, January-February 1961.
4. Pineo, V.C., Kraft, L.G., and Briscoe, H.W., "Ionospheric Backscatter Observation at 440 Mc/s", Journal of Geophysical Research, Vol. 65, pp. 1620-1621, May 1960.
5. Pineo, V.C., Kraft, L.G., and Briscoe, H.W., "Some Characteristics of Ionospheric Backscatter Observed at 440 Mc/s", Journal of Geophysical Research, Vol. 65, pp. 2629-2633, September 1960.
6. Millman, G.H., Moceyunas, A.J., Sanders, A.E., and Wyrick, R.F., "The Effect of Faraday Rotation on Incoherent Backscatter Observations", Journal of Geophysical Research, Vol. 65, pp. 1564-1568, May 1961.
7. Salpeter, E.E., "Scattering of Radio Waves by Electrons above the Ionosphere", Journal of Geophysical Research, Vol. 65, pp. 1851-1852, June 1960.
8. Dougherty, J.P. and Farley, D.T., "A Theory of Incoherent Scattering of Radio Waves by a Plasma", Proceedings of the Royal Society, A, Vol. 259, pp. 79-99, 1960.
9. Fejer, J.A., "Scattering of Radio Waves by an Ionized Gas in Thermal Equilibrium", Canadian Journal of Physics, Vol. 38, pp. 1114-1133, 1960.
10. Fejer, J.A., "Scattering of Radio Waves by an Ionized Gas in Thermal Equilibrium in the Presence of a Uniform Magnetic Field", Canadian Journal of Physics, Vol. 39, pp. 716-740, 1961.
11. Renau, J., "Scattering of Electromagnetic Waves from a Non-Degenerate Ionized Gas", Journal of Geophysical Research, Vol. 65, pp. 3631-3640, November 1960.
12. Renau, J., Camnitz, H., and Flood, W., "The Spectrum and the Total Intensity of Electromagnetic Waves Scattered from an Ionized Gas in Thermal Equilibrium in the Presence of a Static Quasi-Uniform Magnetic Field", Journal of Geophysical Research, Vol. 66, pp. 2703-2732, September 1961.
13. Laaspere, T., "On the Effect of a Magnetic Field on the Spectrum of Incoherent Scattering", Journal of Geophysical Research, Vol. 65, pp. 3955-3959, December 1960.
14. Hagfors, T., "Density Fluctuations in a Plasma in a Magnetic Field, with Applications to the Ionosphere", Journal of Geophysical Research, Vol. 66, pp. 1699-1712, June 1961.

15. Buneman, O., "Fluctuations in a Multicomponent Plasma", Journal of Geophysical Research, Vol. 66, pp. 1978-1979, June 1961.
16. Lawson, J.L. and Uhlenbeck, G.E., "Threshold Signals", Radiation Laboratory Series, Vol. 24, McGraw-Hill Book Co., 1950.
17. Spitzer, L., "Physics of Fully Ionized Gases", Intersciences Publishers, 1956.
18. Heitler, W., "The Quantum Theory of Radiation", Oxford University Press, 1957.
19. Pineo, V.C. and Briscoe, H.W., "Discussion on Incoherent Backscatter Power Measurements at 440 Mc/s", Journal of Geophysical Research, Vol. 66, pp. 3965-3966, November 1961.
20. Kahn, F.D., "Long-Range Interactions in Ionized Gases in Thermal Equilibrium", Astrophysical Journal, Vol. 129, pp. 205-216, 1959.
21. Pines, D. and Bohm, D., "A Collective Description of Electron Interactions: II Collective vs. Individual Particle Aspects of the Interactions", Physical Review, Vol. 85, pp. 338-353, 1952.
22. Buneman, O., "Scattering of Radiation by the Fluctuations in a Non-Equilibrium Plasma", Radioscience Laboratory, Stanford University, Scientific Report No. 4, February 1962.
23. Farley, D.T., Dougherty, J.P., and Barron, D.W., "A Theory of Incoherent Scattering of Radio Waves by a Plasma in a Uniform Magnetic Field", Research Laboratory of Electronics, Chalmers University of Technology, Research Report No. 22, 1961.
24. Pineo, V.C., Private Communication, November 1961.
25. Pineo, V.C., Kraft, L.G., Briscoe, H.W., and Hynek, D.P., "Experimental Studies of the F-region Using the Incoherent Backscatter Technique at Frequencies Around 400 Mc/sec.", Paper presented at the URSI-IRE Meeting, Washington, D.C., May 1961.
26. Laaspere, T., Private Communication, May 1961.
27. Pineo, V.C. and Hynek, D.P., "Diurnal Variation of the Spectral Width and Shape and Other Characteristics of Incoherent Ionospheric Backscatter Observed at 440 Mc/s During a 24-Hour Period in May 1961", Paper presented at the AGU Meeting, Los Angeles, Calif., December 1961.
28. Pineo, V.C. and Hynek, D.P., "Spectral Characteristics of Incoherent Backscatter and Electron Density Profiles Measured at 425 Mc/sec. at Trinidad", Paper presented at the AGU Meeting, Los Angeles, Calif., December 1961.
29. Millman, G.H., "A Study of Ionospheric Winds and Turbulence Utilizing Long Radio Waves", Annales de Geophysique, Vol. 8, pp. 365-384, October-December 1952.
30. Berning, W.W., "A Sounding Rocket Measurement of Electron Densities to 1500 Kilometers", Journal of Geophysical Research, Vol. 65, pp. 2589-2594, September 1960.

31. Nisbet, J.S. and Bowhill, S.A., "Electron Densities in the F-Region of the Ionosphere from Rocket Measurements; Part 1, Method of Analysis", Journal of Geophysical Research, Vol. 65, pp. 3601-3607, November 1960.
32. Nisbet, J.S. and Bowhill, S.A., "Electron Densities in the F-Region of the Ionosphere from Rocket Measurements; Part 2, Results of Analysis", Journal of Geophysical Research, Vol. 65, pp. 3609-3614, November 1960.
33. Garriott, O.K., "The Determination of Ionospheric Electron Content and Distribution from Satellite Observations; Part 1, Theory of Analysis", Journal of Geophysical Research, Vol. 65, pp. 1139-1150, April 1960.
34. Garriott, O.K., "The Determination of Ionospheric Electron Content and Distribution from Satellite Observations; Part 2, Results of the Analysis", Journal of Geophysical Research, Vol. 65, pp. 1151-1158, April 1960.
35. Ross, W.J., "The Determination of Ionospheric Electron Content from Satellite Doppler Measurements; 1. Method of Analysis", Journal of Geophysical Research, Vol. 65, pp. 2601-2606, September 1960.
36. Ross, W.J., "The Determination of Ionospheric Electron Content from Satellite Doppler Measurements; 2. Experimental Results", Journal of Geophysical Research, Vol. 65, pp. 2607-2615, September 1960.
37. Yeh, K.C. and Swenson, G.W., "Ionospheric Electron Content and Its Variation Deduced from Satellite Observations", Journal of Geophysical Research, Vol. 66, pp. 1061-1067, April 1961.
38. Munro, G.H., "Diurnal Variations in the Ionosphere Deduced from Satellite Radio Signals", Journal of Geophysical Research, Vol. 67, pp. 147-156, January 1962.
39. Spencer, N.W., Brace, L.H., and Carignan, G.R., "Electron Temperature Evidence for Nonthermal Equilibrium in the Ionosphere", Journal of Geophysical Research, Vol. 67, pp. 157-175, January 1962.
40. Hutchinson, R. and Shuman, B., "Rocket Measurements of the Magnetic Field Above New Mexico", Journal of Geophysical Research, Vol. 66, pp. 2687-2693, September 1961.
41. Millman, G.H., Sanders, A.E., and Mather, R.A., "Radar-Lunar Investigations at a Low Geomagnetic Latitude", Journal of Geophysical Research, Vol. 65, pp. 2619-2626, September 1960.
42. Millman, G.H., "Ionospheric Investigations by Radar Reflections from Echo I", Paper presented at the NATO Advanced Study Institute on Radio Astronomical and Satellite Studies of the Atmosphere, Corfu, Greece, June 1962.
43. Evans, J.V. and Taylor, G.N., "The Electron Content of the Ionosphere in Winter", Proceedings of the Royal Society, A, Vol. 263, pp. 189-211, 1961.
44. Millman, G.H., "Atmospheric and Extraterrestrial Effects on Radio Wave Propagation", General Electric Technical Information Series Report No. R61EMH29, June 1961. (Lecture notes presented at the "Modern Radar Techniques" course conducted at the Moore School of Electrical Engineering, University of Pennsylvania, June 1961.)

45. Millman, G.H., "The Geometry of the Earth's Magnetic Field at Ionospheric Heights", Journal of Geophysical Research, Vol. 64, pp. 717-726, July 1959.
46. Vestine, E.H., LaPorte, L., Lange, I., and Scott, W.E., "The Geomagnetic Field, Its Description and Analysis", Department of Terrestrial Magnetism, Carnegie Institution of Washington, Publication 580, 1947.
47. Chapman, S. and Bartels, J., "Geomagnetism", Volumes I and II, Oxford University Press, 1940.
48. Millman, G.H., "The Geometry of Radar-Auroral Reflections", General Electric Technical Information Series Report No. R58EMH3, March 1958.
49. Budden, K.G., "A Method for Determining the Variation of Electron Density with Height (N(Z) Curves) from Curves of Equivalent Height Against Frequency", The Physics of the Ionosphere, pp. 332-339, The Physical Society, London, 1955.
50. Millman, G.H. and Rose, F., "A Study of Ionospheric and Lunar Characteristics by Radar Techniques", General Electric Technical Information Series Report No. R61EMH40, August 1961.
51. Wright, J.W., "A Model of the F-Region Above $h_{\max} F2$ ", Journal of Geophysical Research, Vol. 65, pp. 185-191, January 1960.
52. Wright, J.W., "Vertical Cross Sections of the Ionosphere Across the Geomagnetic Equator", National Bureau of Standards Report No. 6726, October 1960.
53. Wright, J.W., "Comment on Models of the Ionosphere Above $h_{\max} F2$ ", Journal of Geophysical Research, Vol. 65, pp. 2595-2596, September 1960.
54. Wright, J.W., Private Communication, March 1961.
55. Hagg, E.L. and Hanson, G.H., "Motion of Clouds of Abnormal Ionization in the Auroral and Polar Regions", Canadian Journal of Physics, Vol. 32, pp. 790-798, 1954.
56. "Solar-Geophysical Data", CRPL-F, Part B, U.S. Department of Commerce, National Bureau of Standards, Central Radio Propagation Laboratory, Boulder, Colorado.
57. Minzer, R.A., Champion, K.S.W., and Pond, H.L., "The ARDC Model Atmosphere", AFCRL, Air Force Surveys in Geophysics No. 115, August 1959.

APPENDIX

SYSTEM REQUIREMENTS FOR THE DETECTION OF
IONOSPHERIC INCOHERENT BACKSCATTER

The incoherent signal-to-receiver noise ratio of the energy backscattered to a monostatic radar by a random distribution of free electrons in an ionized medium such as exists in the ionosphere can be expressed by the function

$$\frac{P_r}{N} = \frac{\pi P_t c \tau A_e \sigma}{8 R^2 K T B F} \quad (\text{A-1})$$

where P_t is the peak transmitted power, c is the free space velocity, τ is the pulse length, A_e is the effective antenna area, σ is the scattering coefficient defined as the power scattered per unit solid angle per unit incident power density per unit scattering volume, R is the radar range to the scatterers, K is Boltzmann's constant (1.38×10^{-23} watt-sec/ $^\circ\text{K}$), T is the ambient temperature, F is the receiver noise figure and B is the receiver noise bandwidth.

For frequencies less than approximately 10,000 megacycles, and assuming that the ionosphere is in thermal equilibrium, the scattering coefficient is defined by

$$\sigma = \frac{1}{2} \sigma_e N_e \quad (\text{A-2})$$

where N_e is the electron density. The parameter, σ_e , which is the scattering cross section of a single free electron, is, in square centimeters, equal to

$$\sigma_e = 7.94 \times 10^{-26} \sin^2 \chi \quad (\text{A-3})$$

where χ is the (polarization) angle between the direction of the incident electric field and the direction of scattering.

Prior to estimating the intensity of the incoherent backscattered signal that could be received by a radar system, Equations (A-1) and (A-2) are combined and the resulting expression is simplified to the general form

$$\frac{P_r}{N} = 11.7 \left[\frac{P_t \tau A_e}{B F} \right] \left[\frac{N_e}{R^2} \right] \quad (\text{A-4})$$

where P_t is in watts, τ is in seconds, A_e is in square centimeters, N_e is in electrons per cubic centimeter, B is in cycles per second, R is in meters, and F is in

dimensionless units. The first parenthesis contains the parameters which would normally describe a radar system while the second merely defines the propagation conditions.

This relationship is plotted in Figure A-1 as a function of radar system parameters for various propagation configurations.

Since the incoherent radiation backscattered from the ionosphere is doppler spread in frequency, caution must be exercised in employing the correct bandwidth in the evaluation of the signal-to-receiver noise ratio.

If the spectral spread imposed by the scattering medium is larger than the receiver noise bandwidth, then it must be used in place of the receiver bandwidth to define the internal receiver noise power.

It should be noted that, for optimum incoherent signal return, the bandwidth of the receiver should be matched to the width of the scatter spectrum.

The spectral bandwidths of the signal power that could be backscattered as a function of altitude at 425 and 1300 megacycles are illustrated in Figure A-2. These calculations are based on Pineo's experimental measurement of a half-power spectral width of 11 kilocycles at a height of 330 kilometers at a frequency of 440 megacycles,⁵ and also on the assumption that the doppler spread is directly proportional to the square root of the kinetic temperature and to the transmission frequency (see Equation (21)). The assumed variation of kinetic temperature with height, also shown in Figure A-2, is the model proposed by Minzer, Champion and Pond.⁵⁷

An estimate of the incoherent signal-to-receiver noise ratio that could possibly be detected from a normal daytime ionosphere is presented in Figure A-3. These computations were derived on the following assumptions: 425 megacycles transmission frequency, 2.5 megawatts transmitted peak power, 500 microseconds pulse width, 3 db receiver noise figure, 2 db line losses, and an 84-foot diameter parabolic antenna having an antenna efficiency factor of 0.6. It is noted that these parameters are approximately the same as those of the Millstone Hill and Trinidad radar employed in the incoherent scatter experiments.

The daytime distribution of the electron density under consideration in this analysis is assumed to follow a Chapman model defined by Equation (38). The parameters of the electron density profile are given by: E-layer, maximum electron density of 1.5×10^5 electrons per cubic centimeter at an altitude of 100 kilometers

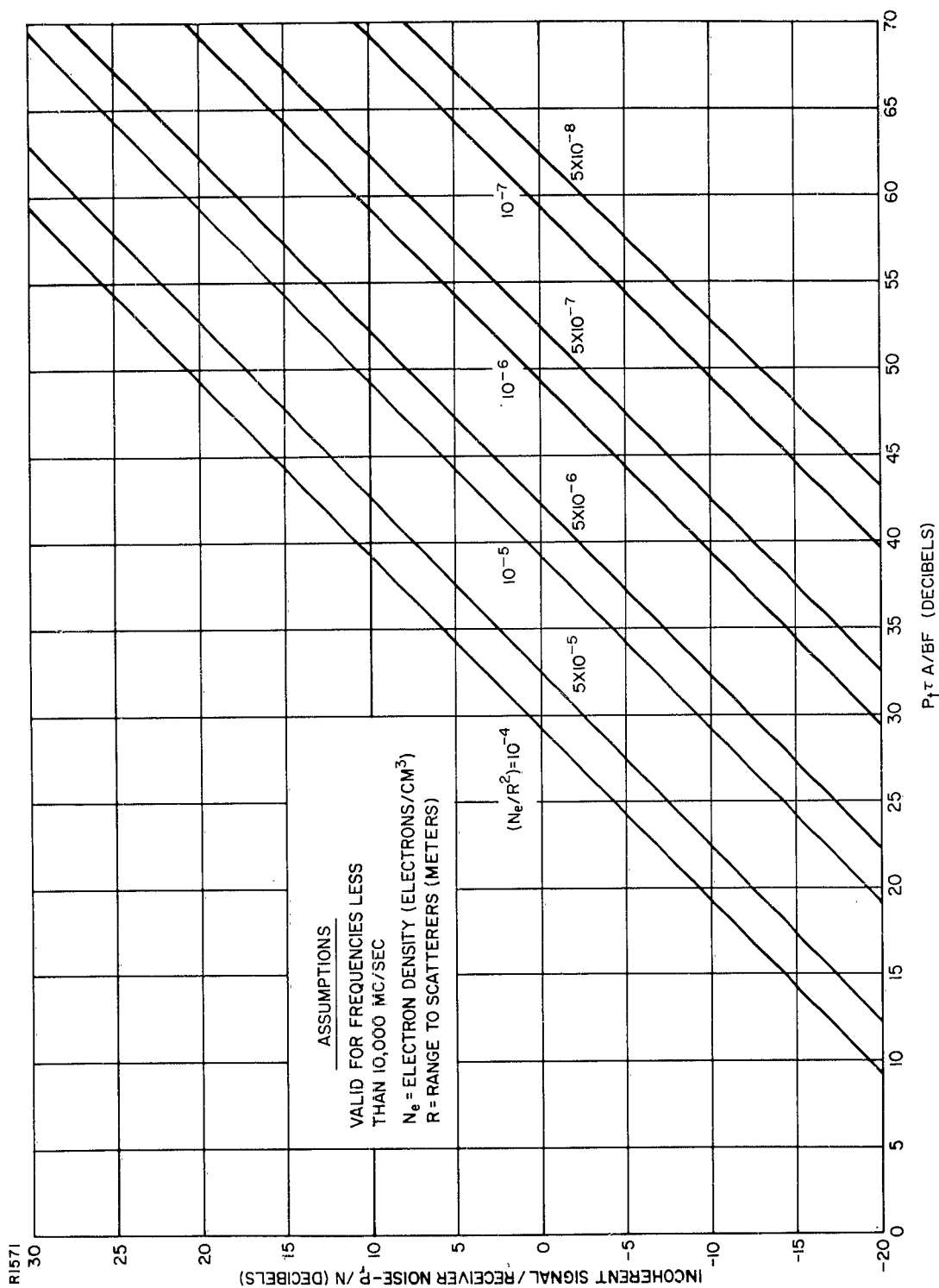


Figure A-1. Incoherent Backscatter Signal-to-Receiver Noise Ratio as a Function of System Parameters

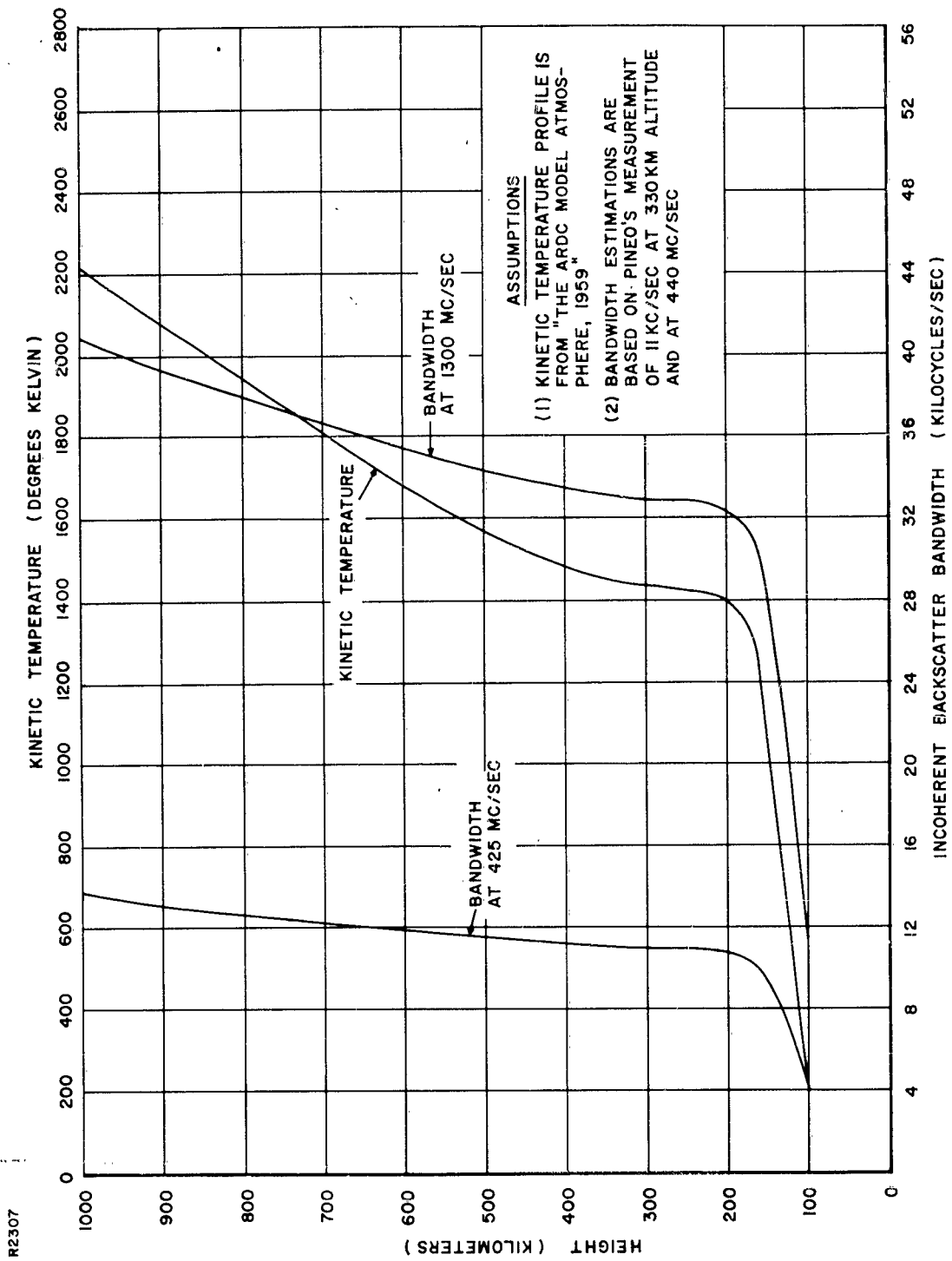


Figure A-2. Estimate of the Bandwidth of Incoherent Signals Backscattered from a Normal Ionosphere at 425 and 1300 Megacycles

with a scale height of 10 kilometers; F₁-layer, maximum electron density of 3.0×10^5 electrons per cubic centimeter at an altitude of 200 kilometers with a scale height of 40 kilometers; F₂-layer, maximum electron density of 12.5×10^5 electrons per cubic centimeter at an altitude of 300 kilometers with a scale height of 50 kilometers.

It is evident from Figure A-3 that, for observations at low elevation angles, the signal intensity from scattering taking place at high altitudes would be extremely weak and that, in order to obtain additional improvement in the signal-to-noise ratio, it would be necessary to employ signal integration techniques.

For nighttime ionospheric conditions, it is estimated that the incoherent signal-to-receiver noise ratio could be from approximately 3 db to 8 db less than the daytime values.

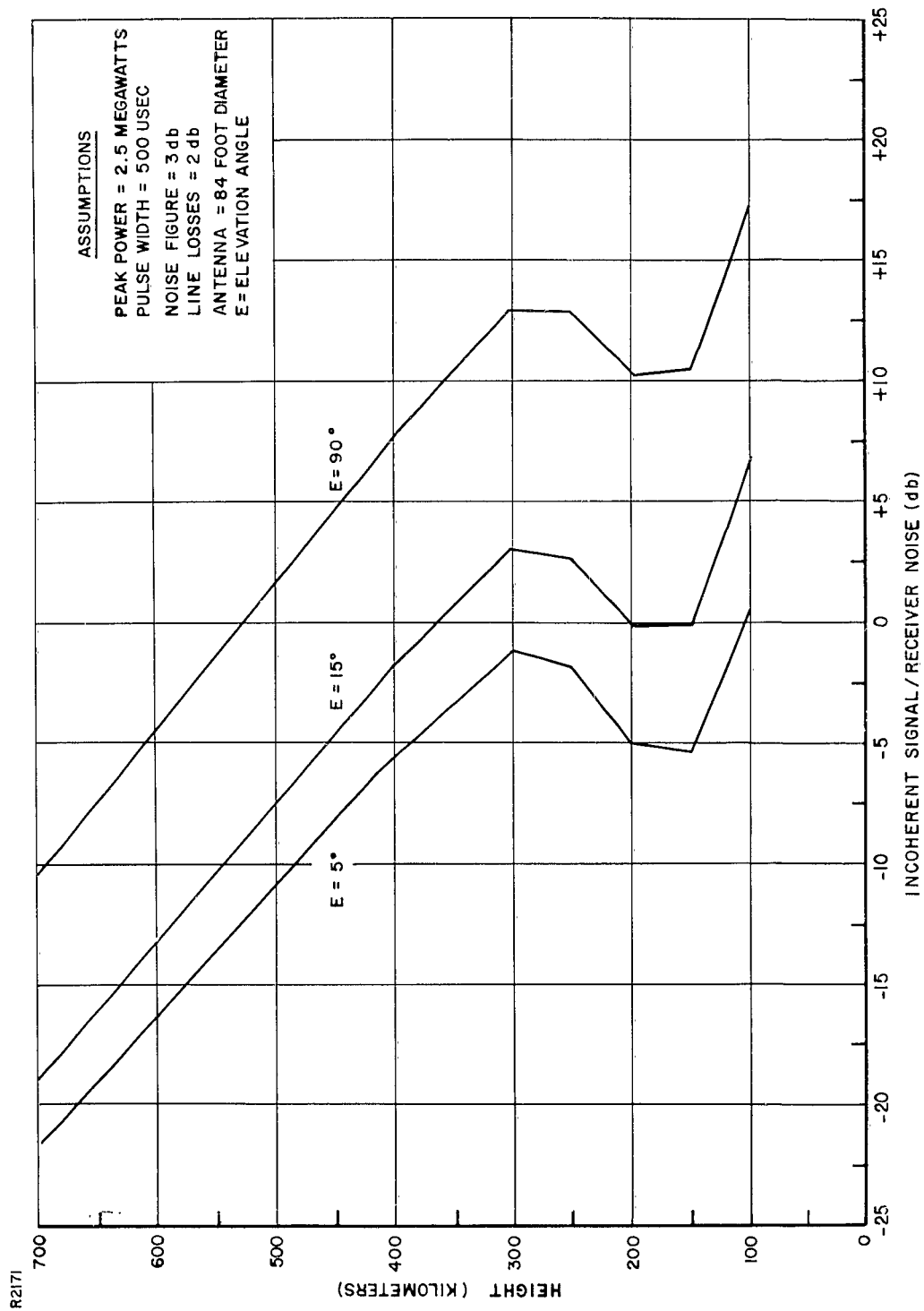


Figure A-3. Estimate of Incoherent Signal-to-Receiver Noise Ratio from a Normal Ionosphere at 425 Megacycles